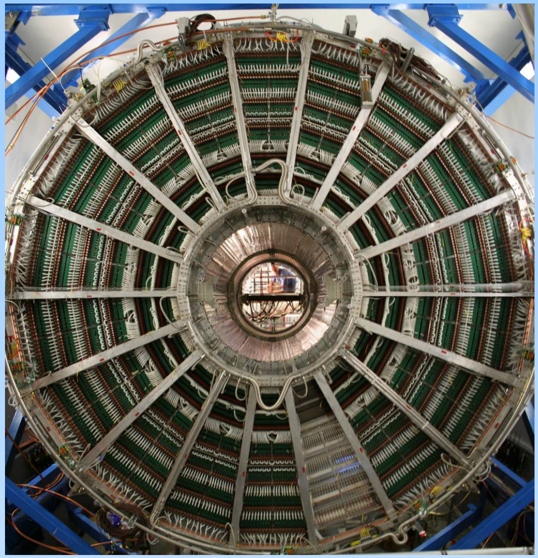

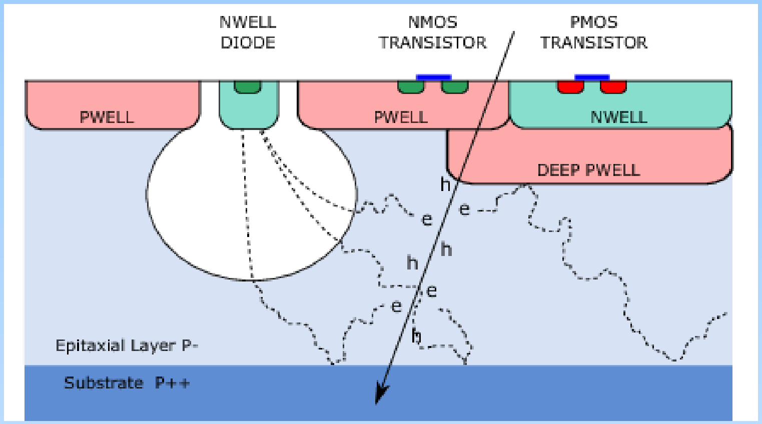

Gaseous detectors

Silvia Masciocchi,
GSI Darmstadt and University of Heidelberg

39^{th} Heidelberg Physics Graduate Days, HGSFP
Heidelberg
October 10, 2017

Gaseous detectors

Schematic Principle
of gas detectors

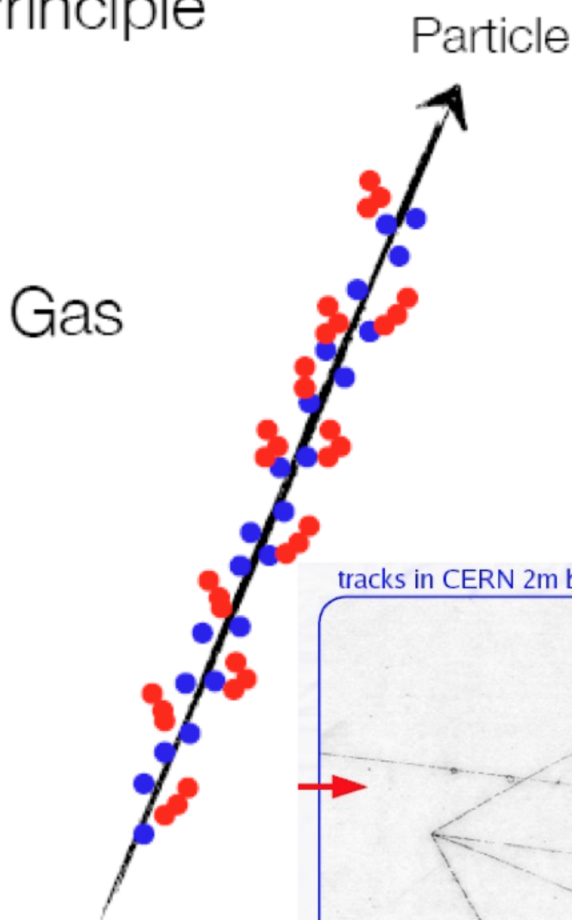

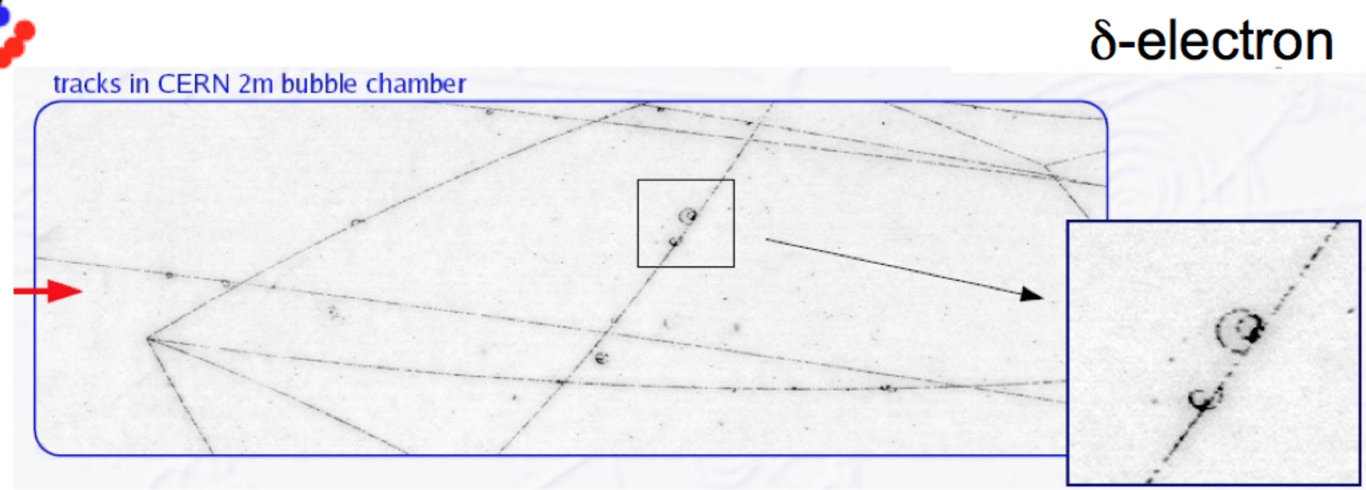

- Primary Ionization
- Secondary Ionization (due to δ-electrons)

Gaseous detectors

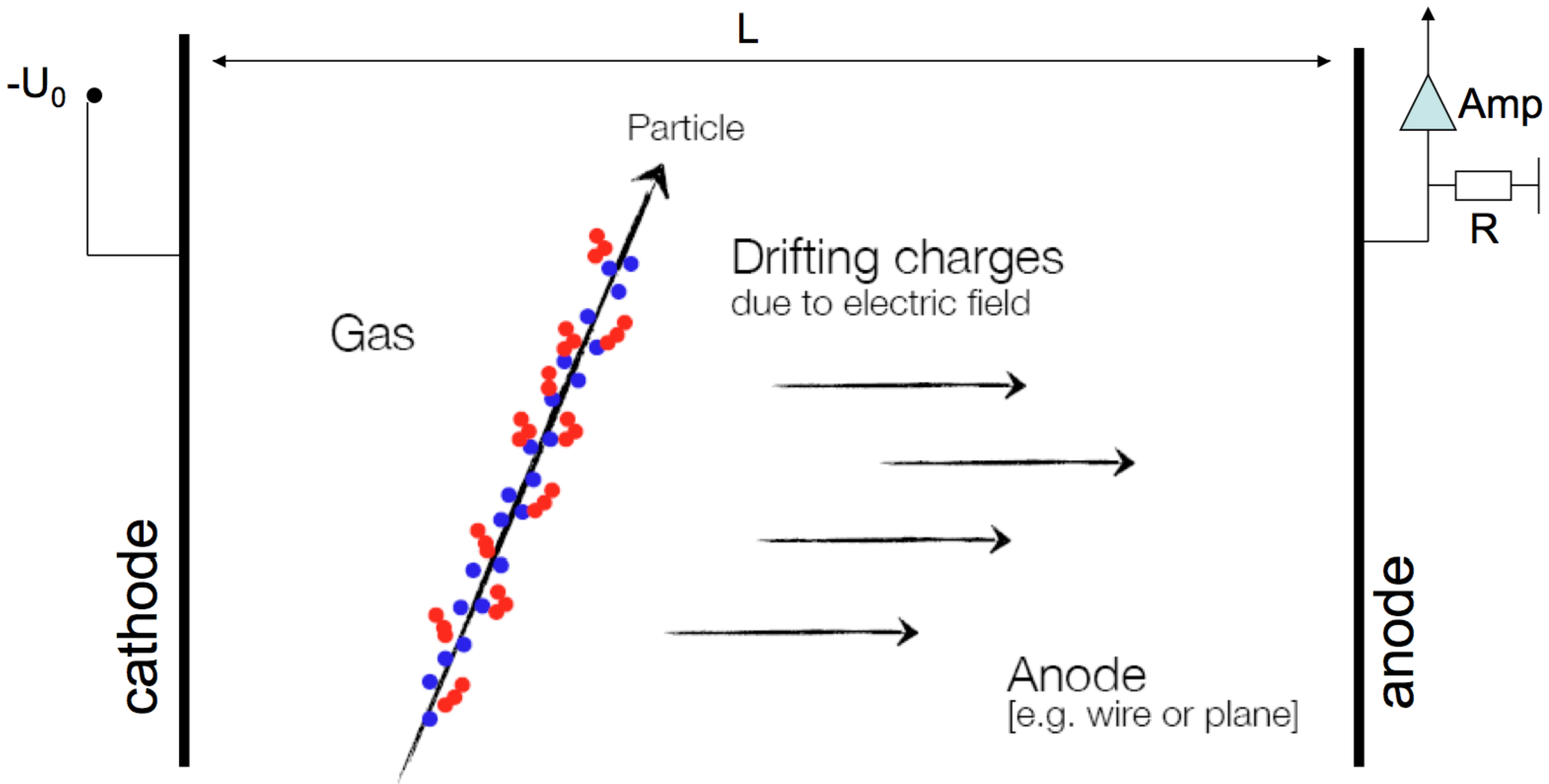

- Primary Ionization
- Secondary Ionization (due to δ-electrons)

Gaseous detectors

Modes of operation, depending on the strength of the electric field

W. Price, "Nuclear Radiation Detection", 1958

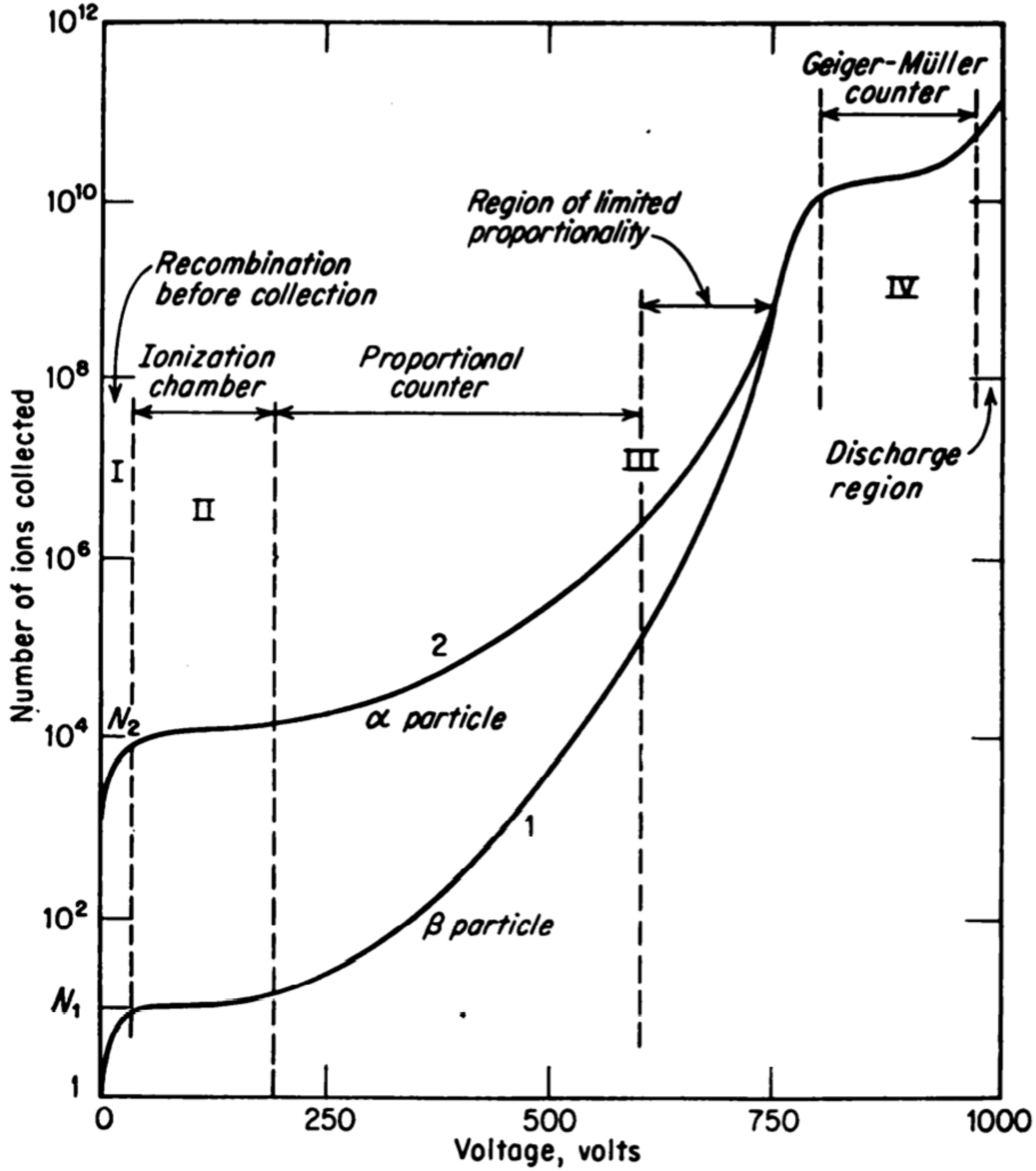

FIG. 2–2. Pulse-height versus applied-voltage curves to illustrate ionization, proportional, and Geiger-Müller regions of operation.

Gaseous detectors: outline

SIGNAL GENERATION

1. Ionization in gas
2. Charge transport in gas
   a) Diffusion
   b) Electron and ion mobility
   c) Drift velocity
3. Charge multiplication / gas amplification

DETECTOR TYPES

A) Ionization chamber
B) Proportional counter
   - Multiwire proportional chambers
C) Drift chambers
   - Cylindrical wire chambers
   - Jet drift chambers
D) Time projection chambers

Gaseous detectors: Signal generation

1. Ionization in gas
2. Charge transport in gas
   a) Diffusion
   b) Electron and ion mobility
   c) Drift velocity
3. Loss of electrons
4. Charge multiplication / gas amplification

Gaseous detectors: Signal generation

1. **Ionization in gas**

2. Charge transport in gas
   a) Diffusion
   b) Electron and ion mobility
   c) Drift velocity

3. Loss of electrons

4. Charge multiplication / gas amplification

Ionization in gas

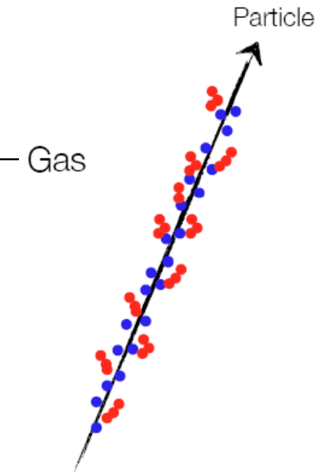

p: charged particle traversing the gas

X: gas atom or molecule

Primary ionization:

$$p + X \rightarrow p + X^{+} + e^{-}$$

Secondary ionization: if E_e is high enough ($E_e > E_i$, δ electrons)

$$e^{-} + X \rightarrow X^{+} + e^{-} + e^{-}$$

length scale ~ 10-20 μm

Relevant parameters for gas detectors:

- Ionization energy: E_i
- Average energy per e-ion pair: W_i
- Average # of primary e-ion pairs [per cm]: n_p
- Average # of e-ion pairs [per cm]: n_T

$$\langle n_T \rangle = \frac{L \cdot \left\langle \frac{dE}{dx} \right\rangle_i}{W_i}$$

L = layer thickness

n_T ~ 2-6 times n_p

Typical values: E_i ~ 30 eV

n_T ~ 100 pairs / 3 keV incident particle

Ionization in most common gases

$(E_i = I_o)$

Gas	ρ (g/cm^3) (STP)	I_0 (eV)	W_i (eV)	dE/dx (MeVg^{-1}cm^2)	n_p (cm^{-1})	n_t (cm^{-1})
H_2	$8.38 \cdot 10^{-5}$	15.4	37	4.03	5.2	9.2
He	$1.66 \cdot 10^{-4}$	24.6	41	1.94	5.9	7.8
N_2	$1.17 \cdot 10^{-3}$	15.5	35	1.68	(10)	56
Ne	$8.39 \cdot 10^{-4}$	21.6	36	1.68	12	39
Ar	$1.66 \cdot 10^{-3}$	15.8	26	1.47	29.4	94
Kr	$3.49 \cdot 10^{-3}$	14.0	24	1.32	(22)	192
Xe	$5.49 \cdot 10^{-3}$	12.1	22	1.23	44	307
CO_2	$1.86 \cdot 10^{-3}$	13.7	33	1.62	(34)	91
CH_4	$6.70 \cdot 10^{-4}$	13.1	28	2.21	16	53
C_4H_{10}	$2.42 \cdot 10^{-3}$	10.8	23	1.86	(46)	195

From: K. Kleinknecht, “Detektoren für Teilchenstrahlung”, B.G. Teubner, 1992

Gaseous detectors: Signal generation

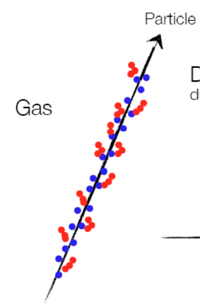

~30 eV per e-ion pair

1. **Ionization in gas**

2. **Charge transport in gas**
   a) Diffusion
   b) Electron and ion mobility
   c) Drift velocity

3. Loss of electrons

4. Charge multiplication / gas amplification

Charge transport

- Thermal motion: diffusion
- Motion under the influence of external fields
- Collisions with gas atoms/molecules

Charge transport: diffusion

Thermal motion

E = B = 0

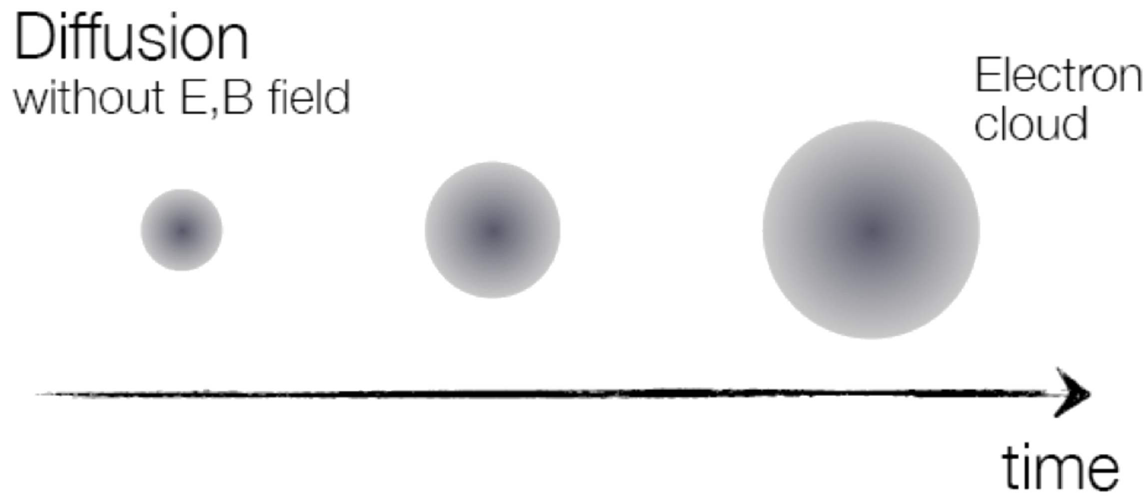

Classical kinetic theory of gases:

$$\frac{dN}{dx} = \frac{N_0}{\sqrt{4\pi D t}} \exp\left(-\frac{x^2}{4 D t}\right)$$

After a time t, the cloud of electrons/ions has diffused to a Gaussian distribution with width:

$$\sigma(r) = \sqrt{6 D t}$$

D: diffusion coefficient:

$$D = \frac{1}{3} v \lambda$$

Longitudinal	1/3 D
Transversal	2/3 D

Charge transport: diffusion

D: diffusion coefficient:

$$D = \frac{1}{3} v \lambda$$

Mean free path of electrons/ions in gas:

$$\lambda = \frac{1}{\sqrt{2}} \frac{kT}{\sigma_0 P}$$

Mean velocity according to the Maxwell distribution:

$$v = \sqrt{\frac{8kT}{\pi m}}$$

m=mass of particle (note difference e / ion!)

Therefore:

$$D = \frac{1}{3} v \lambda = \frac{2}{3\sqrt{\pi}} \frac{1}{\sigma_0 P} \sqrt{\frac{(kT)^3}{m}}$$

Diffusion depends on the **gas pressure P and temperature T** !!!

Charge transport: ion mobility

- **Action of external electric field**

  Ions move along the lines of the electric field E and gain a velocity $\vec{v}_D$, in addition to their random thermal motion (isotropic)

- **Collisions with non-ionized gas atoms**

  Ions keep colliding with other (non-ionized) atoms of the gas. In such collisions (comparable mass) they transfer typically half of their kinetic energy → ion kinetic energy is approximately equal to thermal energy

$$\langle T_{ion}(E\neq 0)\rangle = \langle T_{ion}(\text{Therm})\rangle = \frac{3}{2}kT$$

- **Drift velocity develops between collisions** $\tau = \lambda(T_{kin})/v_{therm} = \text{const.}$

  Assume: $v_D(t=0) = 0$; after τ = typical collision time the velocity is

$$\vec{v} = \vec{a}\cdot\tau = \frac{e\vec{E}}{M}\cdot\tau$$

$$\vec{v}_D = \langle\vec{v}\rangle = \frac{1}{2}\vec{v} = \frac{e|\vec{E}|}{2M}\cdot\tau = \mu_+|\vec{E}|$$

$$v_D^{ions} \propto E\,!$$

μ_+ = **ion mobility**

E.g. μ_+ = 0.61 cm²/Vs for C_4H_{10}. E = 1 kV/cm. Typical drift distances = few cm → typical ion drift time = few ms

Electron mobility: old and hot gases

Situation different for electrons ($m_e \ll M$) → $\mu_+ \ll \mu_-$

Two cases for the electron mobility, depending on the gas used:

- **Cold gases**: gas atoms have many low-lying levels → electrons in a collision can loose substantial part of the kinetic energy which they gain between collisions (similar to ions!!):

  $T_e \approx kT$; $\mu \approx$ const. → $v_D^e \propto E$!

  Examples: Ar/Co_2, Ne/CO_2

  In Ne/CO_2, $\mu \approx 7.0 \times 10^{-3}$ cm²/μsV at 10% CO_2, or v_D = 2 cm/μs at 300 V/m

  $\mu \approx 3.5 \times 10^{-3}$ cm²/μsV at 20% CO_2, or v_D = 1 cm/μs at 300 V/m

- **Hot gases**: gas atoms have few low-lying levels → electrons loose little energy in collisions with the gas → $T_e \gg kT$

  Acceleration in E field and friction lead to a constant v_D at given E

  But $\mu \propto \tau \propto 1/\sigma(|\vec{E}|)$ not constant!!

  Example: Ar/CH_4 (90:10), v_D = 3-5 cm/μs (saturating with E)

Drift velocity of electrons

in different gases, at normal conditions:

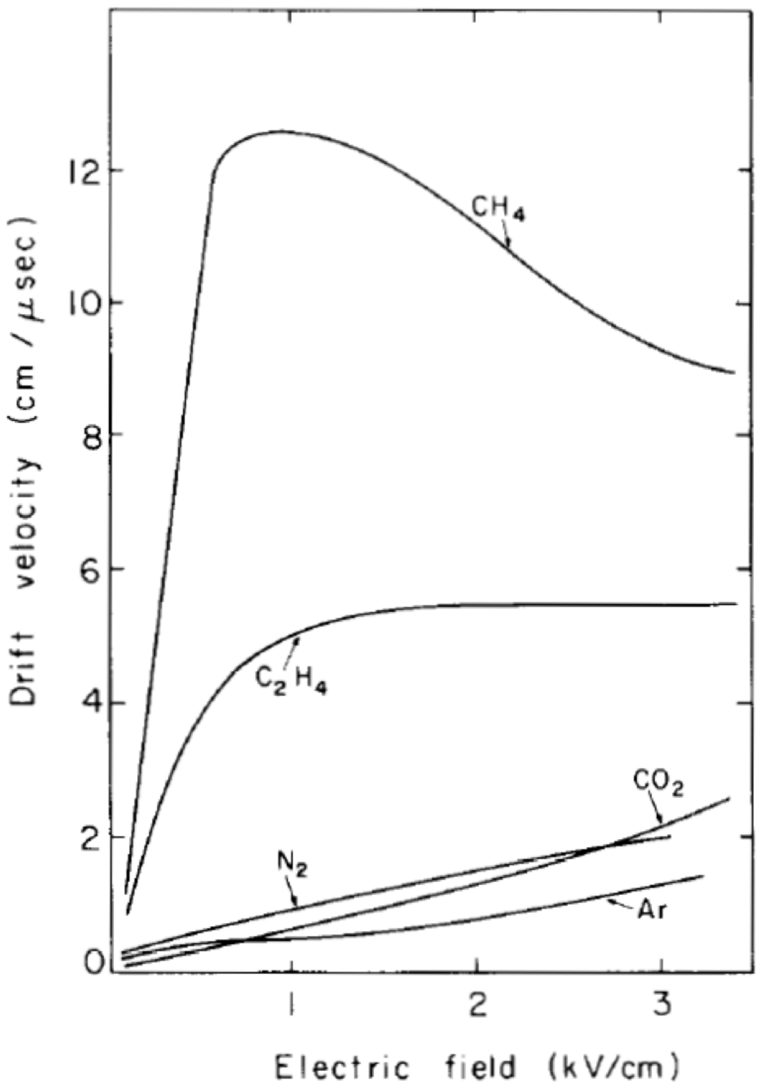

Use gas mixture to obtain constant $\vec{v}_D$
Important for applications using the drift time to get a spatial information

$$x = |\vec{v}_D| \cdot t$$

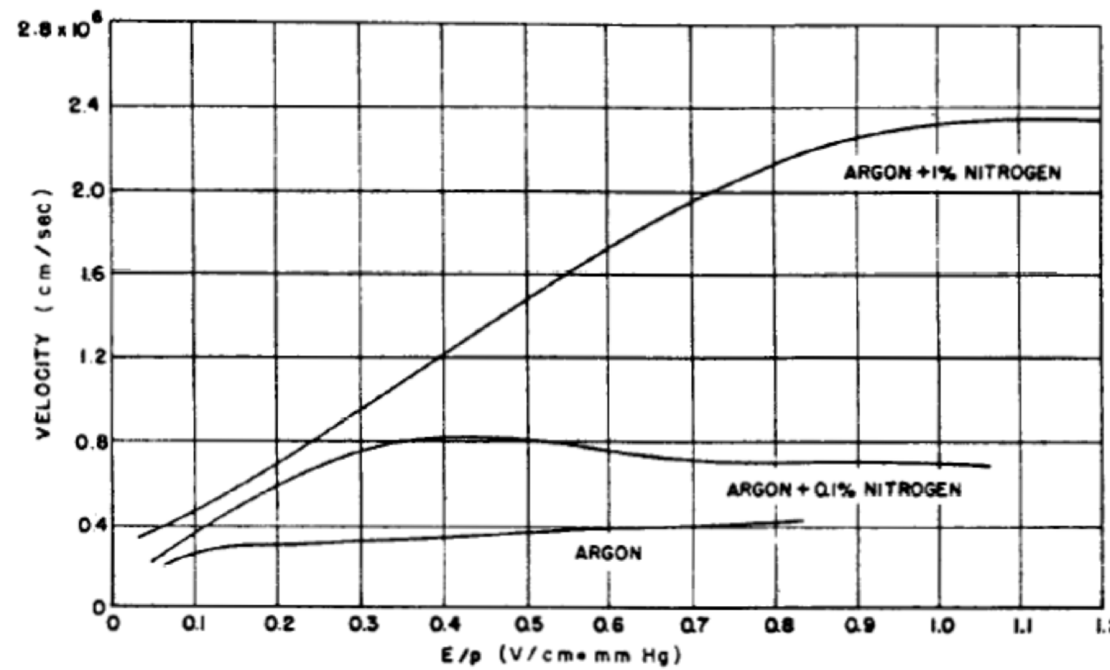

E-Field/pressure

Drift velocity of electrons

Argon-isobutane mixtures:

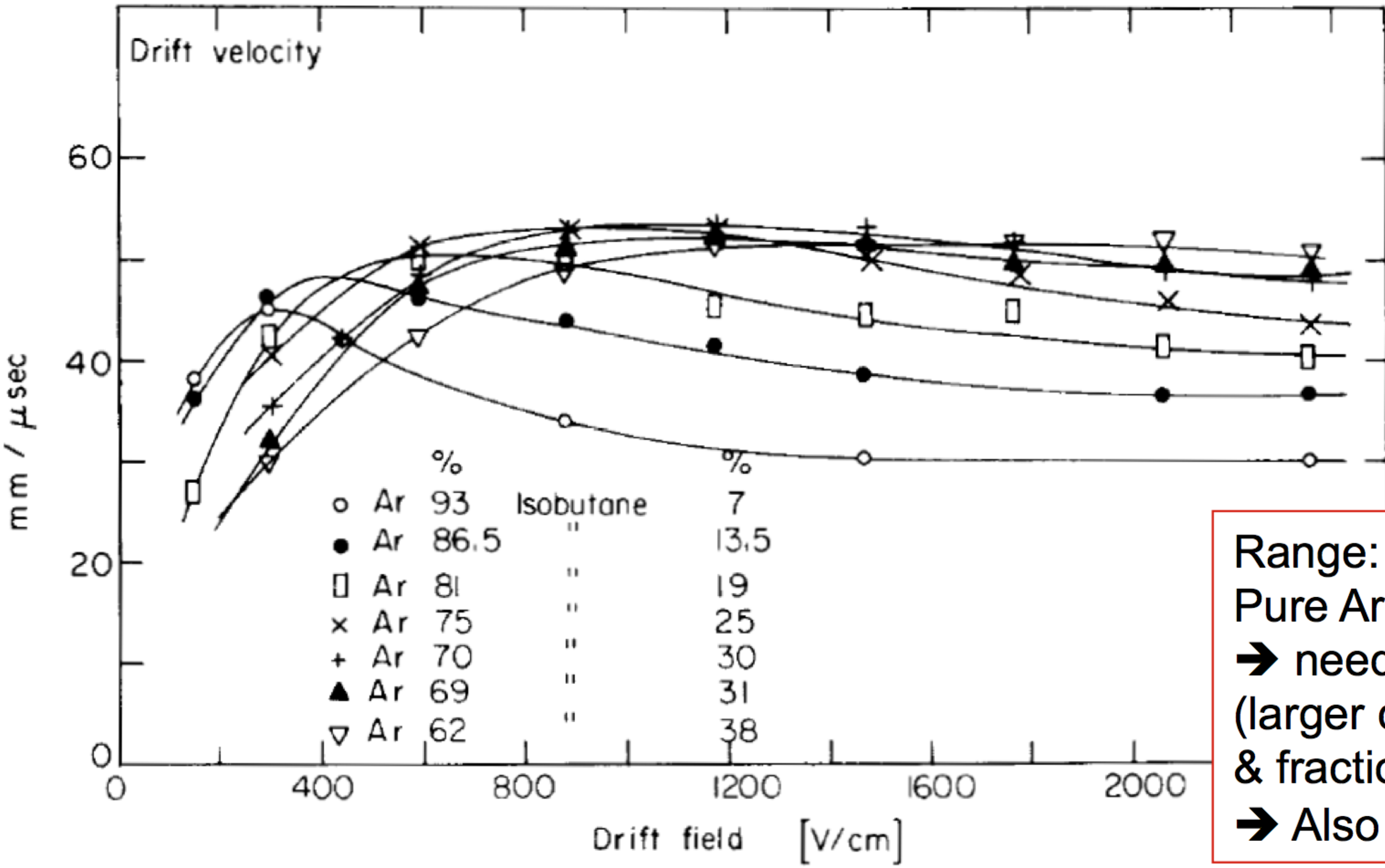

Range: few 10 mm/μs
Pure Ar : ~10 mm/μs
➔ need quenching gas
(larger cross-sections
& fractional energy loss)
➔ Also less diffusion

Diffusion in electric fields

Drift in direction of E-field is superimposed to statistical diffusion

Extra velocity influences the longitudinal diffusion. The transversal diffusion is not affected

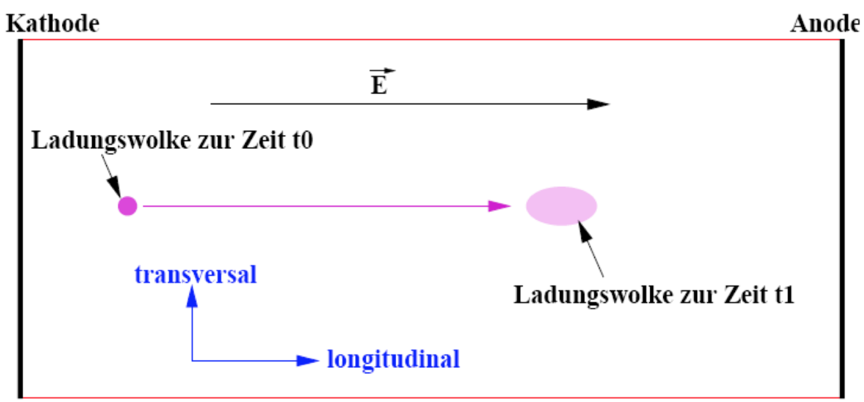

The E-field reduces the longitudinal diffusion

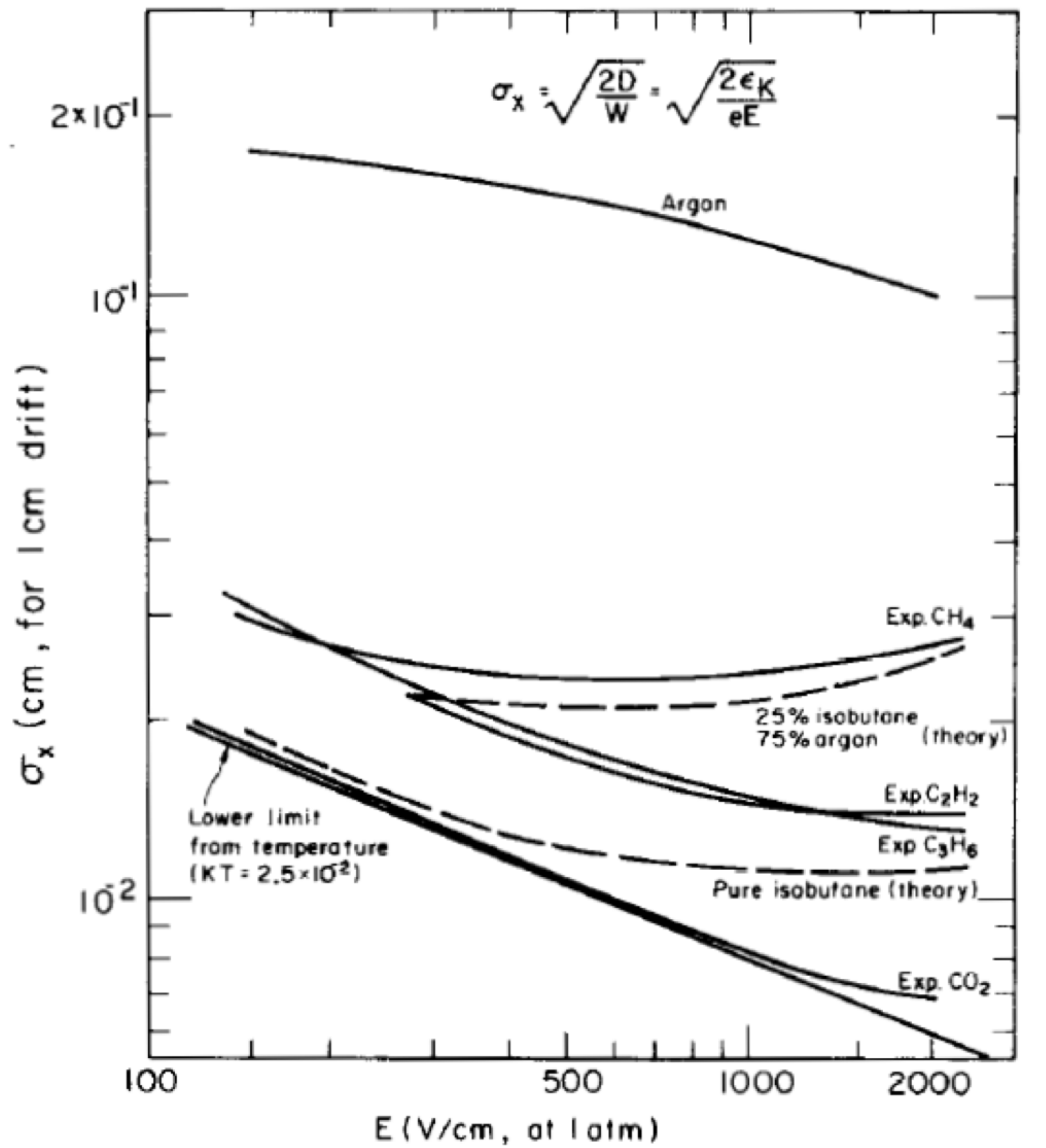

Diffusion in magnetic field

Different effects on longitudinal and transverse diffusion.

No Lorentz force ALONG the direction of the B-field

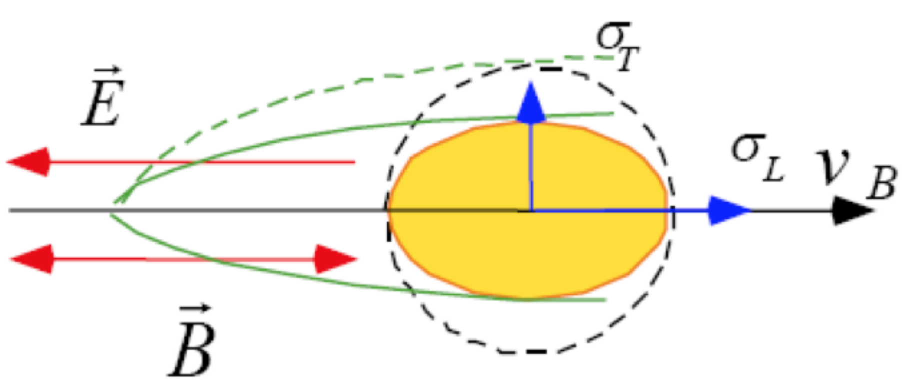

The B-field can substantially reduce the diffusion transversal to its direction

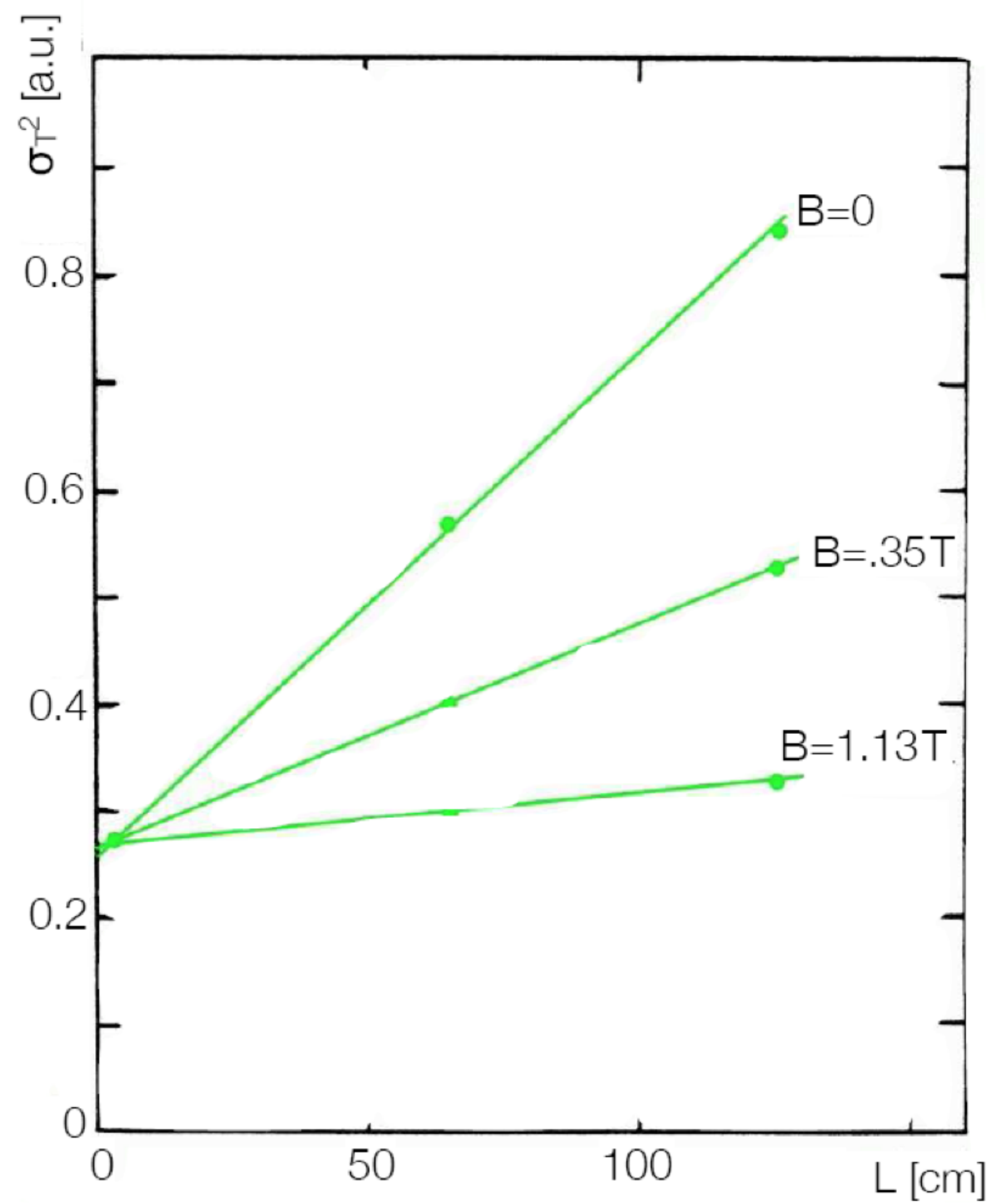

Charge transport: exact solution

For a full and exact solution, need to solve the transport equation for electron density distribution $f(t, \vec{r}, \vec{v})$

$$\frac{\partial f}{\partial t} + \vec{v}\frac{\partial}{\partial \vec{r}} f + \frac{\partial}{\partial \vec{v}}\left(\frac{e\vec{E}}{m} + \vec{\omega}\times\vec{v}\right) f = Q(t)$$

diffusion external forces stochastic collision term

Typically solved numerically, with codes like Magboltz & Garfield:

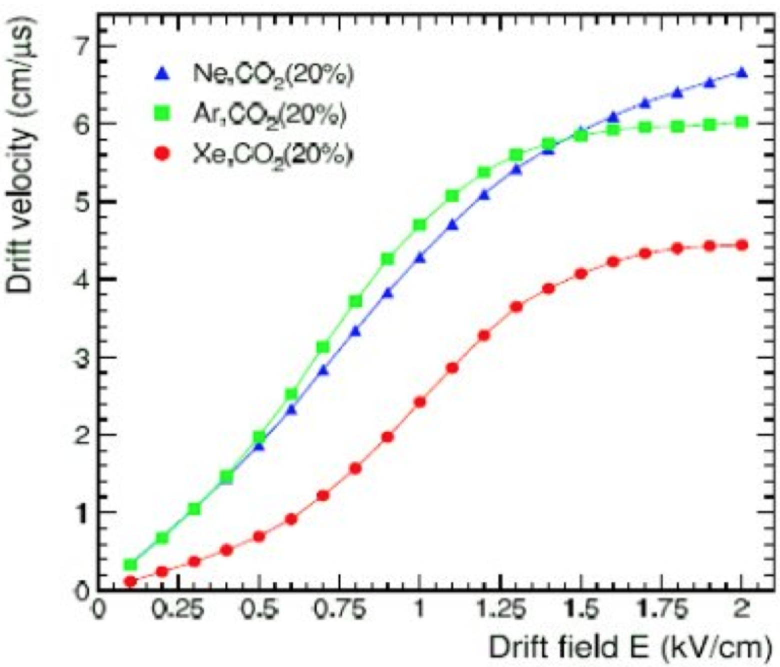

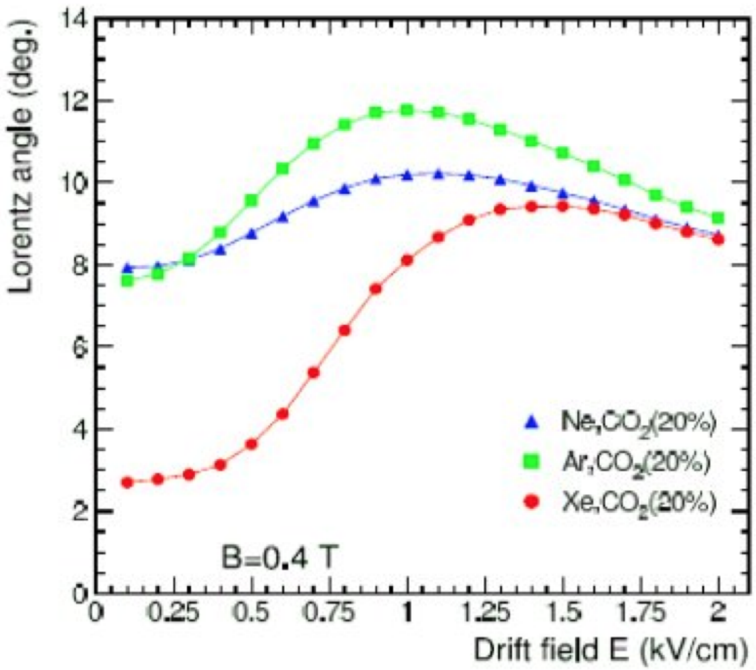

Lorentz angle: angle between E-field and drift velocity of electrons if B not perpendicular to E

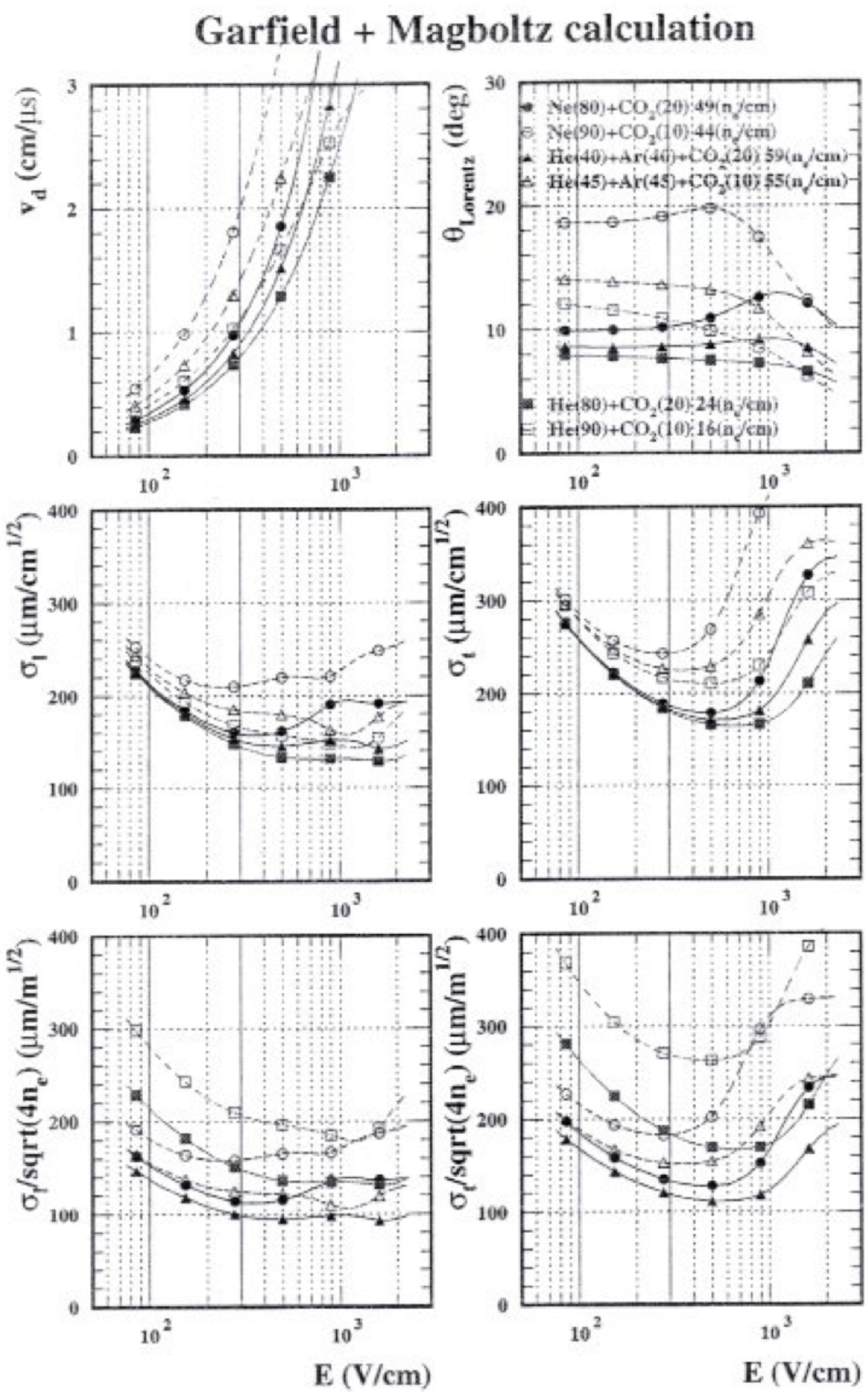

Drift velocity (top left), Lorentz angle (top right), longitudinal and transverse diffusion constants (middle) and longitudinal and transverse diffusion constants normalized to the square root of the number of charge carriers (bottom) for different mixtures of noble gas and CO_2.

Lorentz angle: angle between E-field and drift velocity of electrons in presence of B not $\perp$ to E

Gaseous detectors: Signal generation

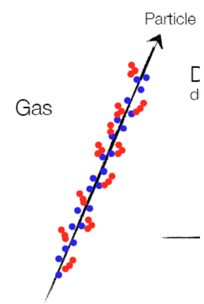

~30 eV per e-ion pair

1. **Ionization in gas**

2. **Charge transport in gas**
   a) Diffusion
   b) Electron and ion mobility
   c) Drift velocity

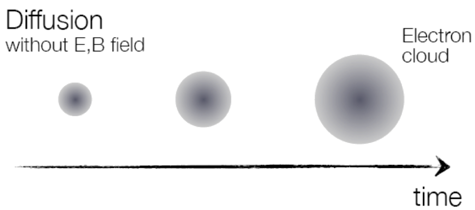

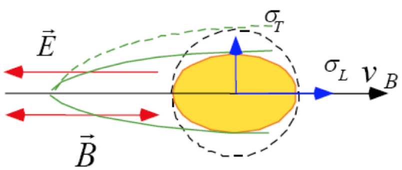

$$\vec{v}_D = \mu \cdot \vec{E}$$

$$x = |\vec{v}_D| \cdot t$$

3. **Loss of electrons**

4. Charge multiplication / gas amplification

Loss of electrons

Electrons might be lost during the drift via:

- **Recombination** of ions and electrons

  Depends on number of charge carriers and recombination coefficient. Generally not too significant

- **Electron attachment**:
  - electro-negative gas molecules (O_2, Freon, …) bind electrons:

    $e^- + M \rightarrow M^-$ for $T_e \approx 1$ eV or $e^- + XY \rightarrow X + Y^-$
  - electron attachment coefficient h is strongly energy dependent (Ramsauer effect)
  - Example O_2: $h = 10^{-4}$ at 1 eV. Collisions for electrons/second: 10^{11}

    typical drift time of electrons: 10^{-6} s

    Fraction lost: $X_{loss} = 10^{-4}\ 10^{11}\ s^{-1}\ 10^{-6}\ s\ p = 10\ p$

    $X_{loss} < 1\% \rightarrow p = 10^{-3} \rightarrow$ less than 1‰ in gas mixture!
  - Certain quencher gases such as $C0_2$ enhance the effect of O_2 such that 10 ppm of O_2 can lead to 10% loss within 10 μs

Gaseous detectors: Signal generation

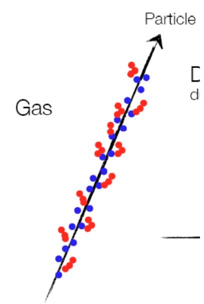

~30 eV per e-ion pair

1. Ionization in gas

2. Charge transport in gas

a) Diffusion

b) Electron and ion mobility

c) Drift velocity

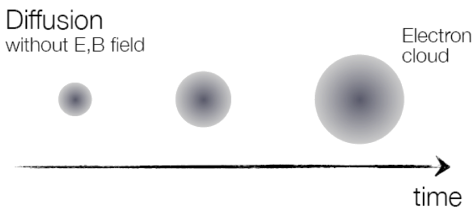

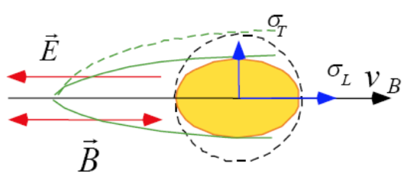

$$\vec{v}_D = \mu \cdot \vec{E} \qquad x = |\vec{v}_D| \cdot t$$

3. Loss of electrons

$$e^- + M \rightarrow M^- \quad \text{or} \quad e^- + XY \rightarrow X + Y^-$$

4. Charge multiplication / gas amplification

Gaseous detector types

A) Ionization chamber

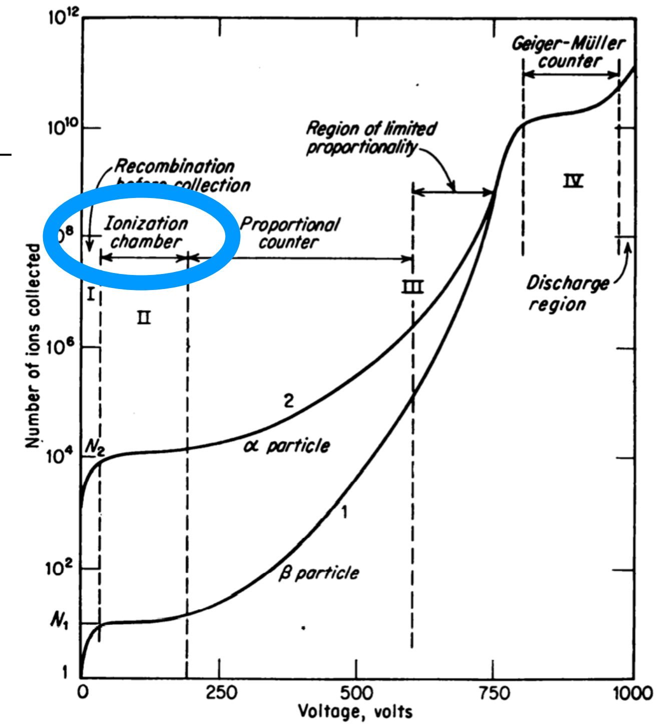

FIG. 2-2. Pulse-height versus applied-voltage curves to illustrate ionization, proportional, and Geiger-Müller regions of operation.

B) Proportional counter

- Multiwire proportional chambers

C) Drift chambers

- Cylindrical wire chambers
- Jet drift chambers

D) Time projection chambers

Ionization chamber

No gas gain: ionization charges move in electric field and induce a signal on the electrodes

Here: planar geometry

2 electrodes → parallel plate capacitor

Free charge q moves: electric field does work → capacitor is charged

$$q\vec{\nabla}\Phi\cdot d\vec{x} = dq_i\cdot U_0$$

leads to induced current:

$$I_{ind} = \frac{q}{U_0}\vec{\nabla}\Phi\cdot\vec{v}_D$$

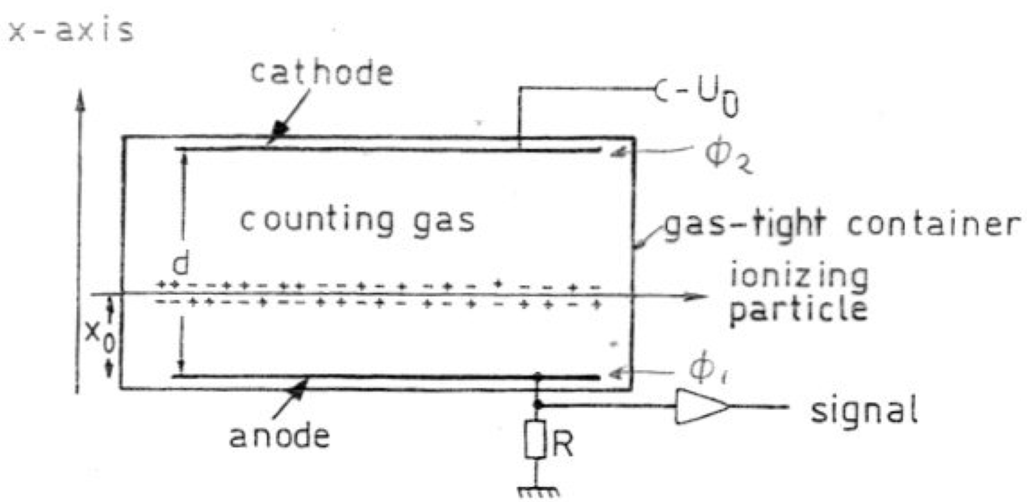

Where:

$$\vec{E} = -\vec{\nabla}\Phi \qquad U_0 = \phi_1 - \phi_2$$

Ionization chamber

- Current is constant while the charge is drifting
- Total induced signal (charge) is independent on x
- Signal induced by electrons:

$$\Delta q_- = \frac{N_e}{U_0}(\phi(x_0) - \phi_1)$$

- Signal induced by ions:

$$\Delta q_- = -\frac{N_e}{U_0}(\phi(x_0) - \phi_2)$$

- $|N_{ion}| = |N_e|$ → total $\Delta q = \Delta q_- + \Delta q_+ = N_e$
- Remember: $\mu_+ = 10^{-3} \ldots 10^{-2}\ \mu_-$ (velocity $w_+ = 10^{-3} \ldots 10^{-2}\ w_-$)

  → induced current and charge for parallel plate case. Ratio between mobilities reduced for purpose of illustration

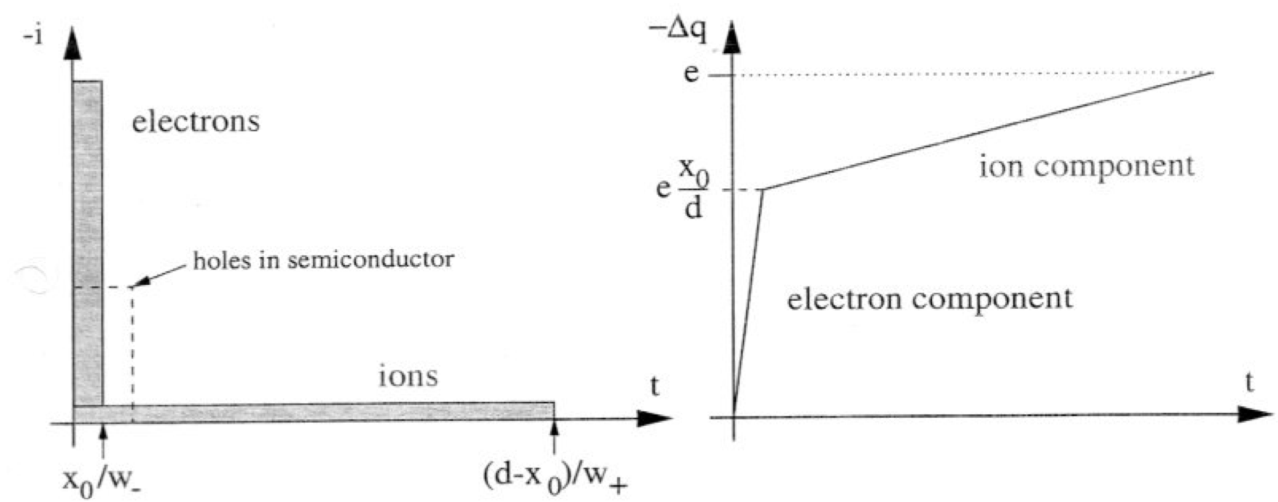

Ionization chamber: pulse shape

Signal generated during drift of charges:

- Induced current ends when the charges reach the electrode
- Induced charge becomes constant (tot el. N_e)
- Signal shape by differentiation (speed of readout) → suppresses slow ion component

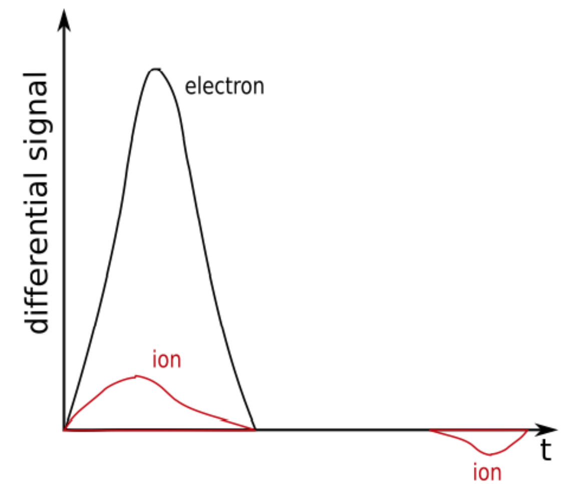

Change in potential $dU = dQ/C$

Typical **time constant** of power supply (+cables ..)

$RC \gg \Delta t^{-}, \Delta t^{+}$ (long!)

Usually some electronic signal shaping is needed

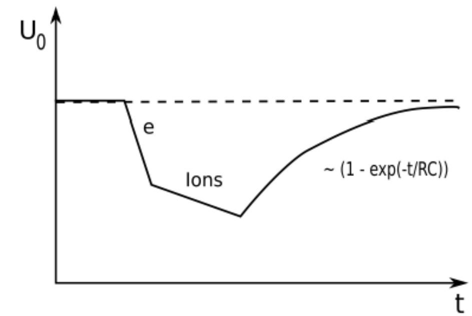

Signal shaping by RC-filter:

Choose it such that $\Delta t^{-} \ll RC \ll \Delta t^{+}$ → damps ion component

$$\Delta U = \Delta U^{-} + \Delta U^{+} = \frac{\Delta Q^{-}}{C} + \frac{\Delta Q^{+}}{C}$$

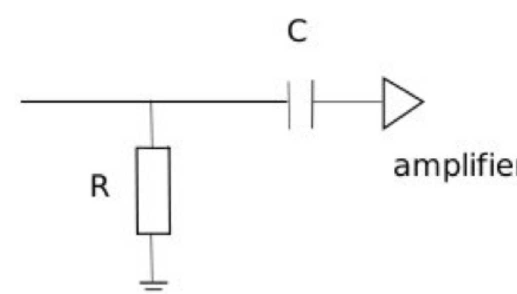

ΔQ= charge induced in the anode by electrons and ions for total n. of ionizations N_e

Ionization chamber: general difficulty

Signals in ionization chambers are generally VERY SMALL

Example: 1 MeV particle stops in gas

$$
\begin{aligned}
N_e &\simeq \frac{10^6\ \text{eV}}{35\ \text{eV}} \simeq 3 \cdot 10^4 \\
C &\simeq 100\ \text{pF} \\
\Rightarrow \Delta U_{max} &= \frac{3 \cdot 10^4 \cdot 1.6 \cdot 10^{-19}\ \text{C}}{10^{-10}\ \text{F}} \\
&= 4.6 \cdot 10^{-5}\ \text{V}
\end{aligned}
$$

They need very sensitive, low-noise pre-amplifiers

Ionization chamber: examples

- Dosimeter for ionization

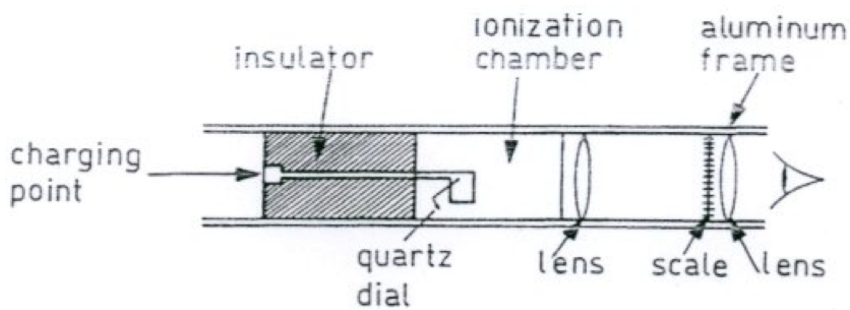

Construction of an ionization pocket dosimeter

- cylindrical capacitor filled with air
- initially charged to potential U_0
- ionization continuously discharges capacitor
- reduction of potential ΔU is measure for integrated absorbed dose (view e.g. via electrometer)

- Nuclear physics experiments, with energies of 10-100 MeV

  Measure the energy deposit of charge particle, it should be highly ionizing or even stop

  Combination of E and ΔE measurement → particle identification (nuclei)

Ionization chamber: MUSIC II - GSI

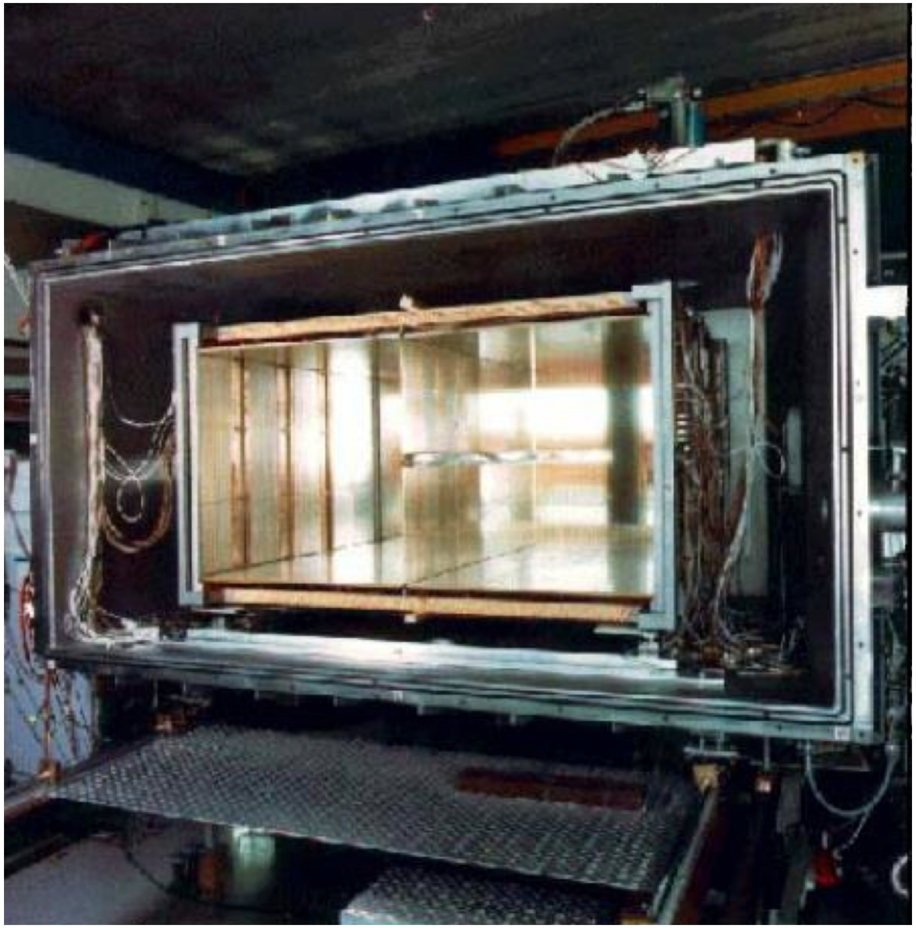

gas	P10 (Ar/Methan 90/10)
pressure	1 atm
active area	102 x 60 cm^2
depth	51 cm
electric field	150 V/cm
potential	9 kV
ionization	70 Z^2 pairs/cm
drift velocity	5 cm/µsec

Multi-sampling ionization chamber to identify the highly charged fragments in nucleus-nucleus collisions at GSI

multiple dE/dx measurements + velocity → charge of the ion

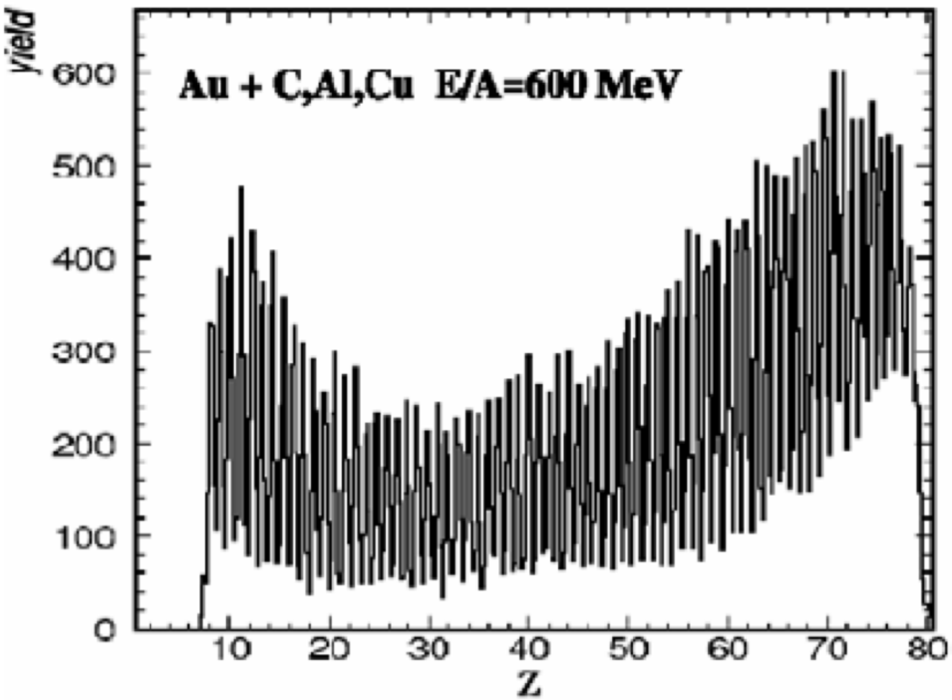

Gaseous detector types

A) Ionization chamber

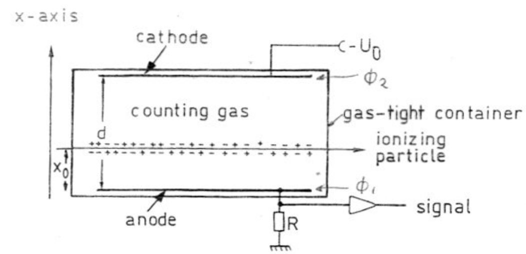

B) Proportional counter

- Multiwire proportional chambers

C) Drift chambers

- Cylindrical wire chambers
- Jet drift chambers

D) Time projection chambers

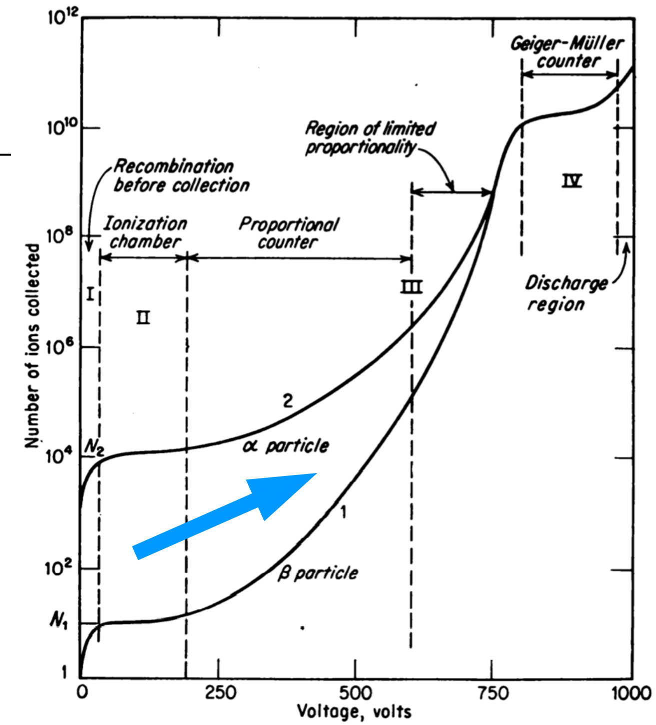

Fig. 2-2. Pulse-height versus applied-voltage curves to illustrate ionization, proportional, and Geiger-Müller regions of operation.

Gaseous detectors: Signal generation

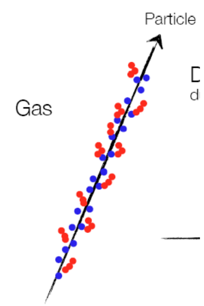

~30 eV per e-ion pair

1. Ionization in gas

2. Charge transport in gas

a) Diffusion

b) Electron and ion mobility

c) Drift velocity

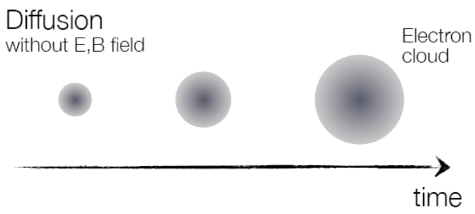

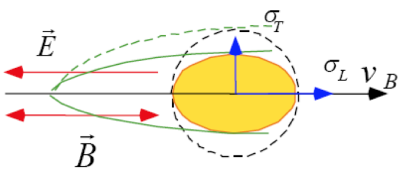

$$\vec{v}_D = \mu \cdot \vec{E} \qquad x = |\vec{v}_D| \cdot t$$

3. Loss of electrons

$$e^- + M \rightarrow M^- \quad \text{or} \quad e^- + XY \rightarrow X + Y^-$$

4. Charge multiplication / gas amplification

Avalanche multiplication

In presence of a very large electric field, the electrons will gain a very large kinetic energy → further ionization

→ Up to avalanche formation

The high mobility of electrons results in liquid-drop-like avalanche, with electrons at the head

Townsend avalanche

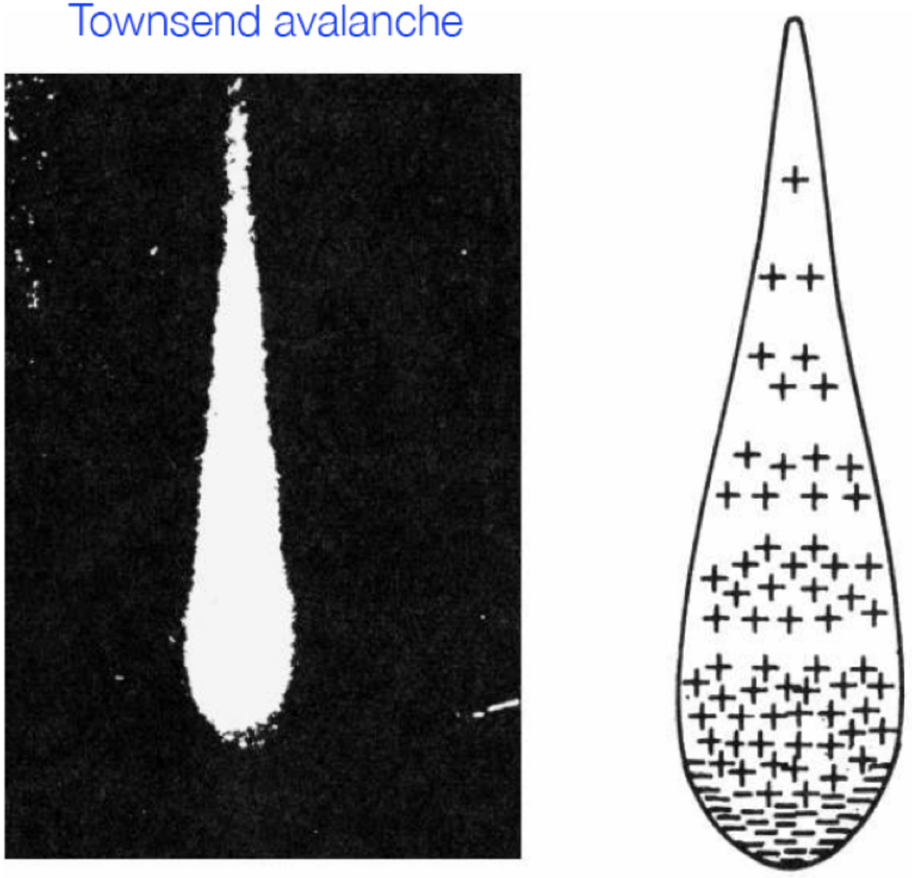

Drop-like shape of an avalanche
Left: cloud chamber picture
Right: hematic view

Mean free path (to secondary ionization): λ_{ion}

Probability of an ionization per unit path length: $\alpha = 1/\lambda_{ion}$

1st Townsend coefficient

n(x) = electrons at location x

$dn = n\,\alpha\cdot dx \quad \rightarrow \quad n = n_0\, e^{\alpha x}$

First Townsend coefficient α

Number of electrons: $n(x) = n_0\, e^{\alpha x}$ ← **GAIN**

Mean free path:

$$\lambda_{ion} = \frac{1}{\alpha} = \frac{1}{n\sigma(T_e)}$$

More precisely: $\alpha = \alpha(x) \rightarrow$

$$G = \frac{n}{n_0} = \exp\left[\int_{x_1}^{x_2} \alpha(x)\,dx\right]$$

Typically 10^4 -10^5, up to 10^6 possible in proportional mode.

Raether limit: $G \approx 10^8 \quad \leftrightarrow \quad \alpha x \approx 20$

Afterwards sparking sets in

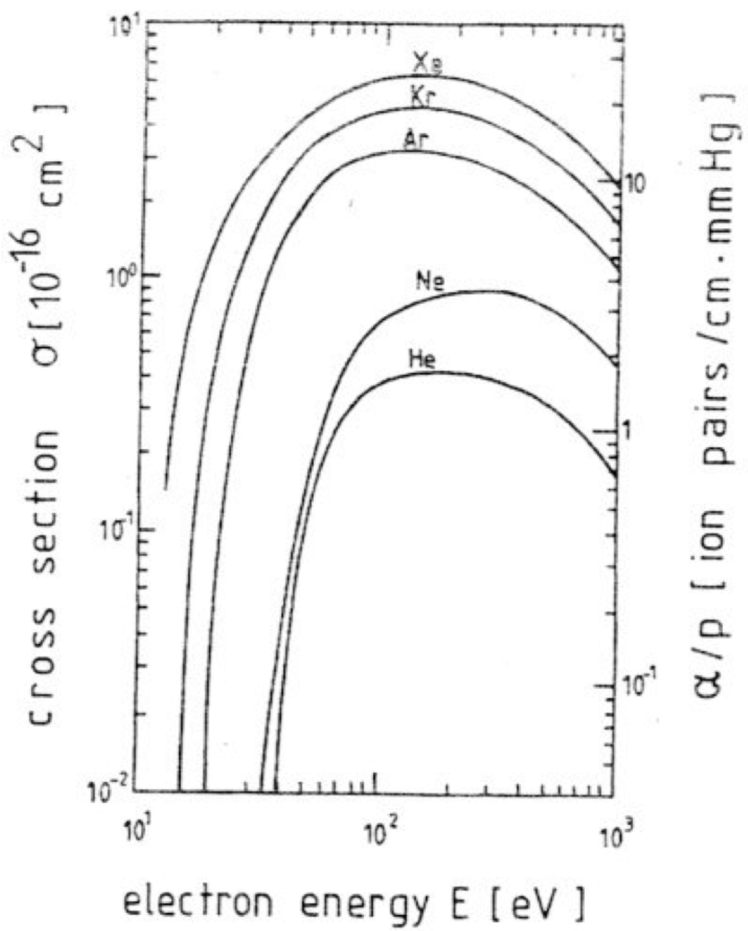

Energy dependence of the cross section for ionization by collision.

Second Townsend coefficient γ

Gas atoms which are excited generate UV photons: they will induce photoelectric effect in the gas and in walls → contribute to the avalanche

$$\gamma = \frac{\text{n. photo effect events}}{\text{n. avalanche electrons}}$$

Gas gain needs to include the photo effect:

$$G_\gamma = G + G(G\gamma) + G(G\gamma)^2 + \ldots = \frac{G}{1-\gamma G}$$

no   one   two   ....

photo effect events

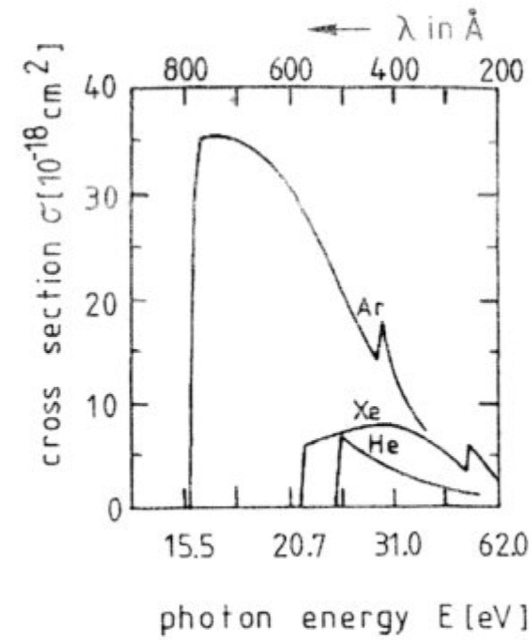

Energy dependence of the cross section for photoionization

Limit: γG → 1 **continuous discharge**, independent from primary ionization

To prevent it: add a quench-gas which absorbs UV photons, leading to excitation and radiationless transitions (e.g. CH_4, C_4H_{10}, CO_2, ...)

Gas amplification: cylindrical geometry

Take cylindrical geometry with anode represented by a very thin wire: E close to wire is very large ($E \propto 1/r$) → electrons gain very large kinetic energy

$$E = \frac{U_0}{r \ln r_0/r_i}$$

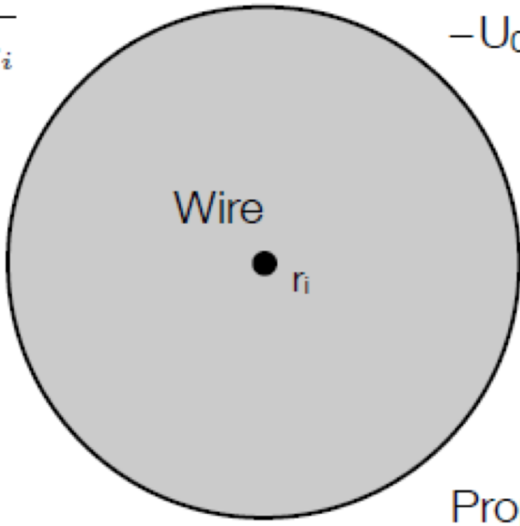

$$\Delta T_e = e \Delta U = e \int_{r_1}^{r_2} E(r)\,dr$$

$$= \frac{eU_0}{\ln \frac{r_o}{r_i}} \int_{r_1}^{r_2} \frac{1}{r}\,dr = eU_0 \frac{\ln \frac{r_2}{r_i}}{\ln \frac{r_o}{r_i}}$$

Gas amplification: cylindrical geometry

- To obtain large E and hence large ΔT_e, use very thin wires ($r_i \approx 10 - 50$ µm)
- Within few wire radii, ΔT_e is large enough or secondary ionization
- Strong increase of E → avalanche formation for $r \to r_i$

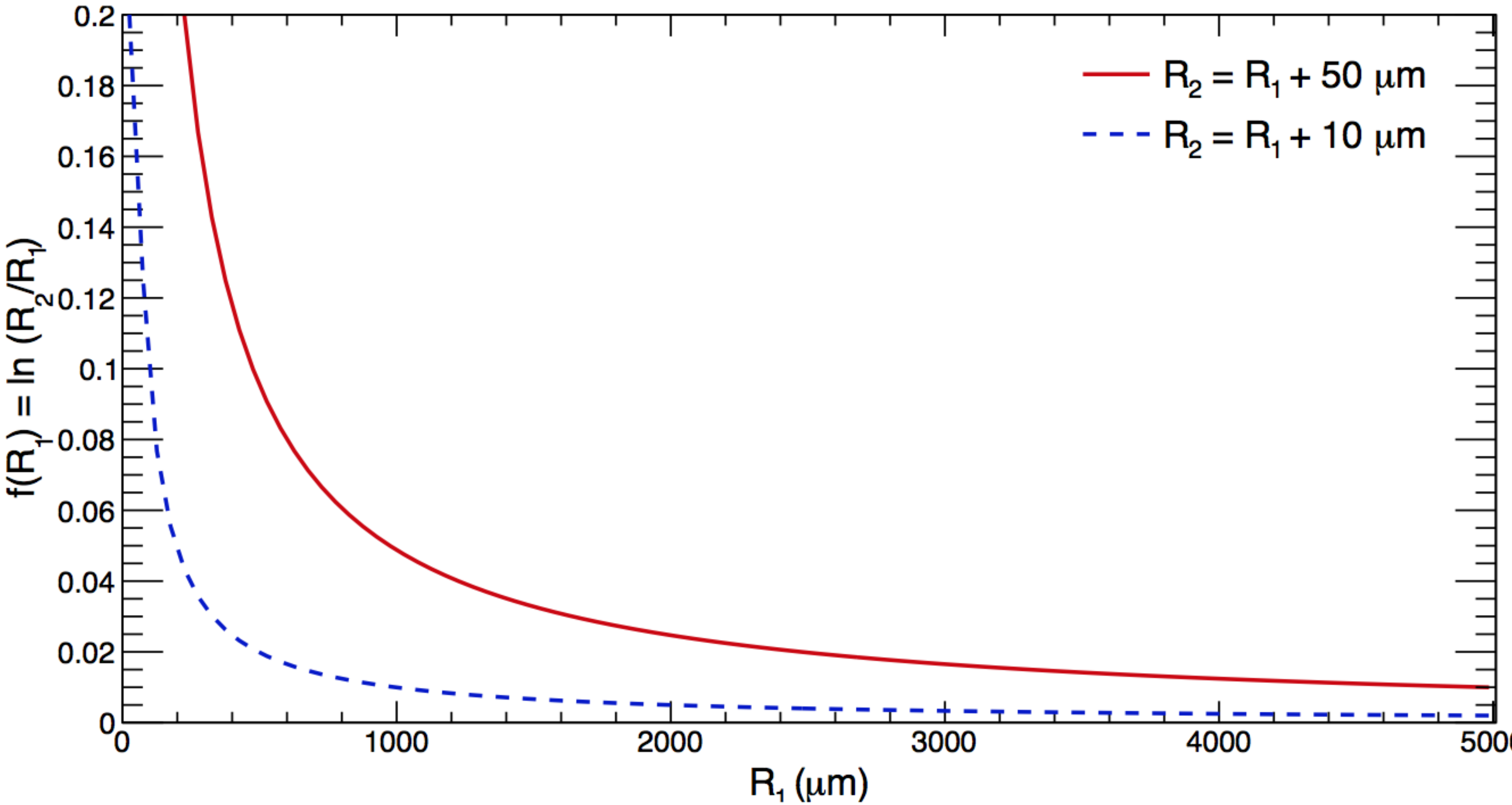

Avalanche formation close to a wire

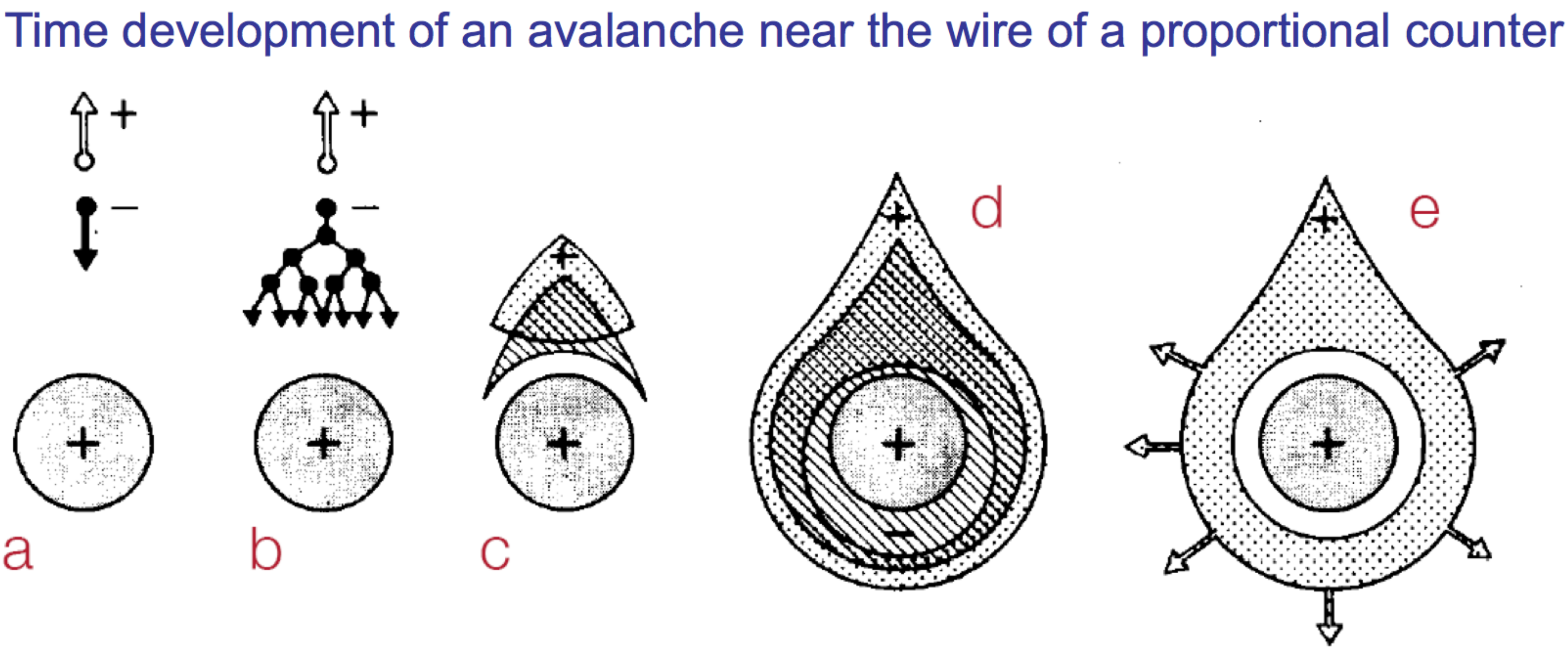

a) a single primary electron proceeds towards the wire anode,
b) in the region of increasingly high field the electron experiences ionizing collisions (avalanche multiplication),
c) electrons and ions are subject to lateral diffusion,
d) a drop-like avalanche develops which surrounds the anode wire,
e) the electrons are quickly collected (~1ns) while the ions begin drifting towards the cathode generating the signal at the electrodes.

Gaseous detectors: Signal generation

1. Ionization in gas

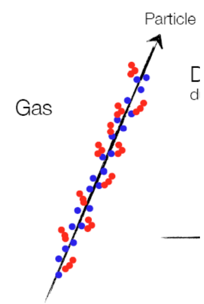

~30 eV per e-ion pair

2. Charge transport in gas

a) Diffusion

b) Electron and ion mobility

c) Drift velocity

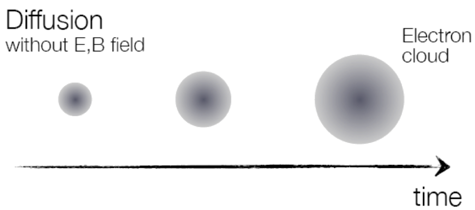

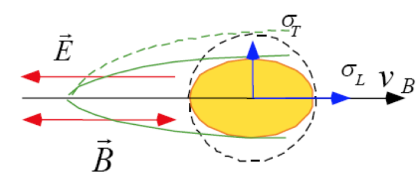

$$\vec{v}_D = \mu \cdot \vec{E} \qquad x = |\vec{v}_D| \cdot t$$

3. Loss of electrons

$$e^- + M \rightarrow M^- \quad \text{or} \quad e^- + XY \rightarrow X + Y^-$$

4. Charge multiplication / gas amplification

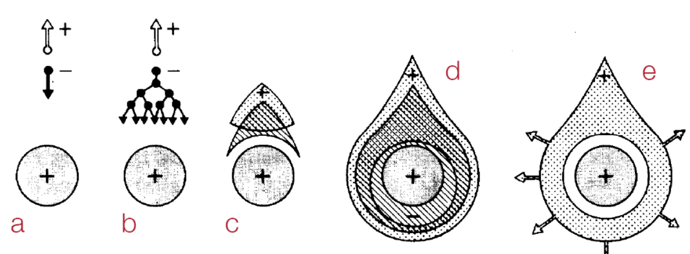

Gaseous detector types

A) Ionization chamber

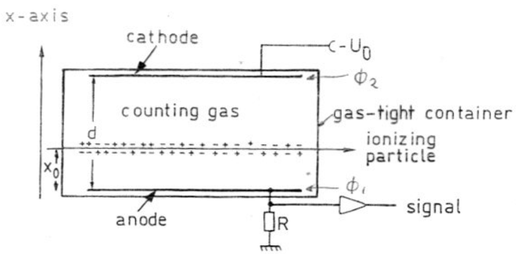

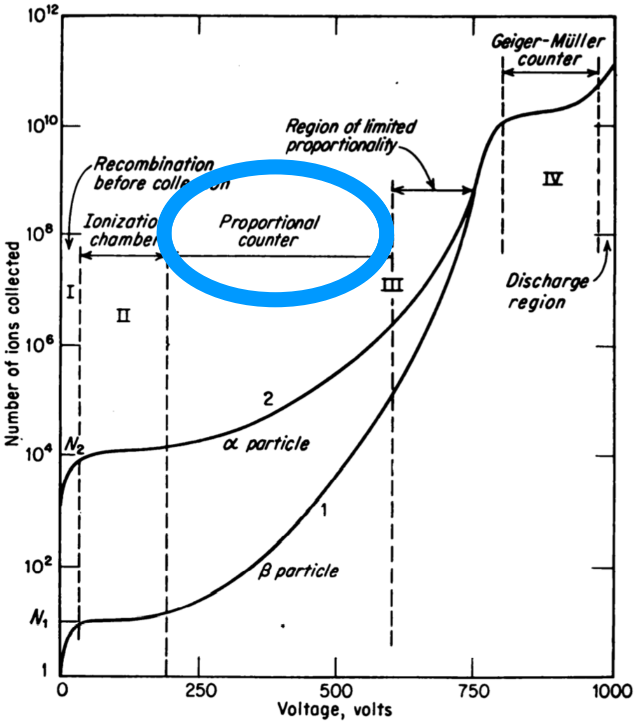

FIG. 2–2. Pulse-height versus applied-voltage curves to illustrate ionization, proportional, and Geiger-Müller regions of operation.

B) Proportional counter

- Multiwire proportional chambers

C) Drift chambers

- Cylindrical wire chambers
- Jet drift chambers

D) Time projection chambers

Proportional counter: cylindrical geometry

Gas amplification:

$$N = A \cdot N_e$$

In the vicinity of the wire:

$$A = \exp \int_{r_0}^{r_i} \alpha(x)\,dx$$

The charge avalanche typically builds up within 20 µm from the wire. Effectively it starts at $r_0 = r_i + k\lambda$, where:

λ = mean free path of electrons (~ µm)

k = number of mean free paths needed for avalanche formation

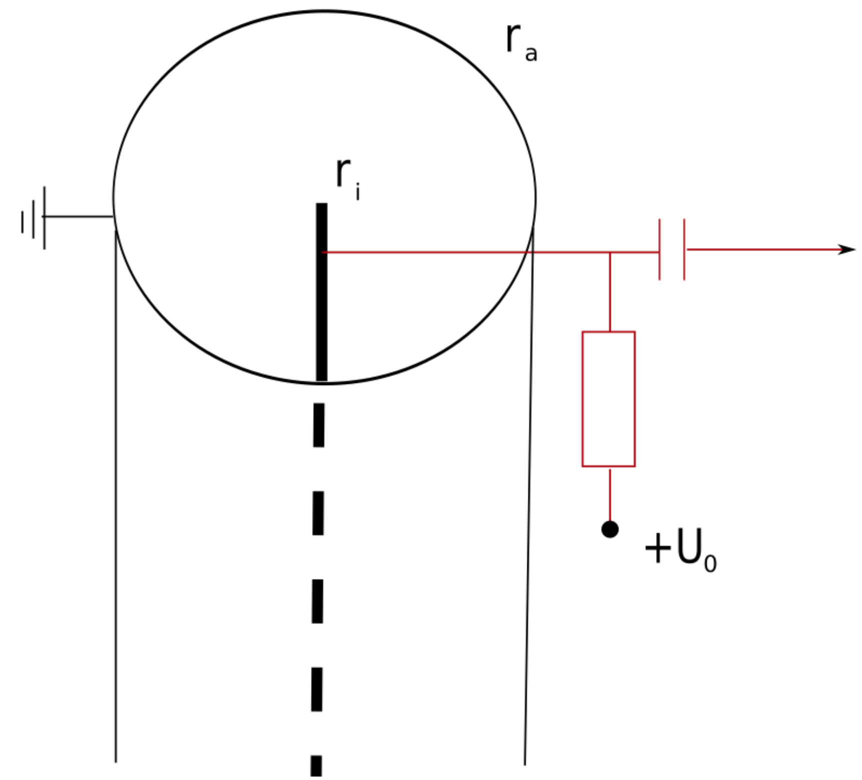

$$\Delta U^- = -\frac{N_e A}{C}\frac{\ln r_0/r_i}{\ln r_a/r_i}$$

$$\Delta U^+ = -\frac{N_e A}{C}\frac{\ln r_a/r_0}{\ln r_a/r_i}$$

Proportional counter: cylindrical geometry

$$\frac{\Delta U^{+}}{\Delta U^{-}} = \frac{\ln r_a / r_0}{\ln r_0 / r_i} = R$$

Typically: r_a = 1 cm, r_i = 30 µm, kλ = 20 µm for Argon at atmospheric pressure

→ R ≃ 10 !

In a proportional counter, the signal at the anode wire is mostly due to the ion drift !!

Signal timing:

- Rise time of electron signal: $\Delta t^{-} = \frac{\ln(r_a/r_i)}{2\mu_{-U_0}} (r_{,}^2 - r_i^2)$ → order of ns
- Ion signal slow, Δt^{+} order of 10 ms

→ differentiate with $R_{diff} \cdot C$

E.g. if $R_{diff} \cdot C \simeq$ 1ns, the time structure of individual ionization clusters can be resolved (see next slide)

Proportional counter

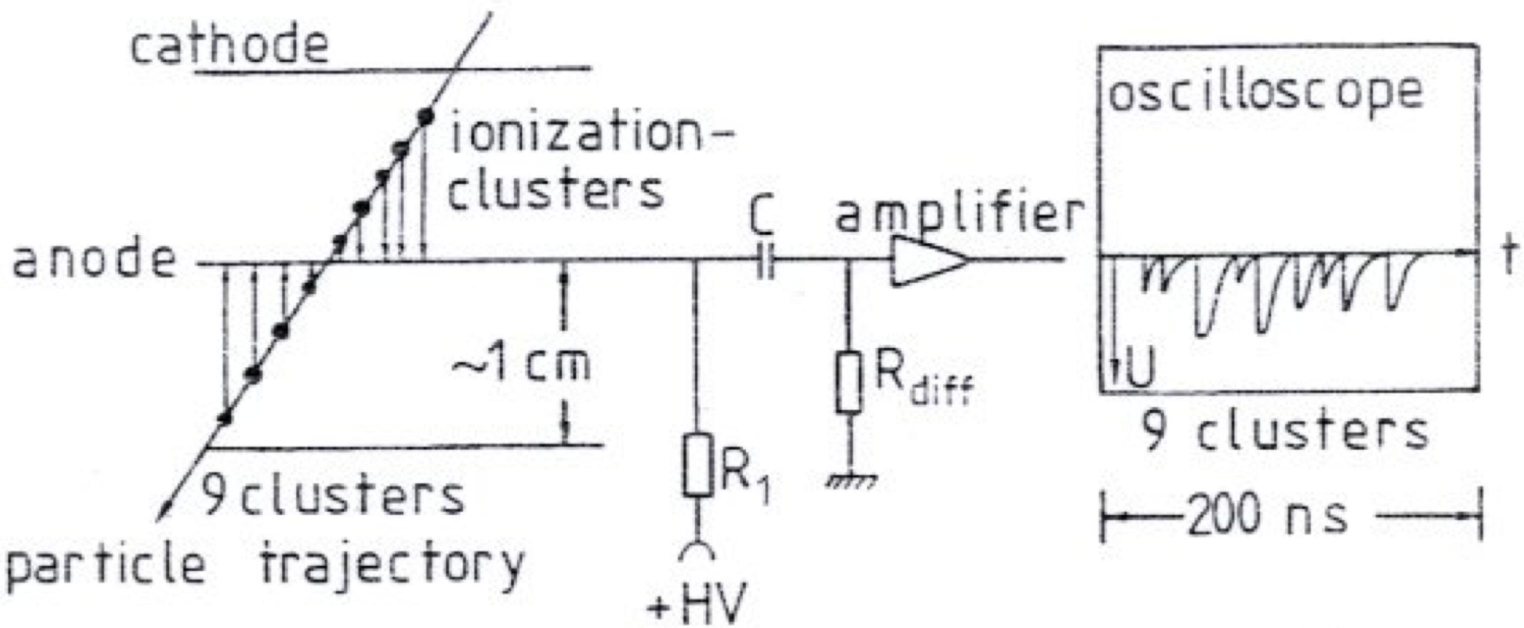

Illustration of the time structure of a signal in the proportional counter

LHCb outer tracker: straw tubes

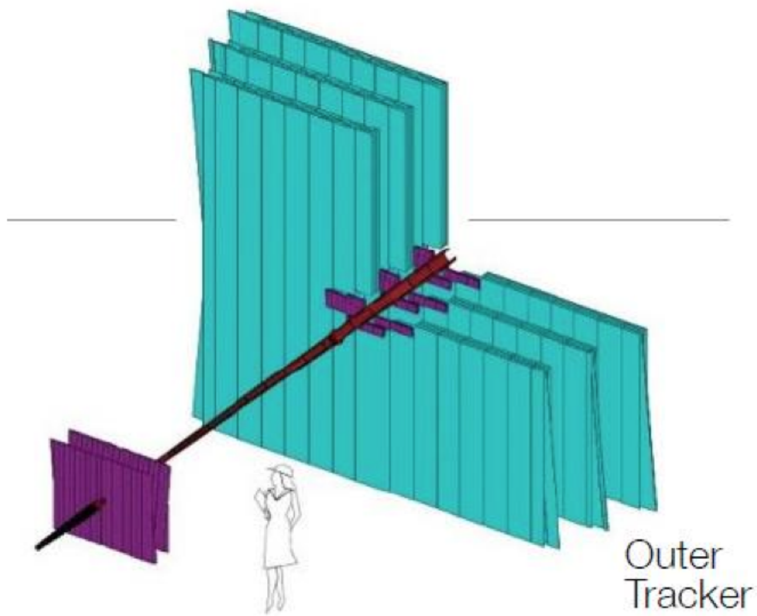

- **double layer of straw tubes**
- **3 chambers with 4 layers (18 modules each)**

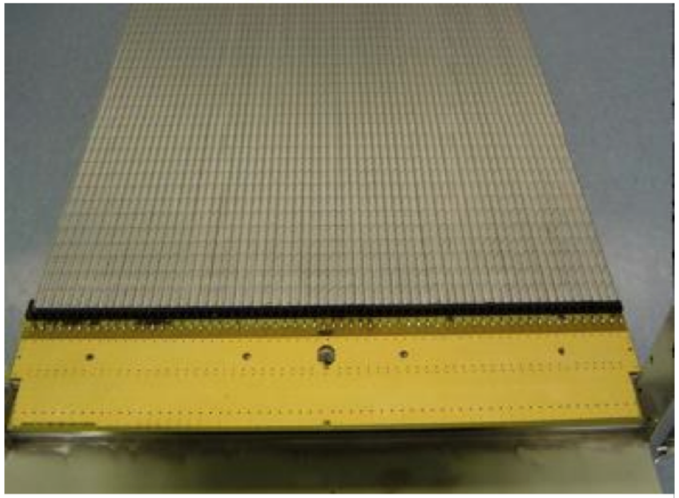

LHCb outer tracker: straw tubes

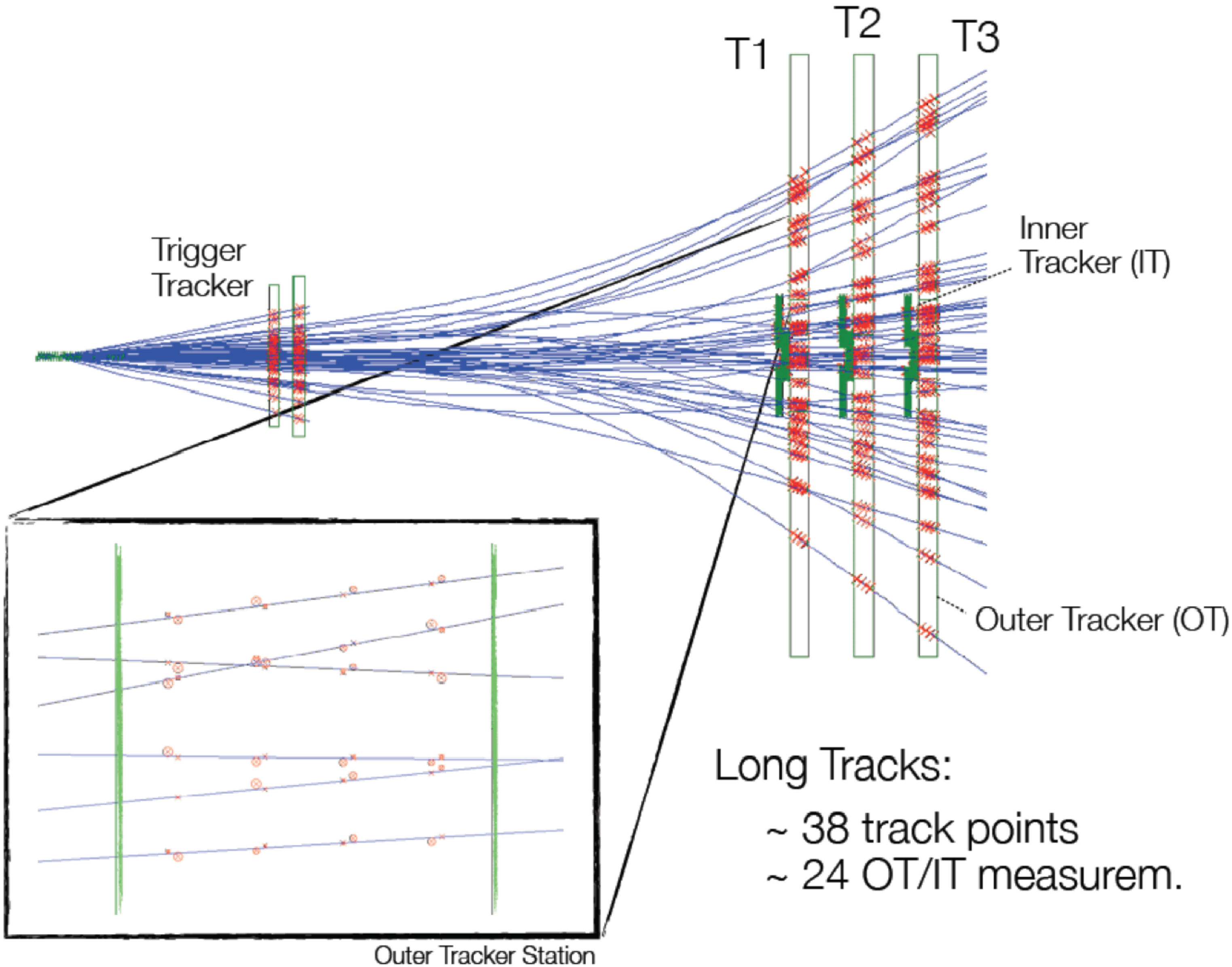

Long Tracks:

~ 38 track points
~ 24 OT/IT measurem.

Gaseous detector types

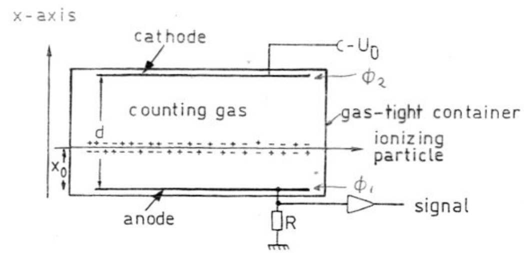

A) Ionization chamber

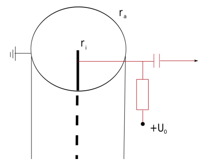

B) Proportional counter

- **Multiwire proportional chambers**

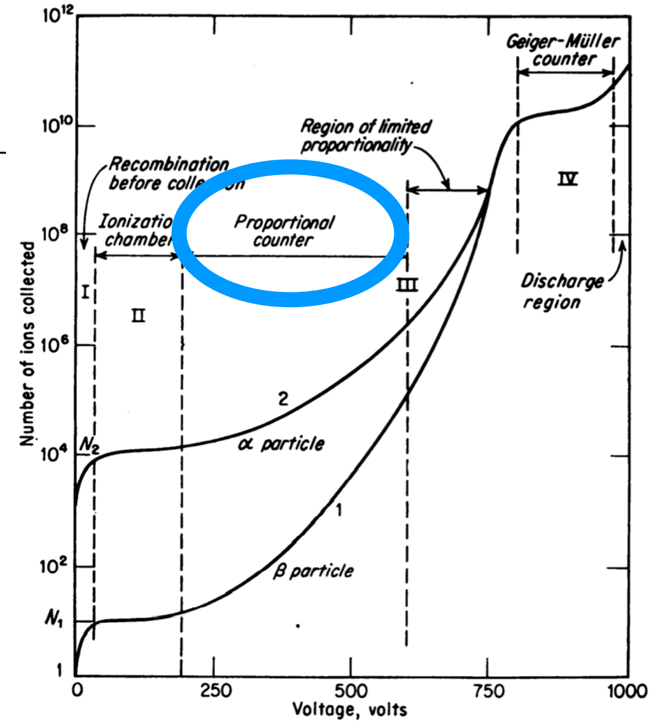

FIG. 2–2. Pulse-height versus applied-voltage curves to illustrate ionization, proportional, and Geiger-Müller regions of operation.

C) Drift chambers

- Cylindrical wire chambers
- Jet drift chambers

D) Time projection chambers

Multi-wire proportional chamber - MWPC

Planar arrangement of proportional counters, without separating walls

G. Charpak at al., NIM 62 (1968) 202

Nobel prize 1992

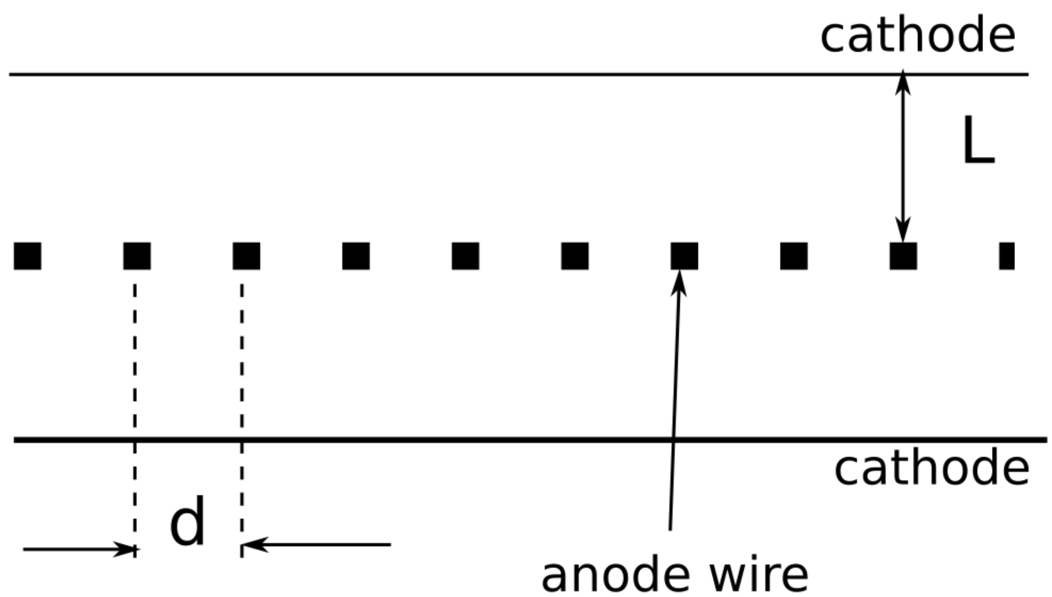

Tracking of charged particles, large area coverage, high rate capability, moderate particle identification capabilities via dE/dx

MWPC: electric field

Typical geometry of electric field lines in MWPC:

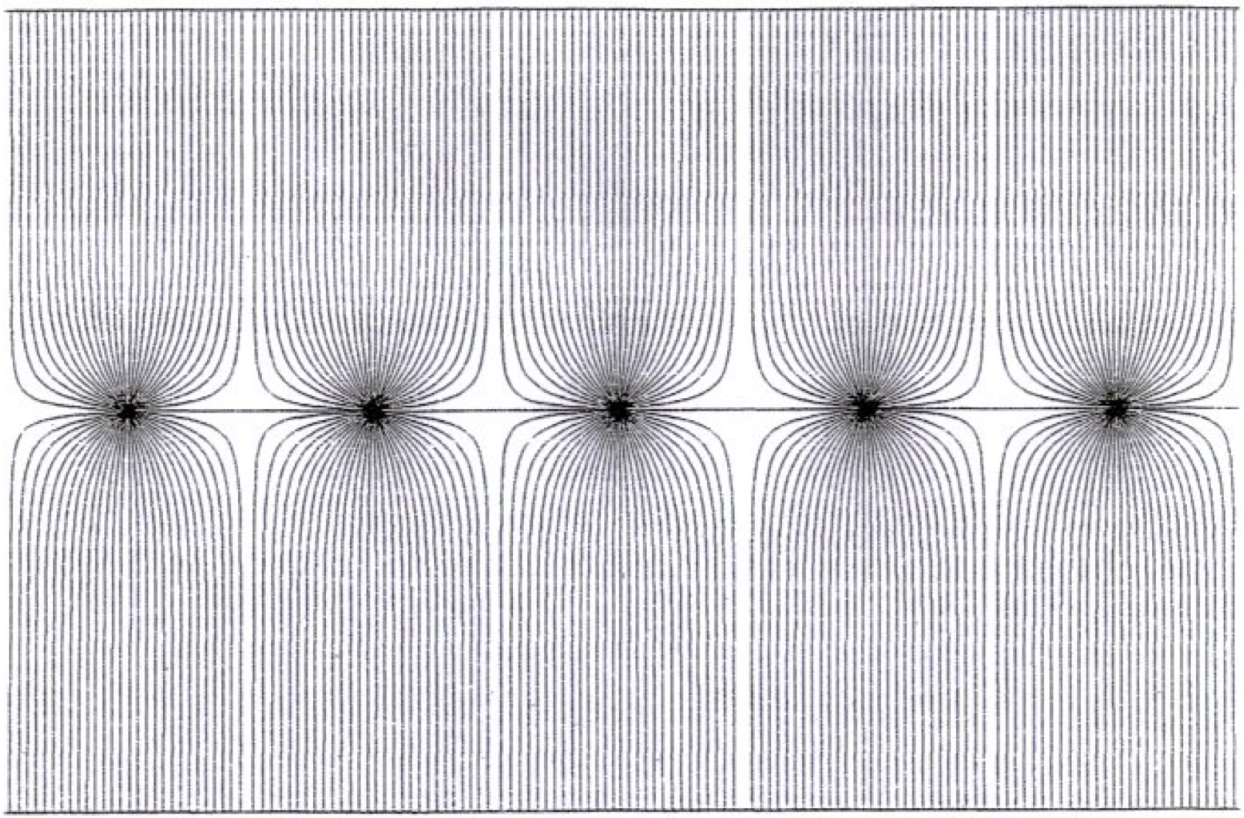

Typical parameters:
d = 2-4 mm
r_i = 15-25 μm
L = 3-6 mm
U_0 = several kV
Total area: many m^2

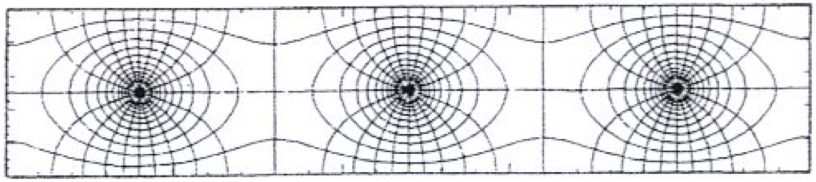

In the vicinity of the anode wires: radial field
Close to the cathodes: homogeneous, as parallel-plate capacitor

MWPC: mechanical precision

Field lines, and equipotential lines

Difficulty evident:

Even small geometric displacements of an individual wire lead to effects on the field quality

Need of high mechanical precision, both for geometry and wire tension (electrostatic effects and gravitational wire sag, see later)

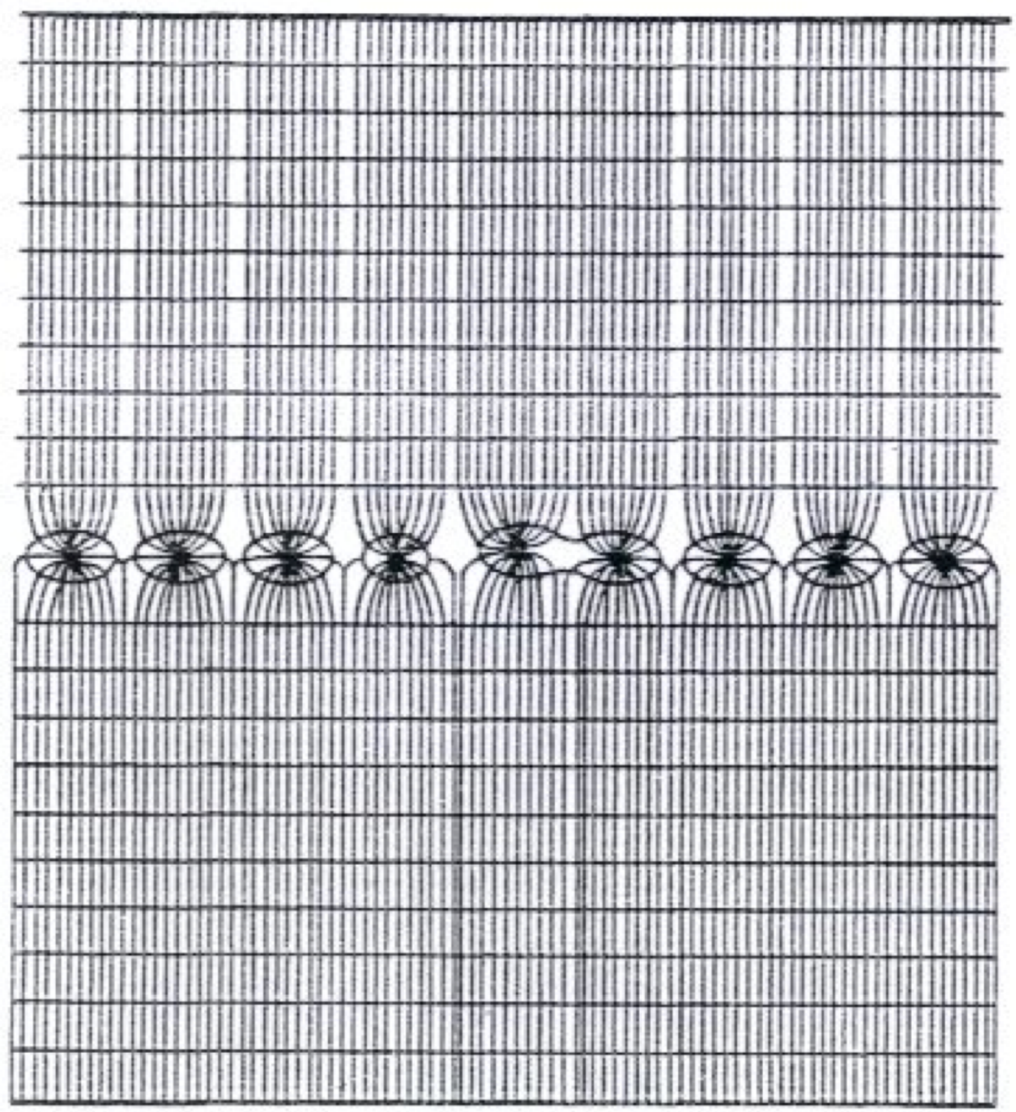

MWPC: signal

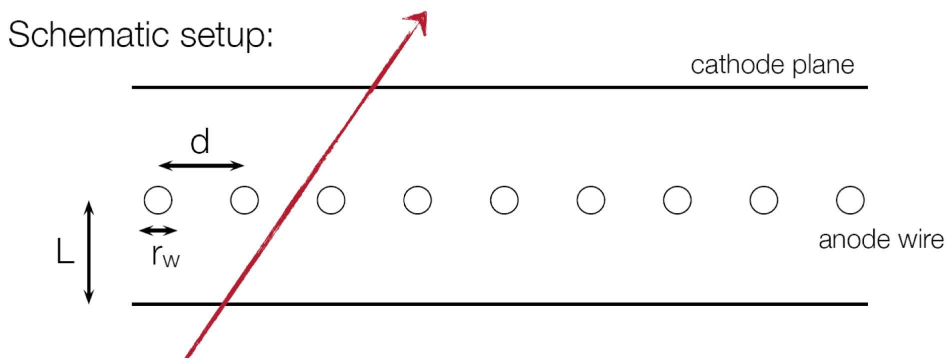

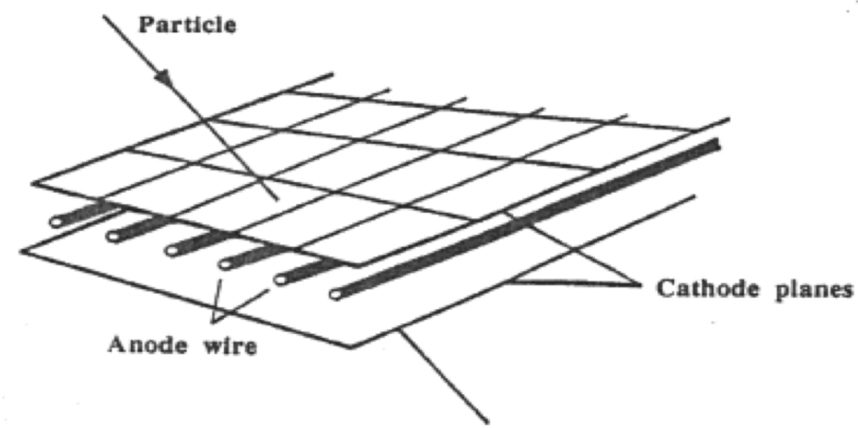

- Electrons from primary and secondary ionization drift to the closest anode wire (signal on 1 wire!)
- In the vicinity of the wire: gas amplification → formation of avalanche Ends when the electrons reach the wire, or when the space charge of positive ions screens the electric field below a critical value
- The signal is generated to electron- and (MOSTLY!) slow ion-drift

MWPC: spatial point resolution

- Perpendicular to wire: since information comes only from closest wire → δx = **d/√12** = e.g. 577 μm for d = 2 mm   not quite so precise!
- Then: segment the cathode in strips: the induced signal is spread over more strips. Using the **center of gravity** of the signal (charge sharing), high precision of 50 – 300 μm can be reached

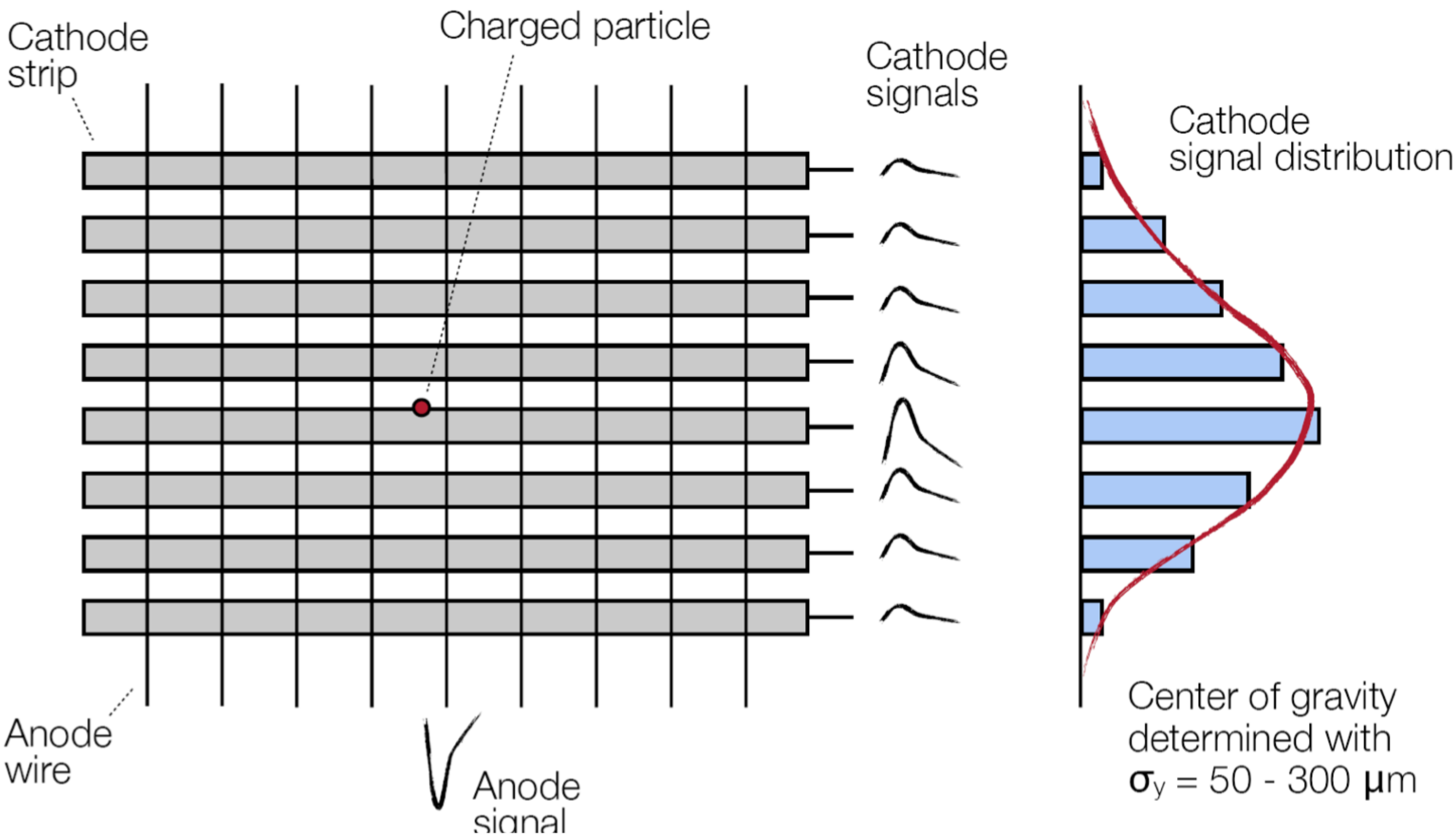

MWPC – resolution of ambiguities

When 2 particles cross the MWPC, with only one orientation of the cathode strips we are left with the ambiguity of the combinations of signals •• ○○

→ 4 possibilities: 2 real, 2 ghosts

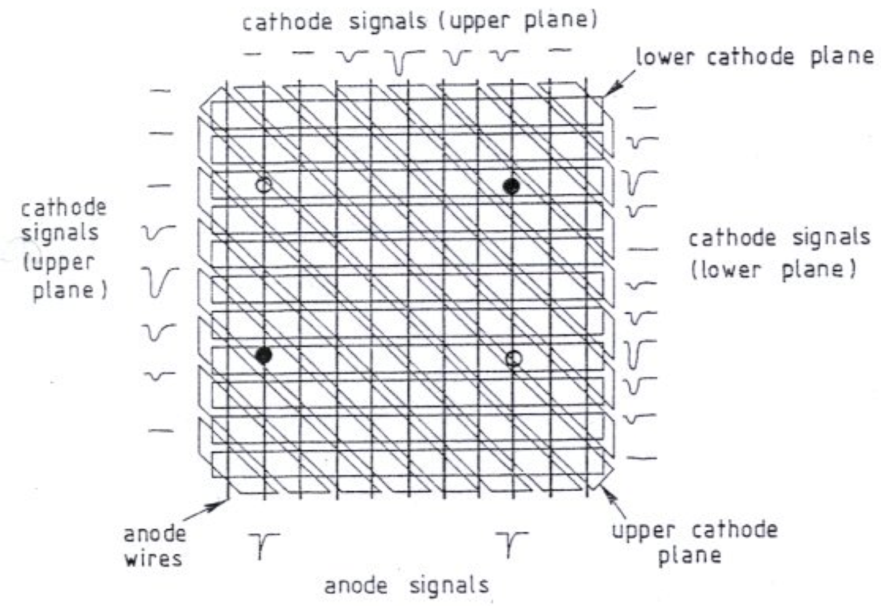

Illustration of the resolution of ambiguities for two particles registered in a multi-wire proportional chamber

Possible solution: use different orientation of strips on the second cathode plane

For high multiplicities and high hit density: segment the **cathode in pads** for a 2-dimensional measurement

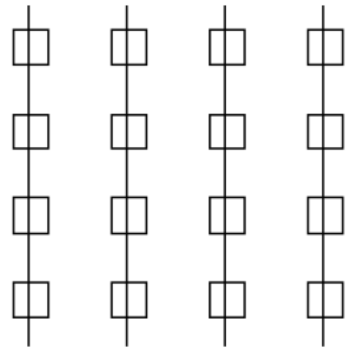

Disadvantage: number of readout channels grows quadratically (expensive!)

MWPC – stability of wire geometry

Can the resolution be improved by mounting the wires closer to each other?

Practical difficulty in stretching wires precisely, closer than 1 mm:

- Electrostatic repulsion between anode wires (particularly for long wires)
  → can lead to "staggering"
  To void this, the wire tension T has to be larger than a critical value T_0 (order of 0.5 N for wires of 1 m and typical chamber geometry)

- For horizontal wires problem of gravity → sag

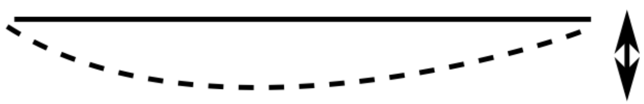

$$f = \frac{\pi r_i^2}{8} \rho g \frac{l^2}{T} = \frac{mlg}{8T}$$

gold-plated W-wire $r_i = 15\ \mu\text{m}$, T as above → $f = 34\ \mu\text{m}$ → visible difference in gain

And remember:

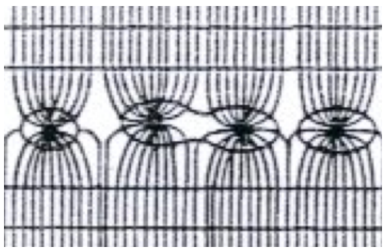

MWPC → straw tube chambers

Some of these troubles are addressed by straw tube chambers: compact assembly of **single-wire proportional chambers**

(see last week, LHCb outer tracker example)

Cylindrical wall = cathode

Aluminized mylar foil

Introduced in the 1990s

Straw diameter: 5-10 mm

Can be operated at overpressure

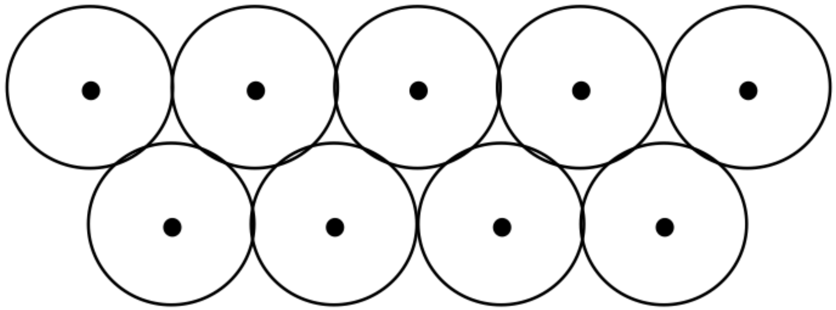

- Further very big advantage: a broken wire affects only one cell!! In a MWPC: large area, if not the entire chamber
- Spatial resolution: down to 160 μm
- Short drift lengths → high rates possible!

  → operation in magnetic field possible without degradation of resolution!

MWPC – wire aging

Avalanche formation can be considered as a micro plasma discharge.

Consequences:

- Formation of radicals, i.e. molecule fragments
- Polymerization yields long chains of molecules
- Polymers may be attached to the electrodes
- Reduction of gas amplification

Important: AVOID unnecessary contaminations!

Harmful are:

- Halogens or halogen compounds
- Silicon compounds
- Carbonates, halocarbons
- Polymers
- Oil, fat ...

Can wires be avoided?

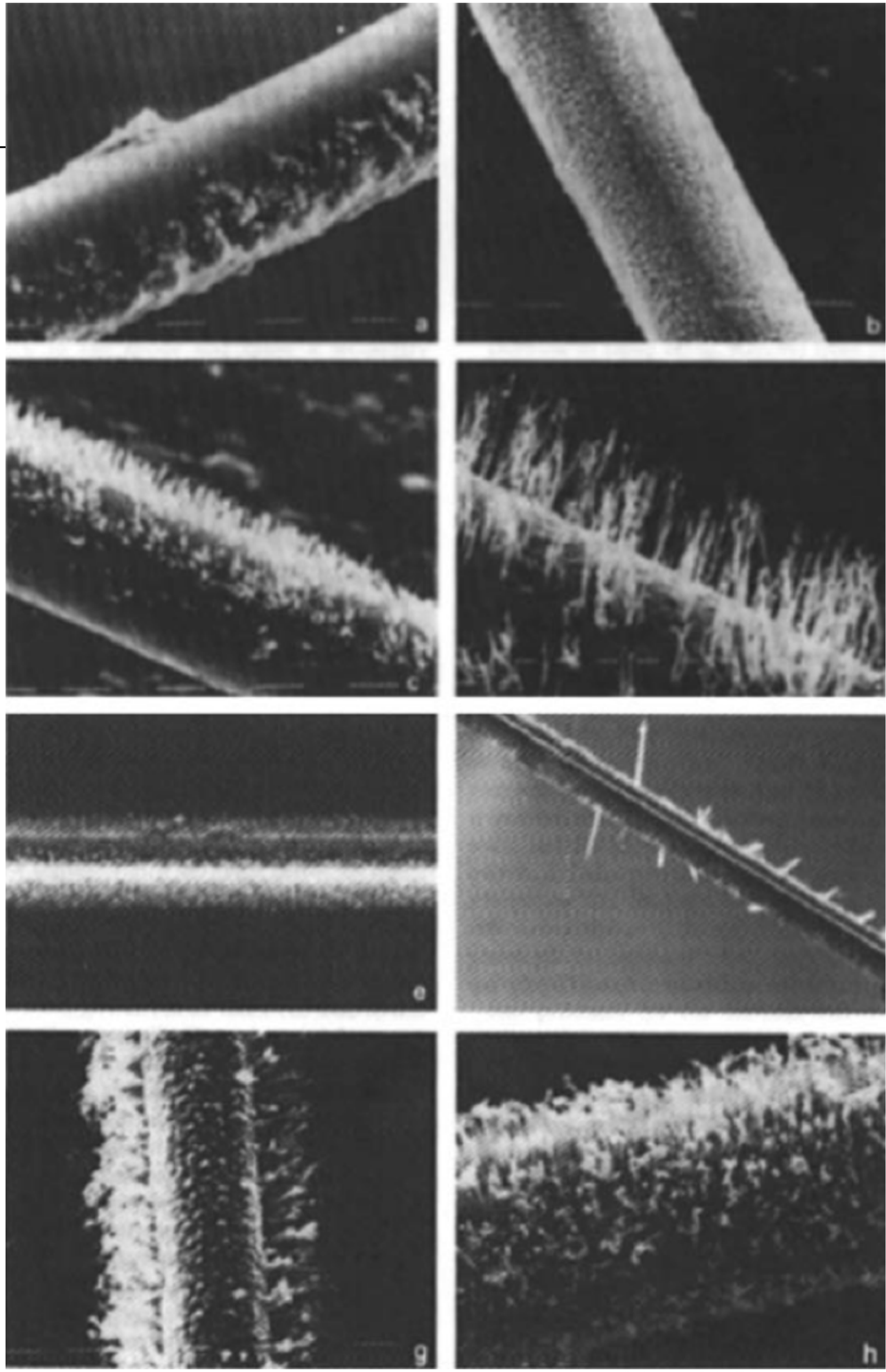

Micro-strip gas chambers

Anodes can be realized via microstructures on dielectrics:

- Simple construction (today)
- Enhanced stability and flexibility
- Improved rate capabilities

First MSGS realized in the 1990s

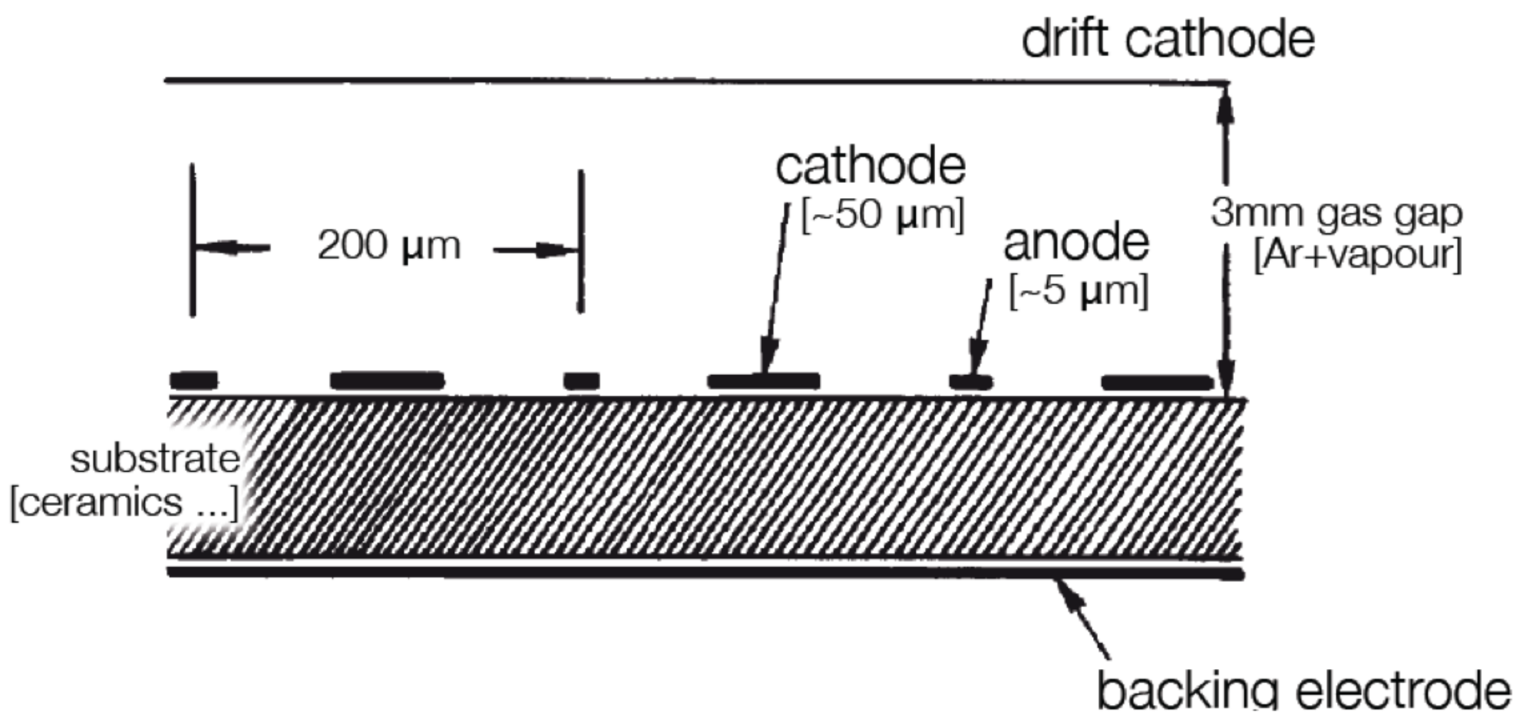

Micro-strip gas chambers

Schematics of MSGC field lines

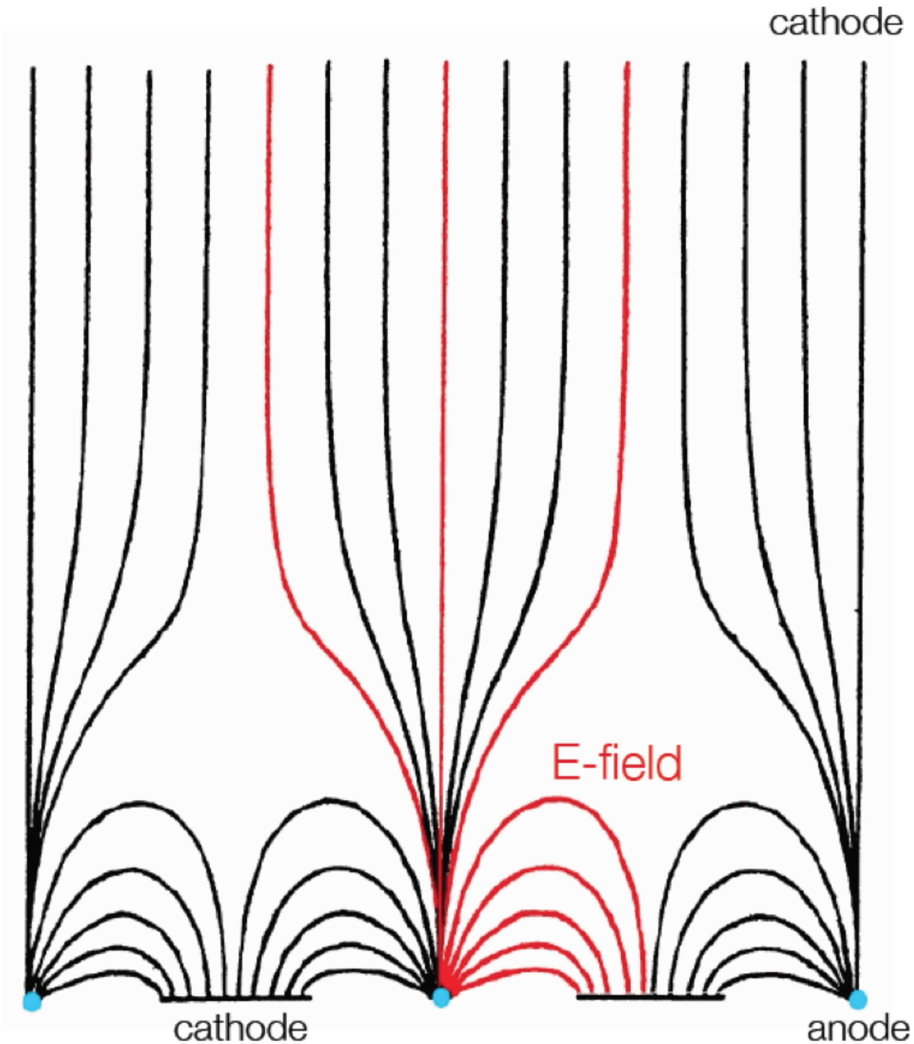

Advantages:

- High field directly above anode
- Ions drift only 100 μm → low dead time, high rate capability without build-up of space charge
- Resolution:
  fine structures can be fabricated by electron lithography on ceramics, glass or plastic foils on which a metal film was previously evaporated

Problems:

- Charging of insulating structures
- Time dependent gain, sparks, anode destruction, corrosion of insulator
- Lifetime of detector too limited

Not quite a success!

MSGC DISCHARGE PROBLEMS:

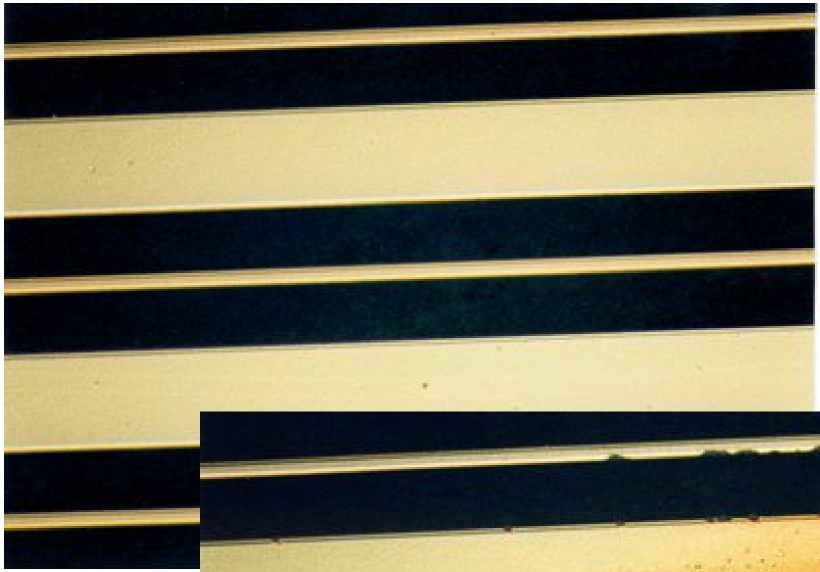

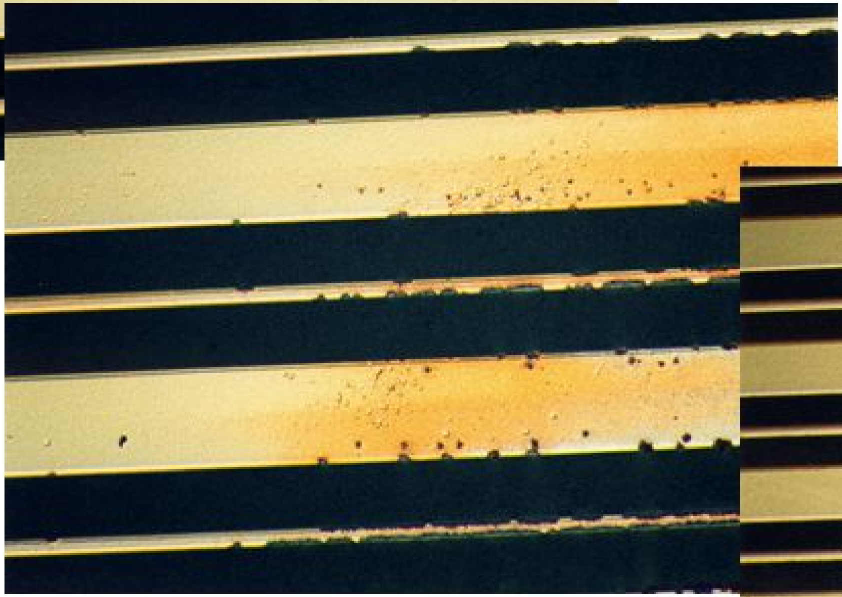

MICRODISCHARGES

FULL BREAKDOWN

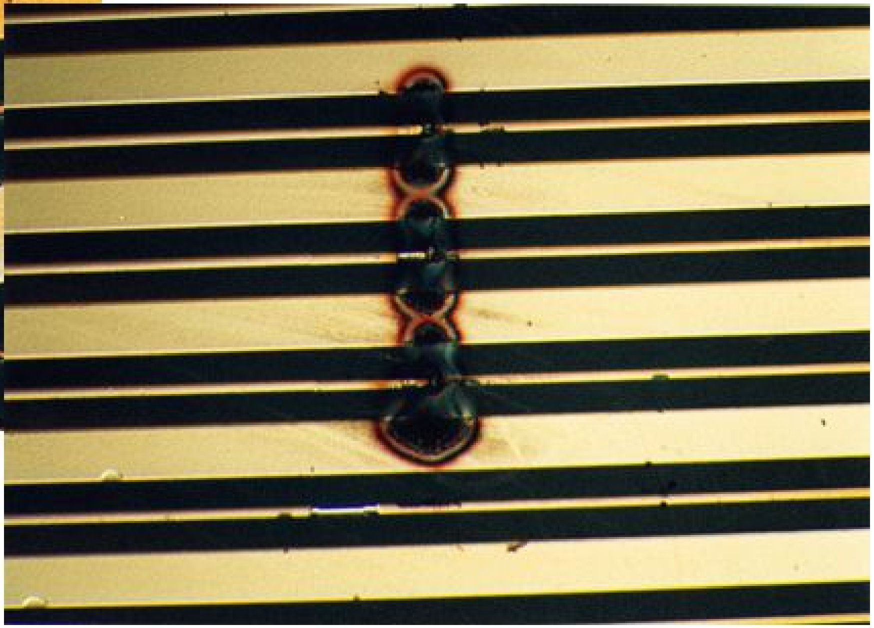

Micro-strip gas chambers

Mitigation of problems: add an intermediate structure

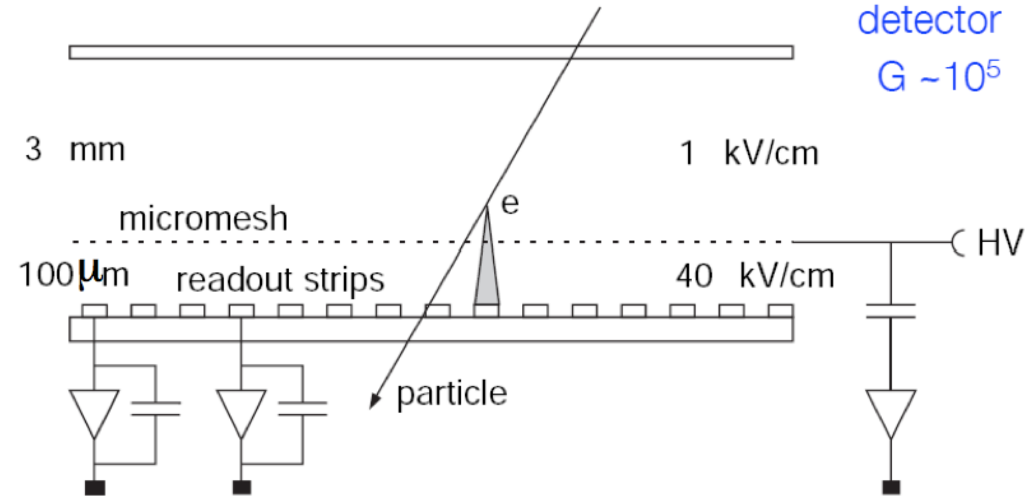

Micromegas detector
$G \sim 10^5$

1. **Micromegas**: fine cathode mesh collects ions. Still fast. No wires

2. **Gas Electron Multiplier** (GEM)

   F. Sauli, CERN, ~1997

   Offers a pre-amplification and allows reduced electric field in the vicinity of the node structures.

   Ease of construction again partly eliminated, risk of discharge on foil (huge capacitance)

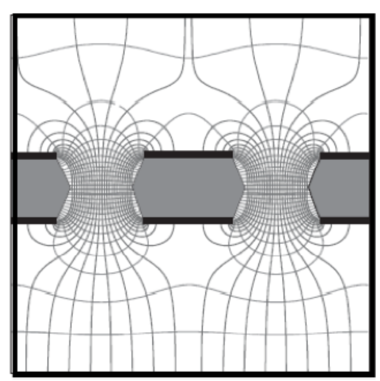

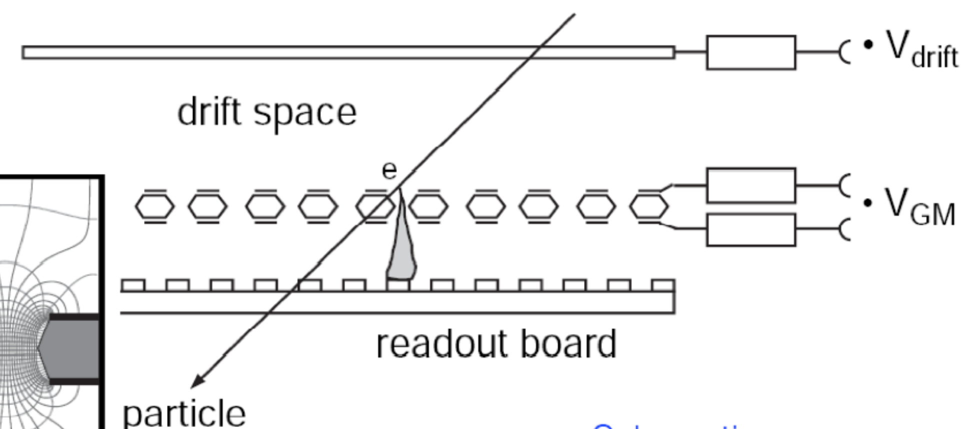

Schematics of GEM detector[30]

GEM detectors

- Copper coated Kapton foils (50µm)
- Holes etched into the foil
- Size ~70µm
- Distance ~140µm

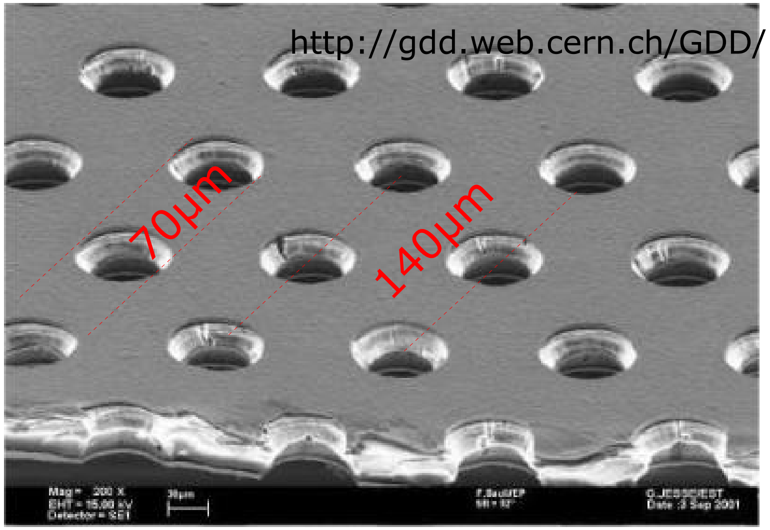

- Apply voltage on copper coating
  - Up to ΔU≈500V
  - Fields up to ~100kV/cm
- Holes act as multiplication channels
- Natural Ion Back-Flow (IBF) suppression

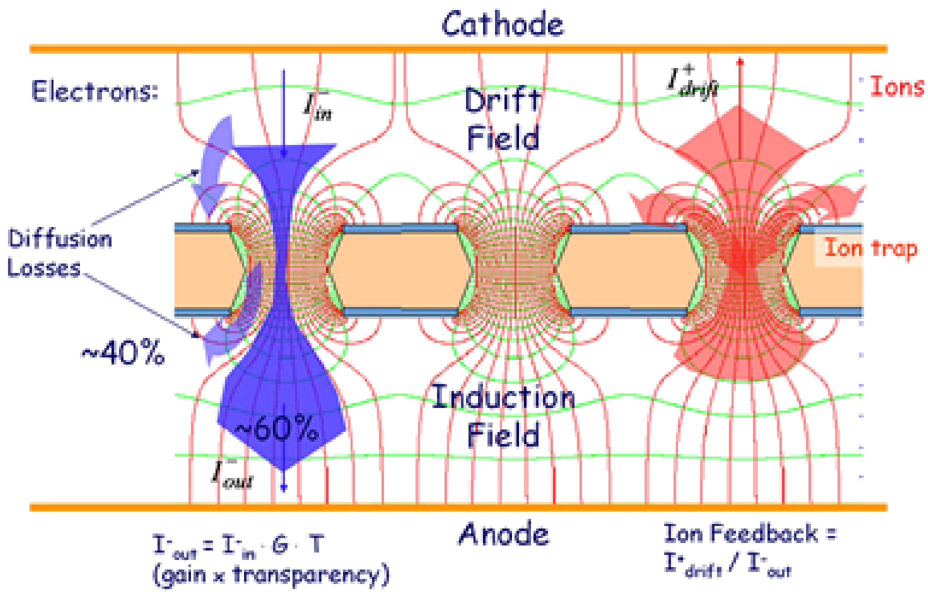

http://www.infn.it/csn5/joomla/GEMINI/

GEM detectors - Ion Back-Flow

- Natural IBF suppression:
  - Asymmetric mobility [low for ions – high for electrons]
    - Electrons move to larger fields in the amplification channel
    - More ions are produced at the edges → trajectory ends on top electrode
  - Asymmetric field [drift – induction]
    - Many field lines end on top electrons (ion capture)
    - Transfer region allows for good electron extraction

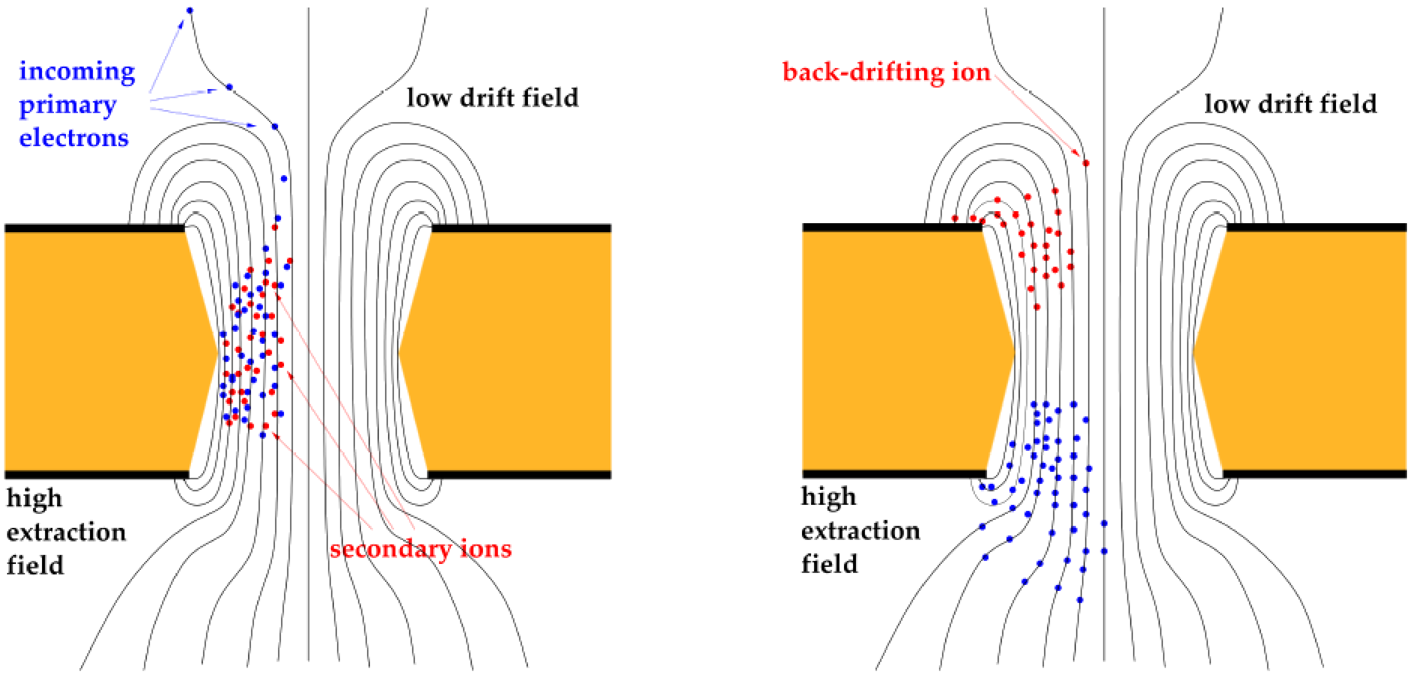

Gaseous detector types

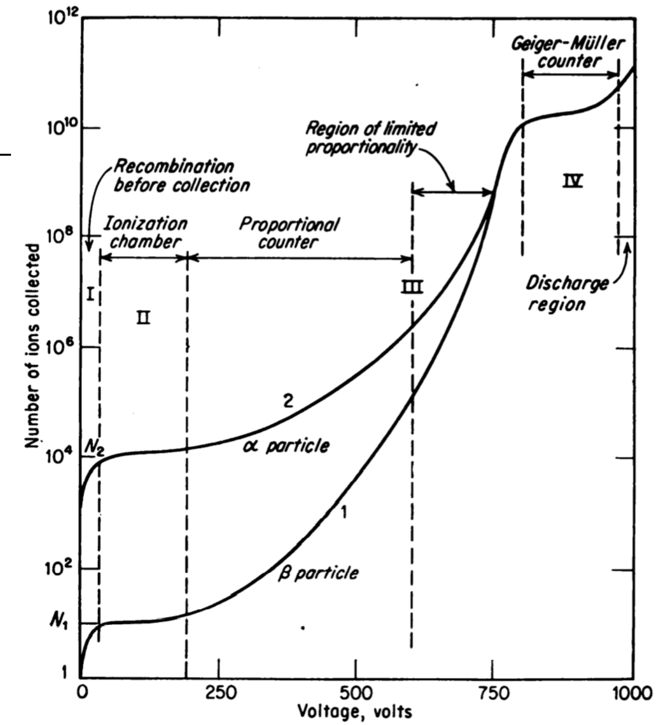

FIG. 2–2. Pulse-height versus applied-voltage curves to illustrate ionization, proportional, and Geiger-Müller regions of operation.

A)Ionization chamber

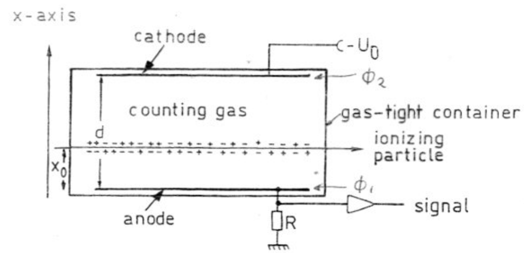

B)Proportional counter

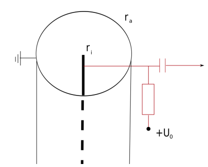

- **Multiwire proportional chambers**

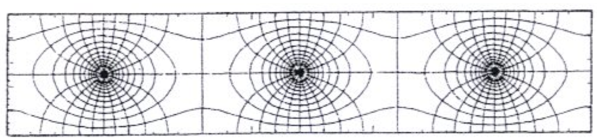

C)Drift chambers

- Cylindrical wire chambers
- Jet drift chambers

D) Time projection chambers

Drift chambers

Obtain spatial information from the electron drift time t_D

Need to know t_0, from a fast scintillator or beam timing

If v_D^- electron drift velocity:

$$x = v_D^- \cdot \Delta t$$

Or, if the drift velocity changes along the electron path:

$$x = \int_{t_0}^{t_D} v_D^-(t)\,dt$$

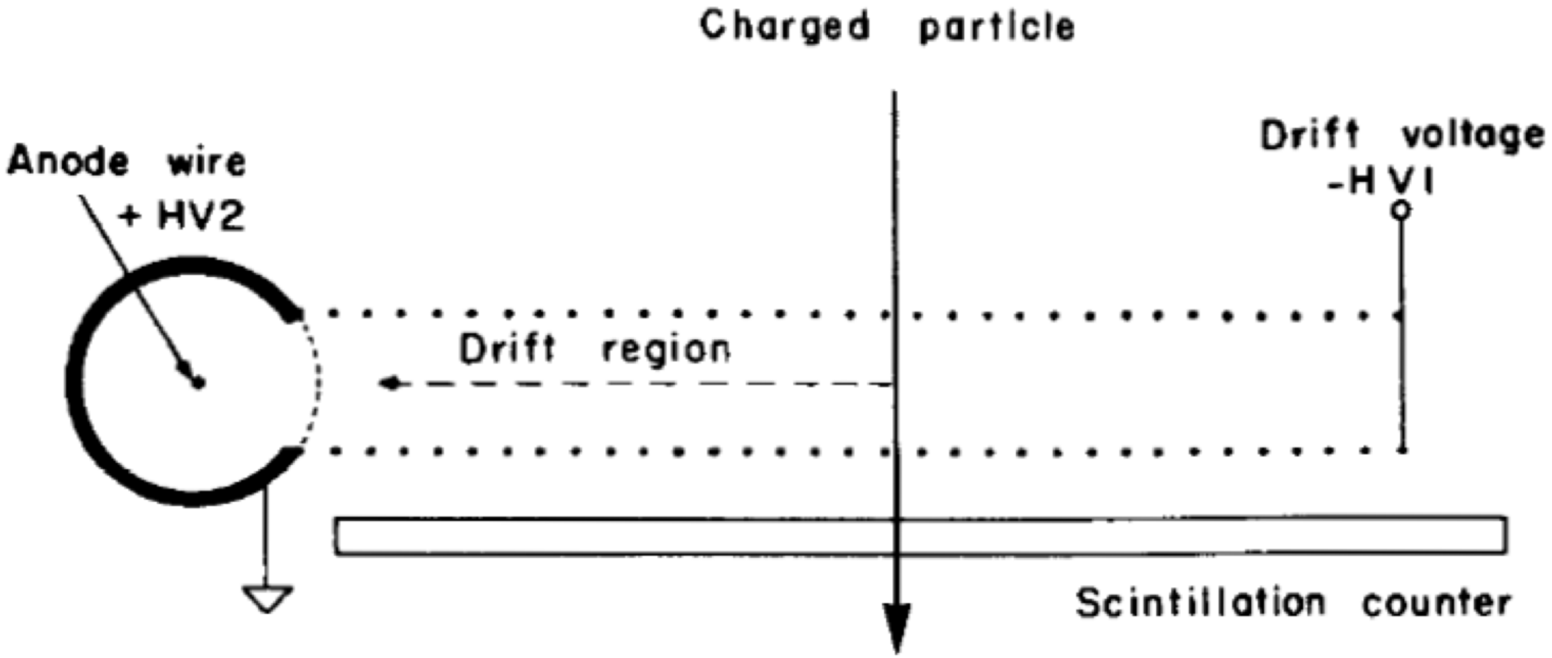

Invented by A. Walenta, J. Heintze in 1970 at Phys. Inst. U.Heidelberg NIM 92 (1971) 373

Drift chambers

Needs well defined drift field → introduce additional field wires in between anode wires

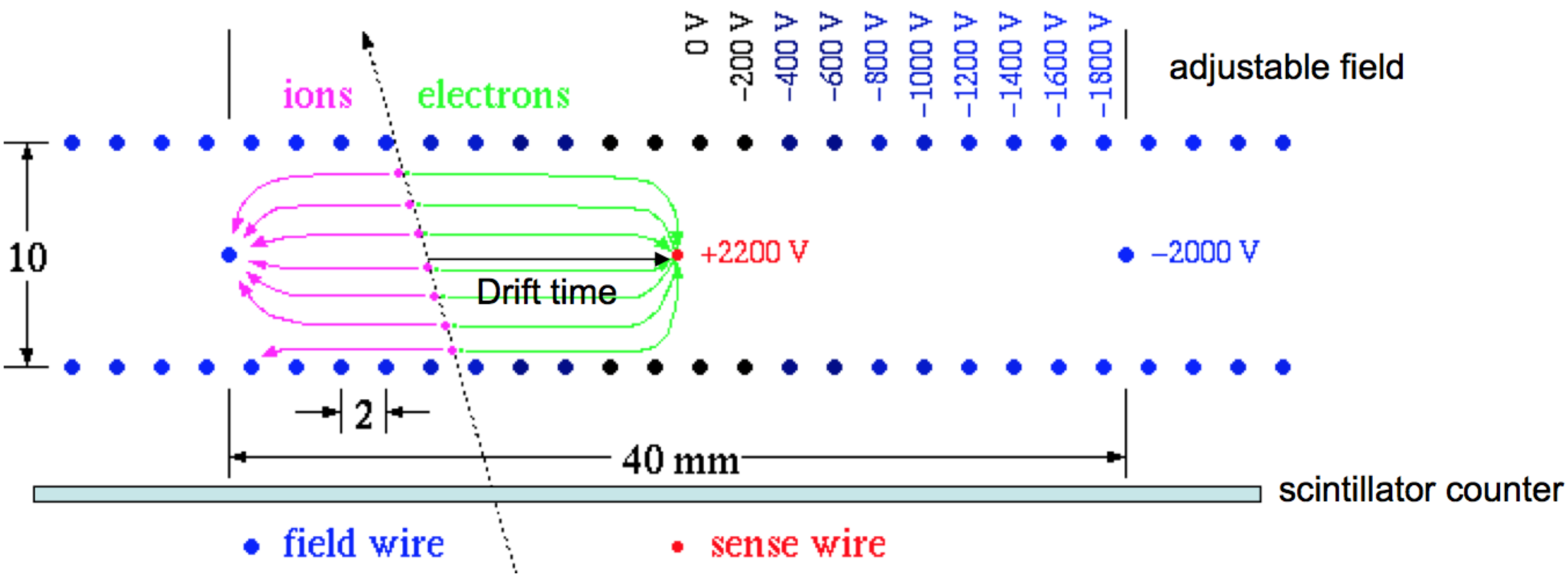

Drift chambers: field wires

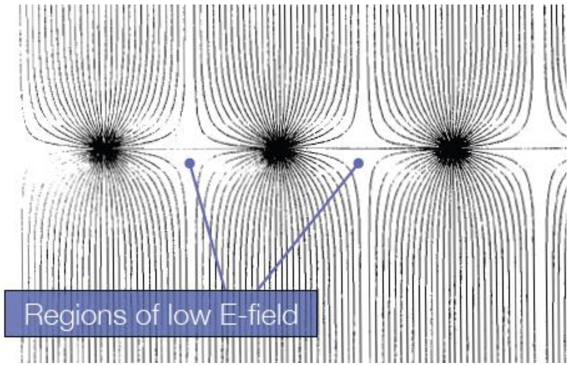

MWPC:

regions of very low electric field between anode wires

Here add **field wires** at negative potential wrt anode wires → strongly improves the quality of the field!

This is essential for drift chambers where **spatial resolution** is dominated by **drift time variations** (and not by segmented electrode structure)

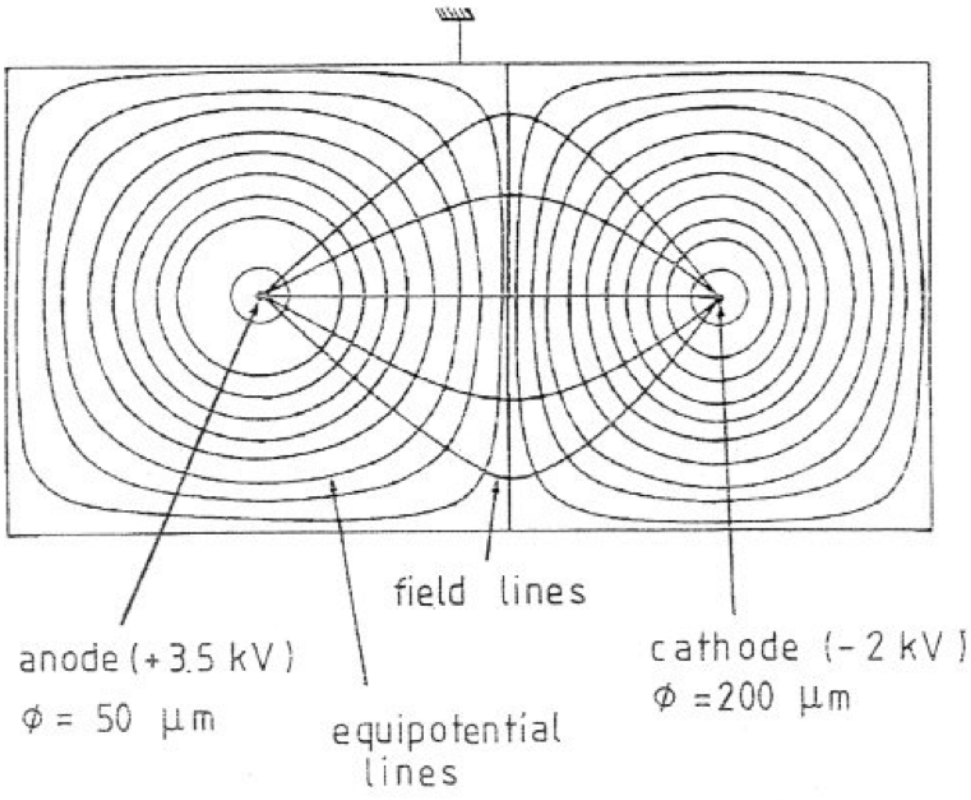

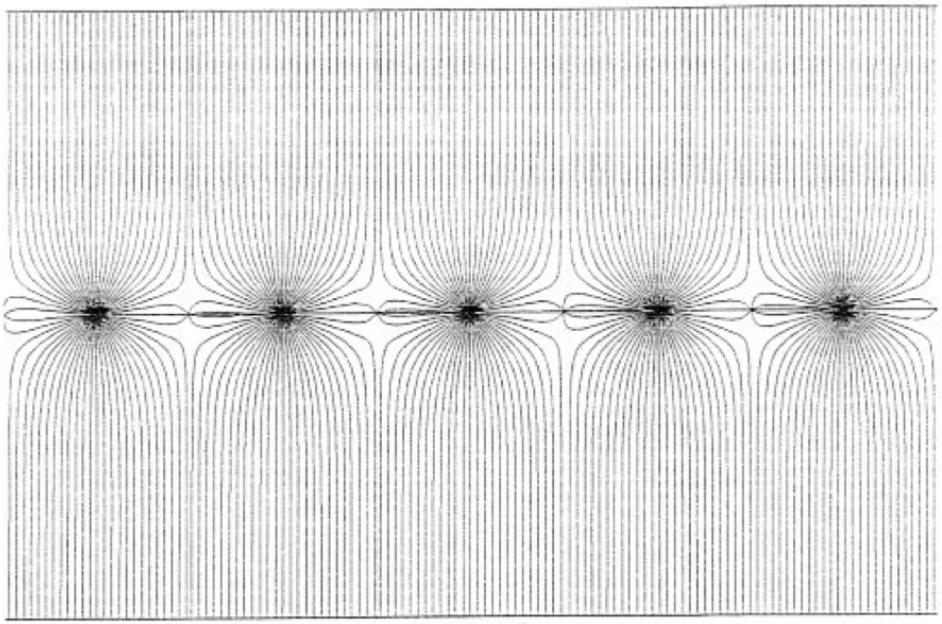

Drift chambers: spatial resolution

Resolution is determined by the accuracy of drift time measurement

Influenced by:

- Diffusion: $\sigma_{diff} \sim \sqrt{x}$
- δ-electrons: σ_{δ} is independent of drift length → constant term in resolution
- Electronics: $\sigma_{electronics}$ = constant, also independent of drift length
- Primary ionization statistics: $\sigma_{prim} \sim 1/x$
  Spatial fluctuations of charge-carrier production result in large drift-path differences for particle trajectories close to the anode.
  It has minor influence for tracks far away from the anode

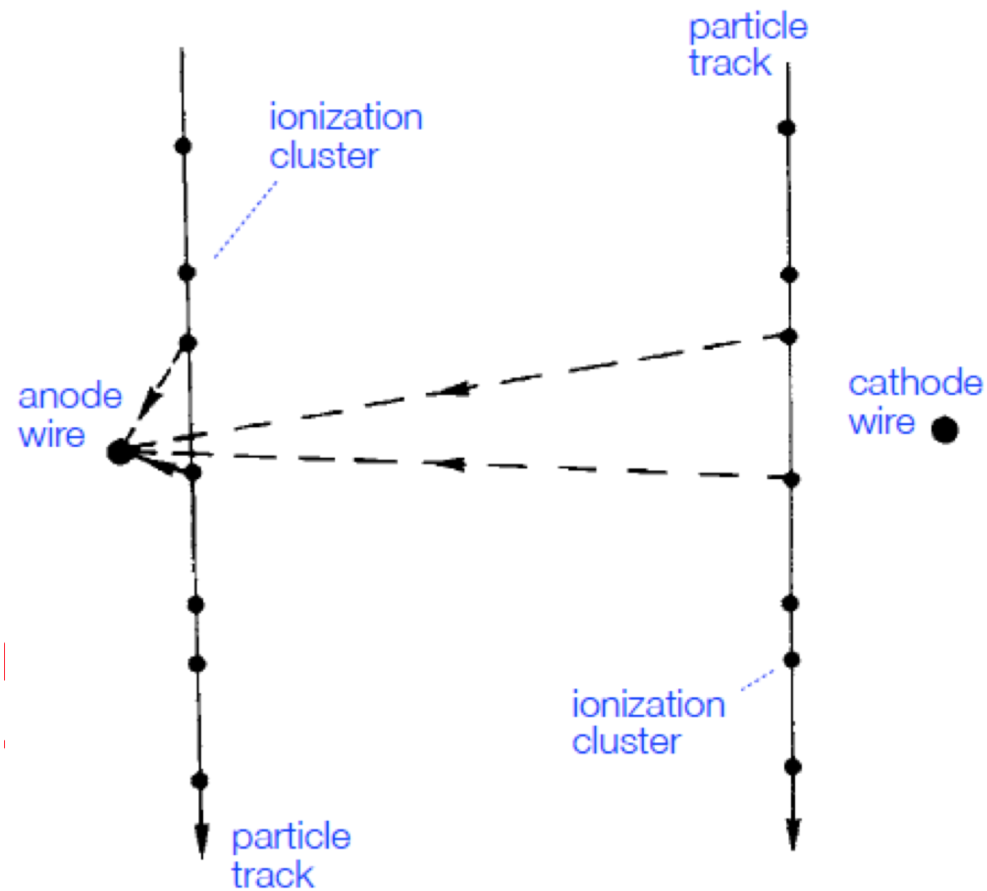

Drift chambers: spatial resolution

$$\sigma_x^2 = \underbrace{\left(\frac{1}{64N^2}\right)\cdot\frac{1}{x^2}}_{\text{1st ionization statistics}} + \underbrace{\frac{2D}{v_d}}_{\text{diffusion}}\cdot x + \underbrace{\sigma_{\text{const}}^2}_{\substack{\text{electronics}\\ \delta\text{-electrons}}}$$

Possible improvements:

- Increase N by increasing the pressure
- Decrease D by increasing the pressure

$$D \sim \frac{\lambda_0^2}{\tau} \sim \frac{1/n^2}{1/n} \sim \frac{1}{n}$$

[n: particle density in gas]
[increases with pressure]

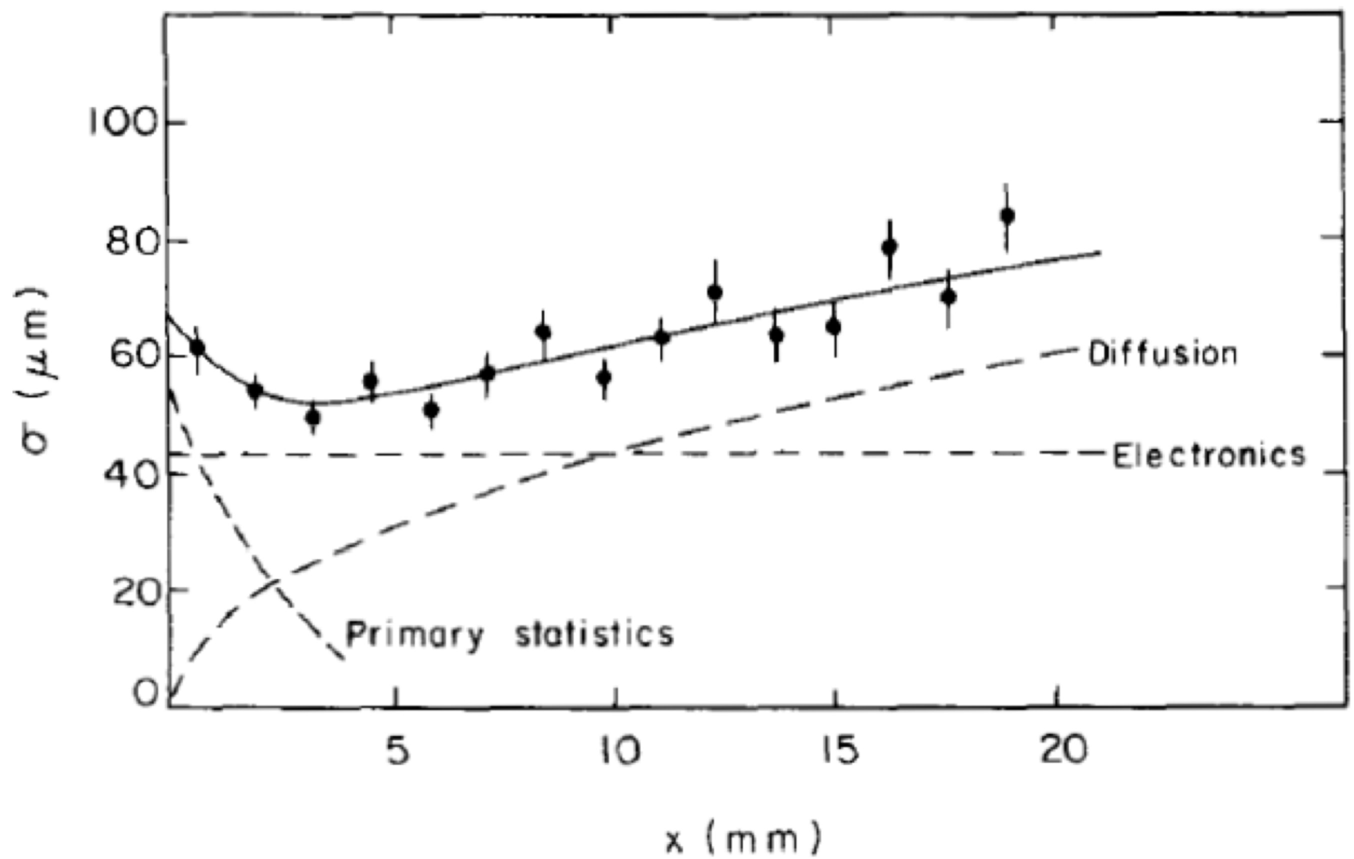

INCREASE the pressure!
Up to 4 atm possible

Position of coordinate along the wire

Possibilities to measure the position of the signal in the wire direction:

- Charge division: measure the current at both ends of anode wire:
  precision ~1% of wire length

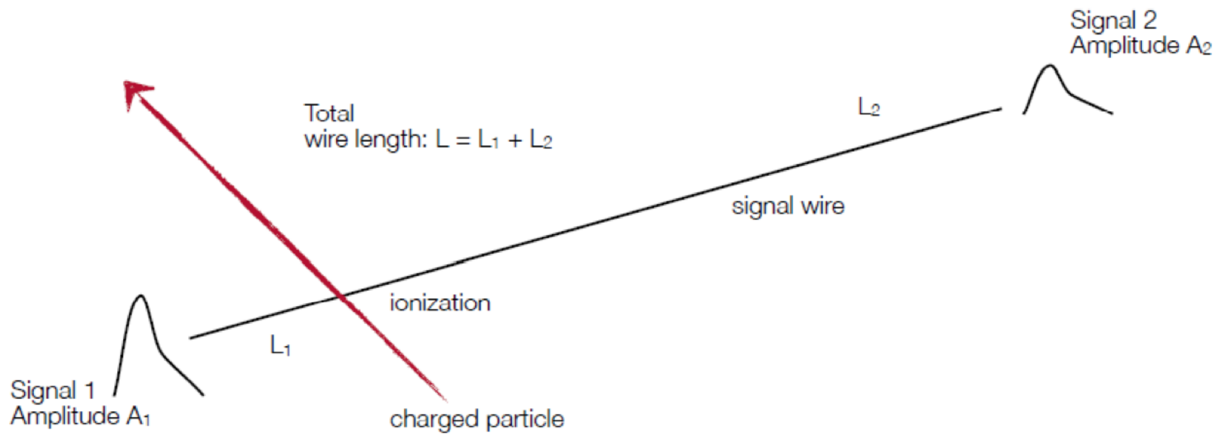

- Time measurement at both ends of the wire

- Stereo wires: layer of anode wires inclined by a small angle γ (“stereo angle) →

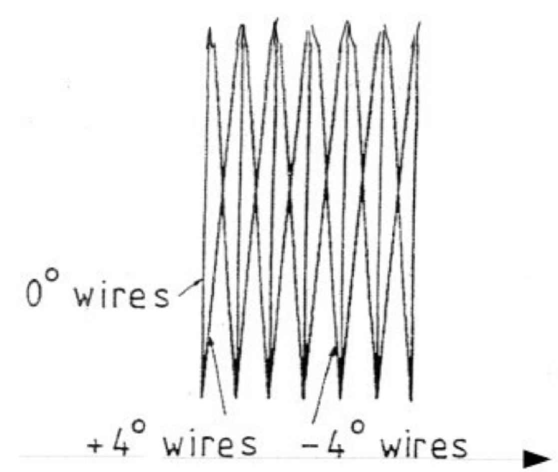

Drift chambers: staggered wires

Difficulty: time measurement cannot distinguish between particle passing to the left or to the right of the anode wire → 'left – right ambiguity'

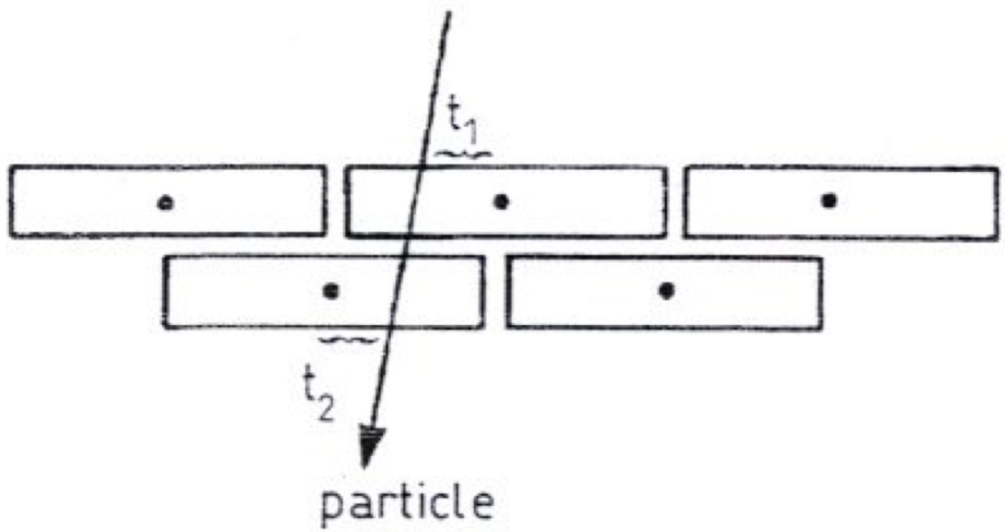

Use two layers displaced relative to each other by half the wire distance: Staggered wires

Drift chambers: field and resolution

Very large drift chambers possible, introducing a voltage divider = cathode strips connected via resistors, and very few or even only one wire

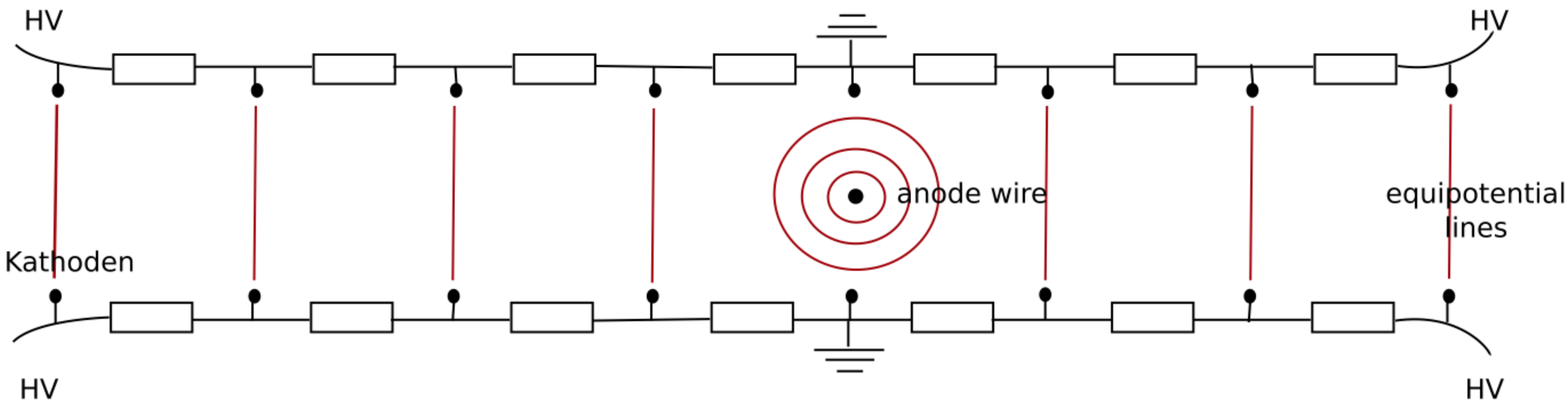

Space point resolution limited by mechanical tolerance:

Very large chambers:
100 cm x 100 cm → ≃ 200 μm

Small chambers
10 cm x 10 cm → ≃ 20 μm

Limit! The hit density has to be low!

Drift time – space relation in a large drift chambers (80 cm x 80 cm) with only one anode wire (Ar + isobutane 93:7)

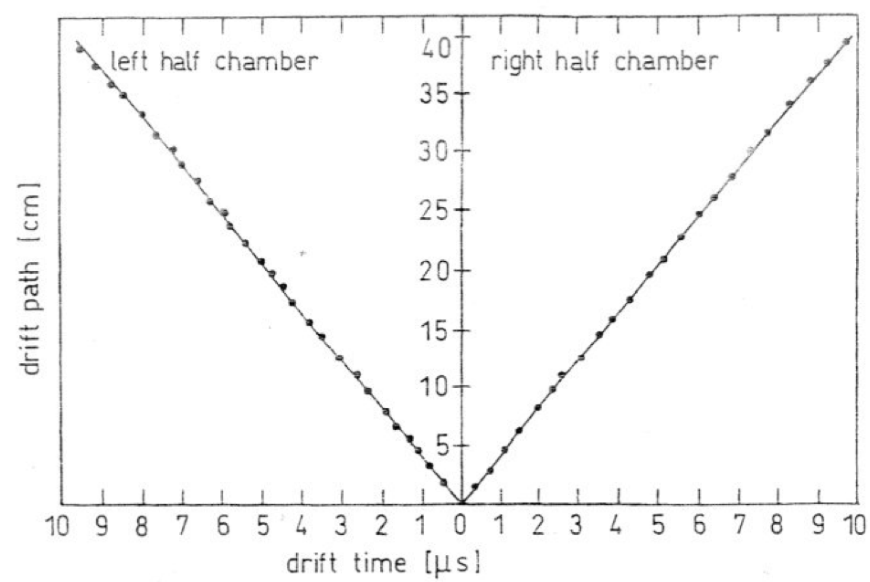

Resistive plate chambers

Electrode-less drift chamber:

Field can be formed by charging up an insulating chamber wall with ions.

After some charging time, ions cover the insulating layer → no field lines end there and the drift field is well defined:

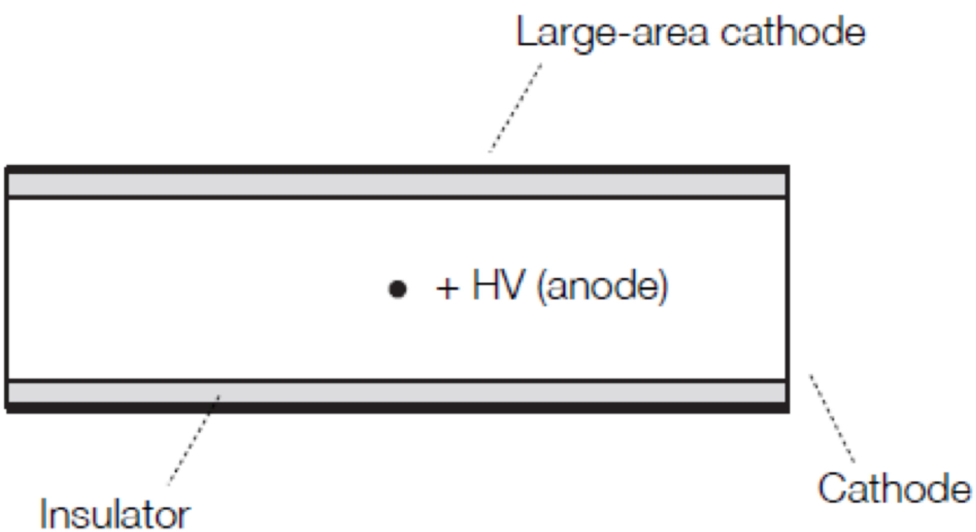

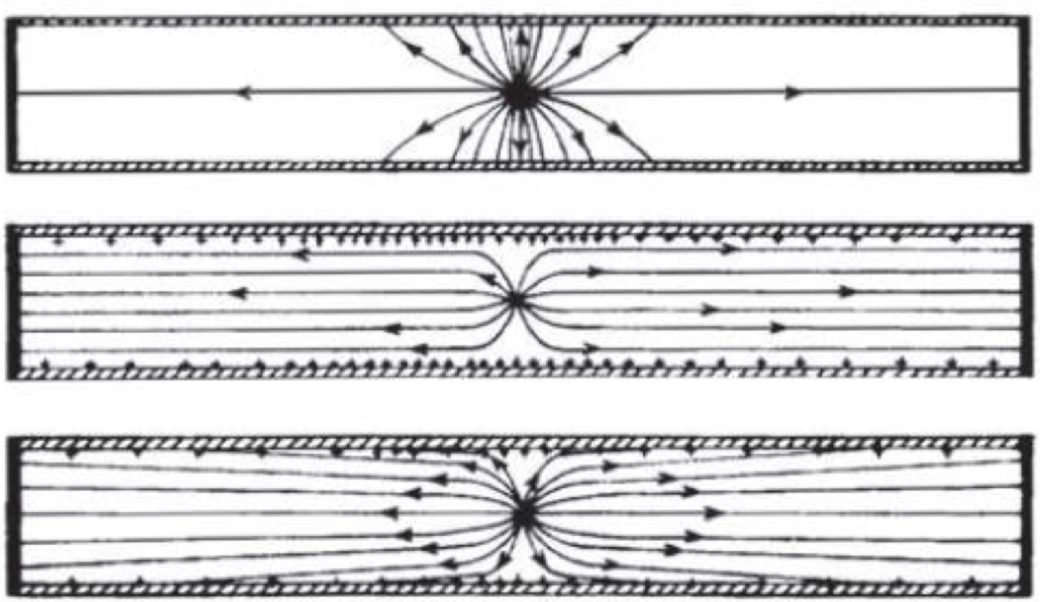

To avoid overcharging, finite resistance of the insulator (some field lines end at the cathode)

Cylindrical wire chambers

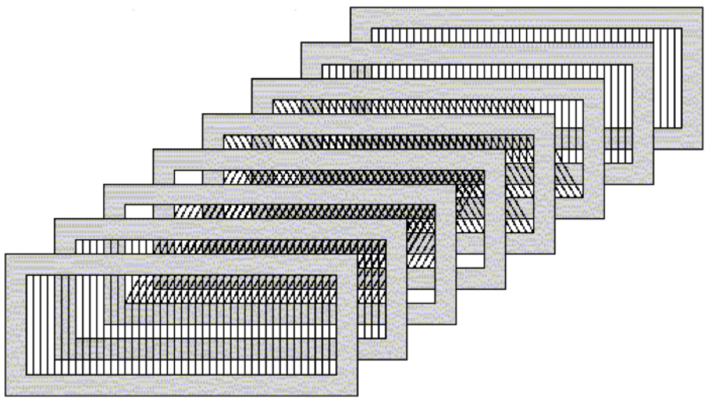

- Fixed target experiments:
  multi-layer MWPC or drift chambers
- Collider experiments, to cover the maximum solid angle:
  - Initially multi-gap spark chambers or MWPCs
  - Later cylindrical drift chambers, jet chambers
  - Today Time Projection Chambers (TPC)

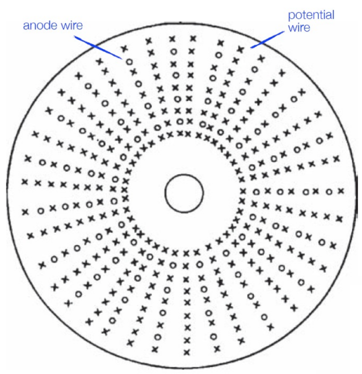

Generally these chambers are operated in a magnetic field → measurement of radius ρ of curvature of a track → momentum determination (internally in one detector)

$$p\ (\mathrm{GeV}/c) = 0.3 \cdot B\ (\mathrm{T}) \cdot \rho\ (\mathrm{m})$$

Cylindrical drift chambers

Principle of a cylindrical drift chamber: wires in axial direction, parallel to the beam axis AND the magnetic field

Alternating anode and field wires:

- One field wire between two anode wires
- Cylindrical layers of field wires between layers of anode wires → very good drift cell

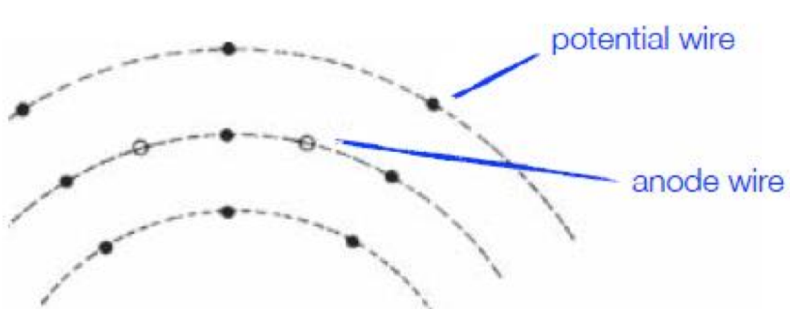

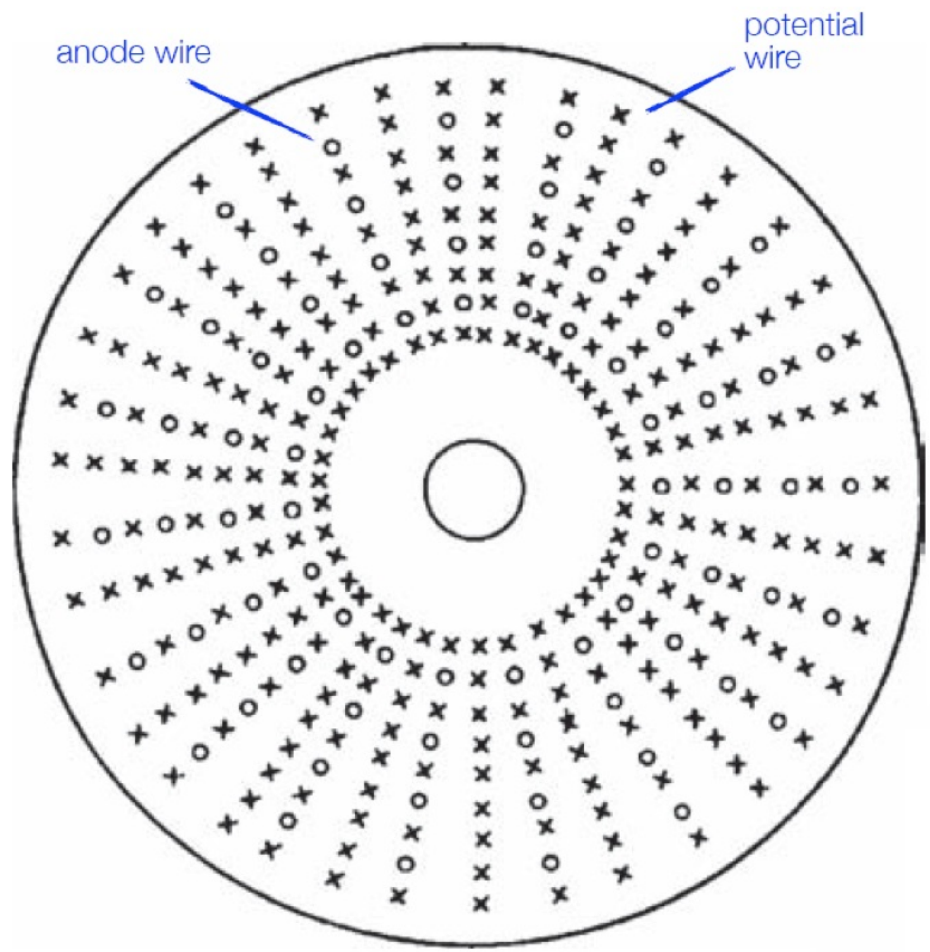

Cylindrical drift chambers: cell geometries

Different drift cell geometries:

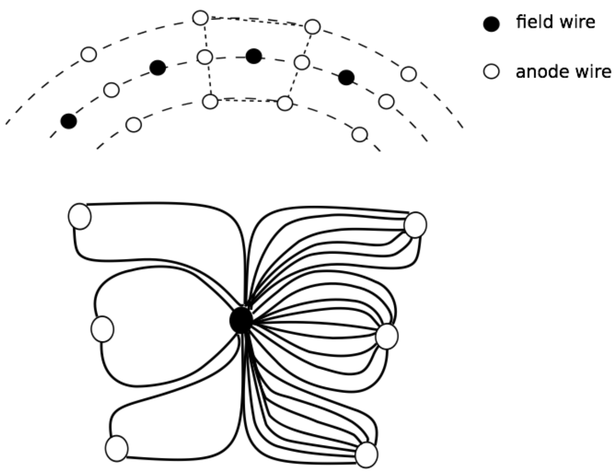

open drift cell

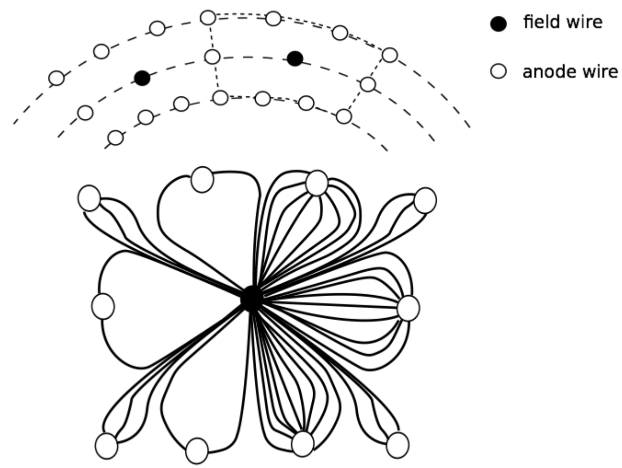

closed drift cell

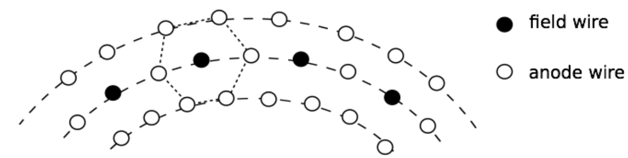

also hexagonal drift cell

- Thin anode wires (⌀ ≃ 30 μm)
- Thicker field wires (⌀ ≃ 100 μm)
- Field quality better with more wires per drift cell

However:

- More labor-intensive construction
- Wire tension applies enormous stress on the end plates (e.g. 5000 anode wires + 15000 field wires → 2.5 t on each end plate!)

In E + B fields

Here in general the electric drift field E is perpendicular to the magnetic field B → Lorentz angle for drifting charges must be considered!

Drift trajectories in an open rectangular drift cell for:
a) without, and
b) with magnetic field

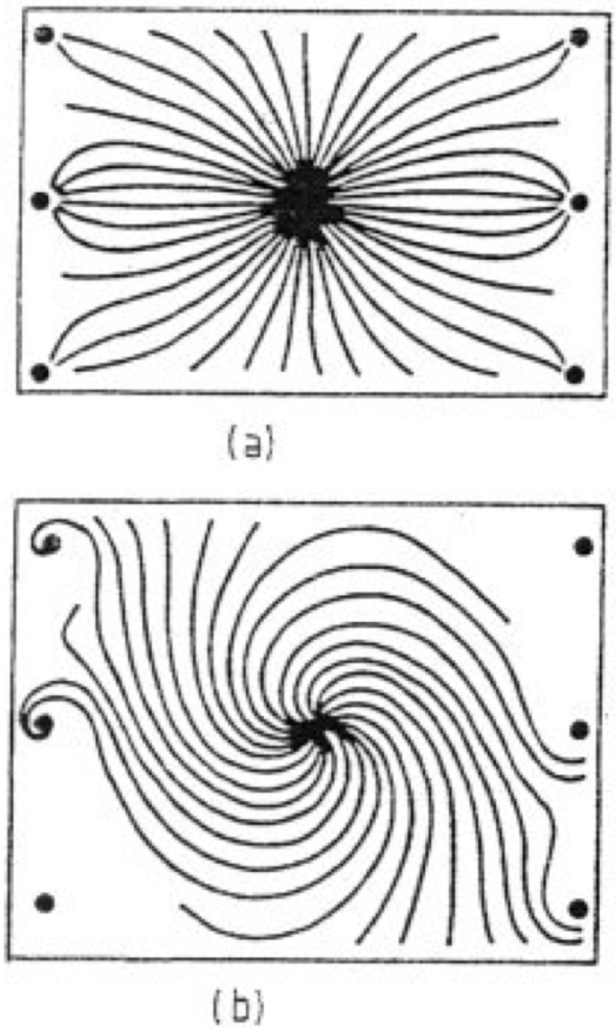

Jet drift chambers

- Very large drift cells
- Optimize number of measurements per track

  Typically 1/cm

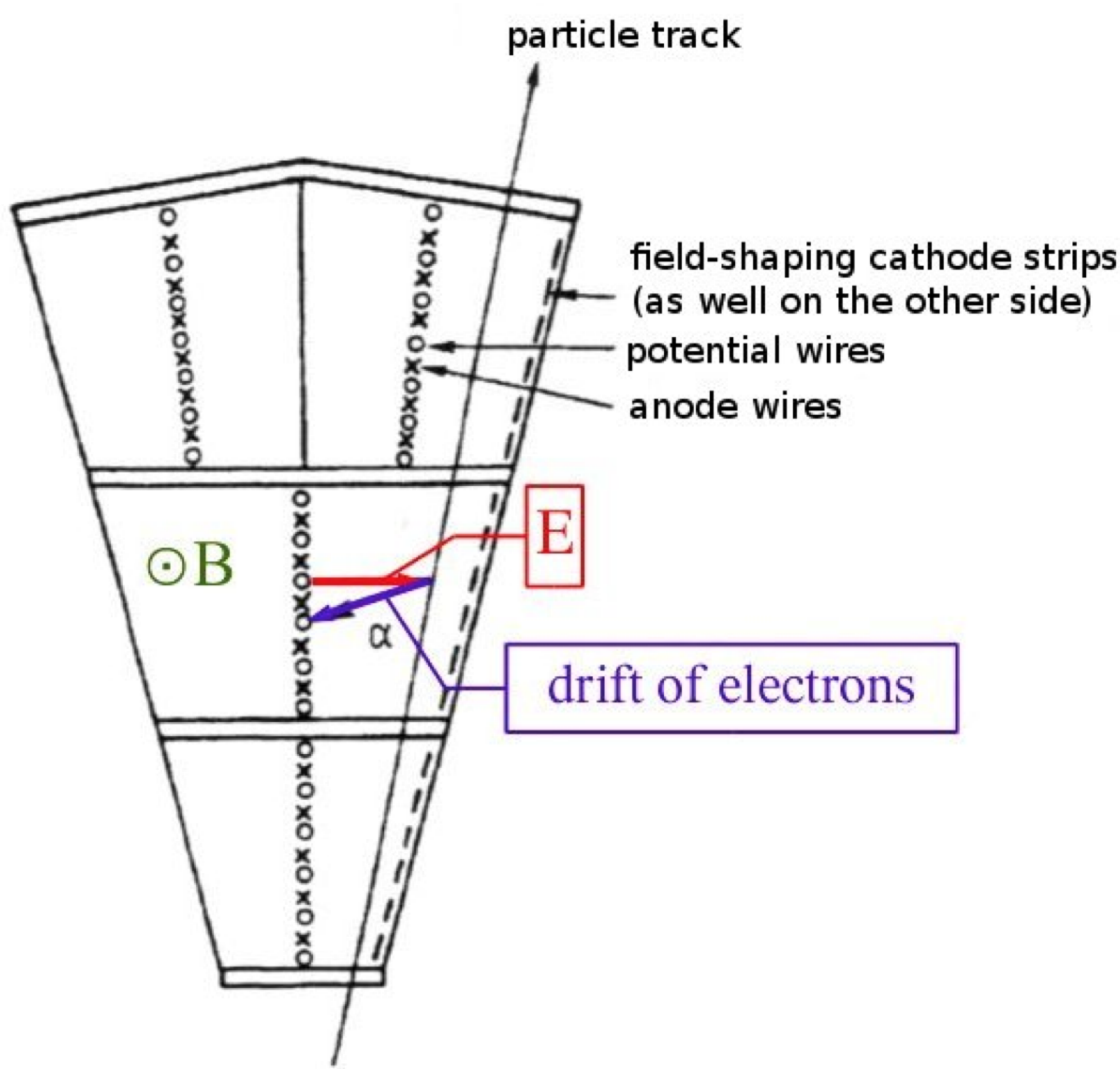

JADE jet chamber for PETRA (DESY)

example: JADE jet chamber for PETRA, built by J.Heintze et al. Phys. Inst. U. Heidelberg
length: 2.34 m, radial track length: 57 cm, 47 measurements per track
$\sigma_{r\phi} = 180\ \mu$m, $\sigma_z = 16$ mm

JADE jet chamber for PETRA (DESY)

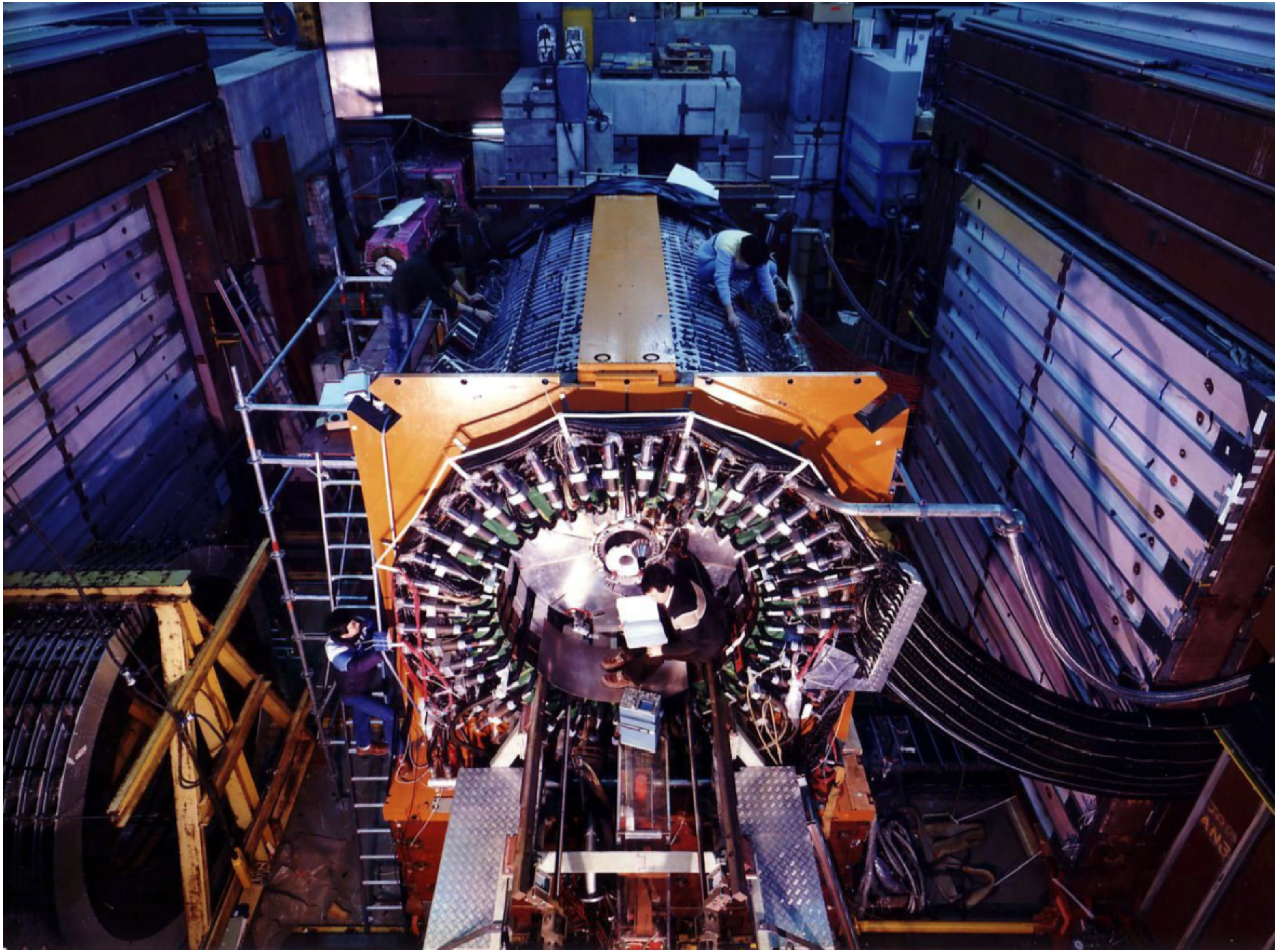

JADE jet chamber for PETRA (DESY)

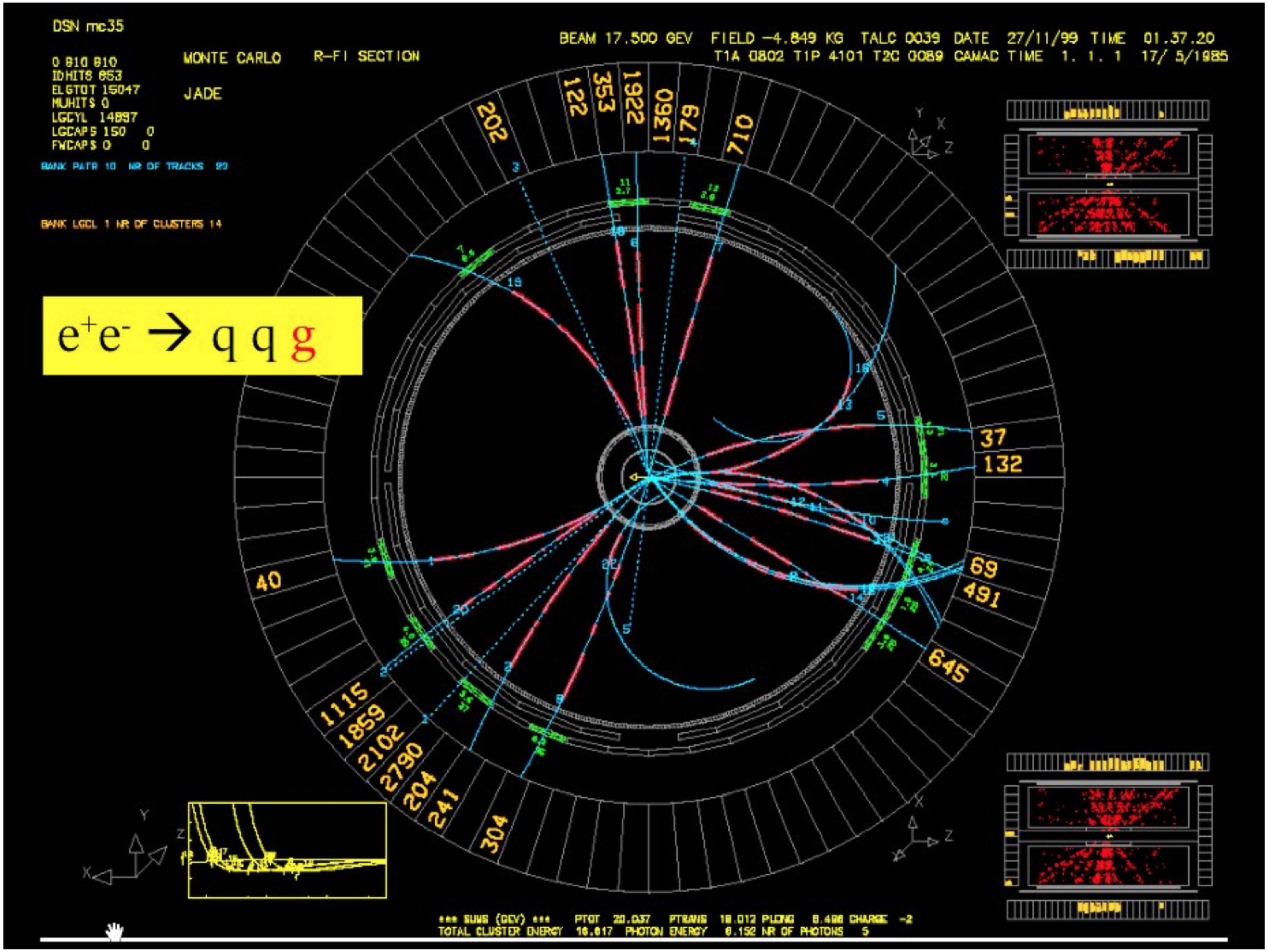

3-jet event by JADE – measurements taken at PETRA → discovery of gluon

Jet chamber in OPAL, at LEP

length: 4 m, radius: 1.85 m, 159 measurements per track, gas: $Ar/CH_4/C_4H_{10}$ at 4 bar
$\sigma_{r\phi} = 135\ \mu m$, $\sigma_z = 60$ mm

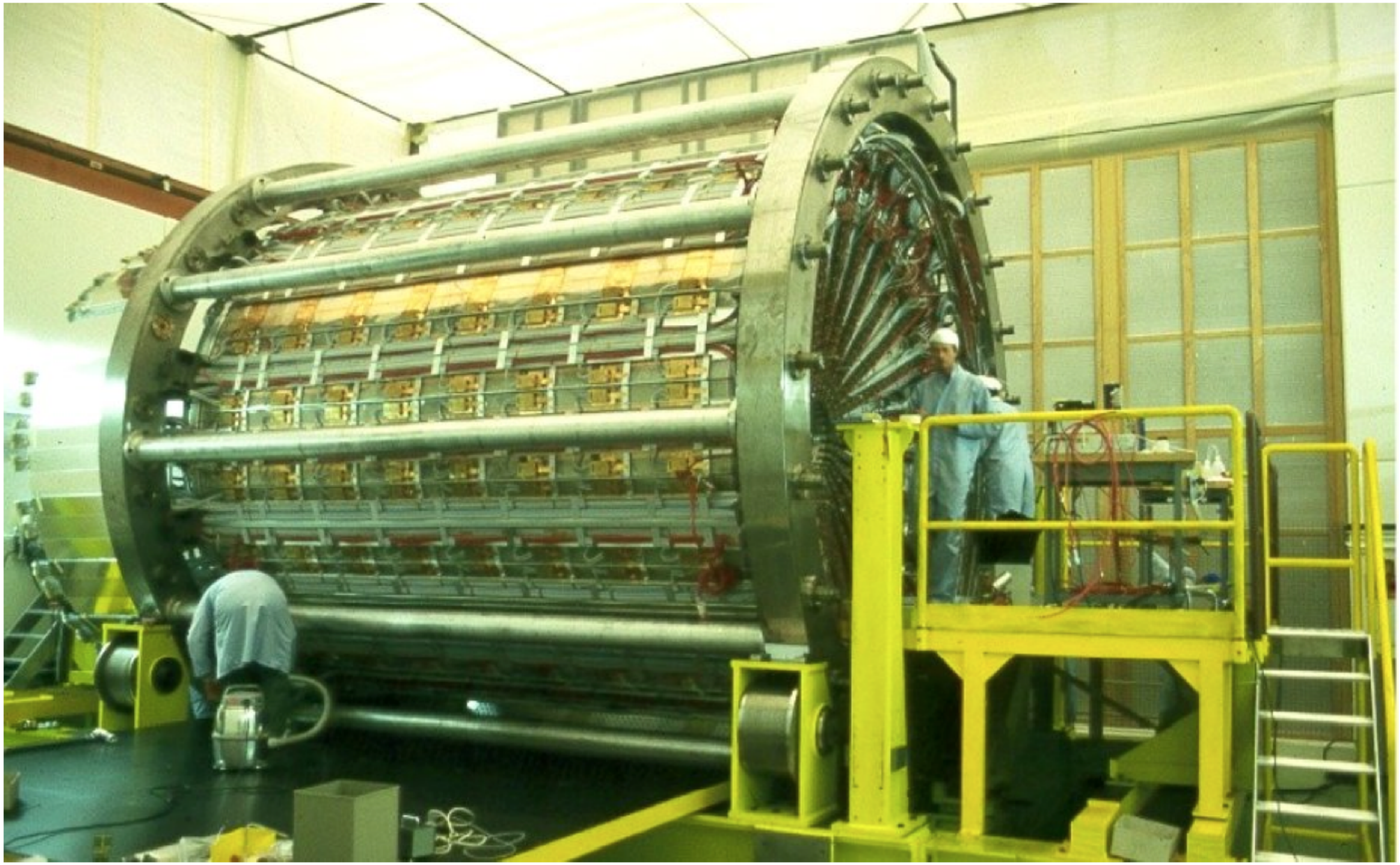

Jet chamber in OPAL, at LEP

interior of jet chamber of OPAL

Central drift chamber (CDC) in FOPI

application for heavy ion collisions: FOPI (experiment at SIS at GSI):
central drift chamber (CDC), D. Pelte and N. Herrmann Phys. Inst. U.Heidelberg

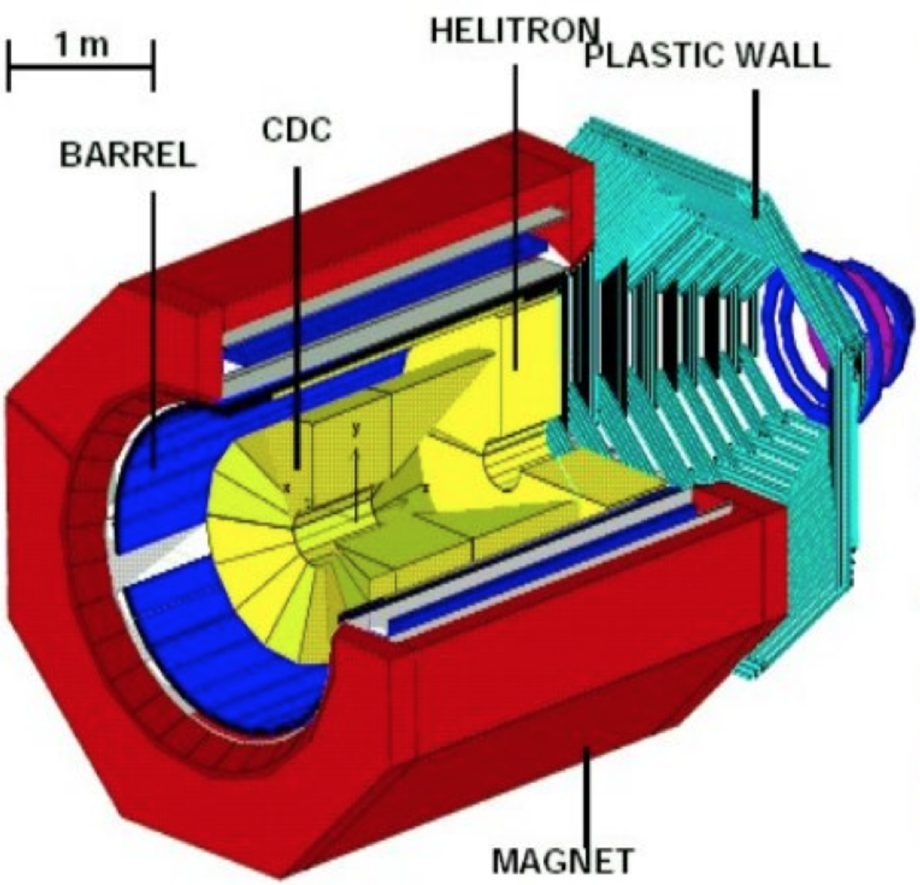

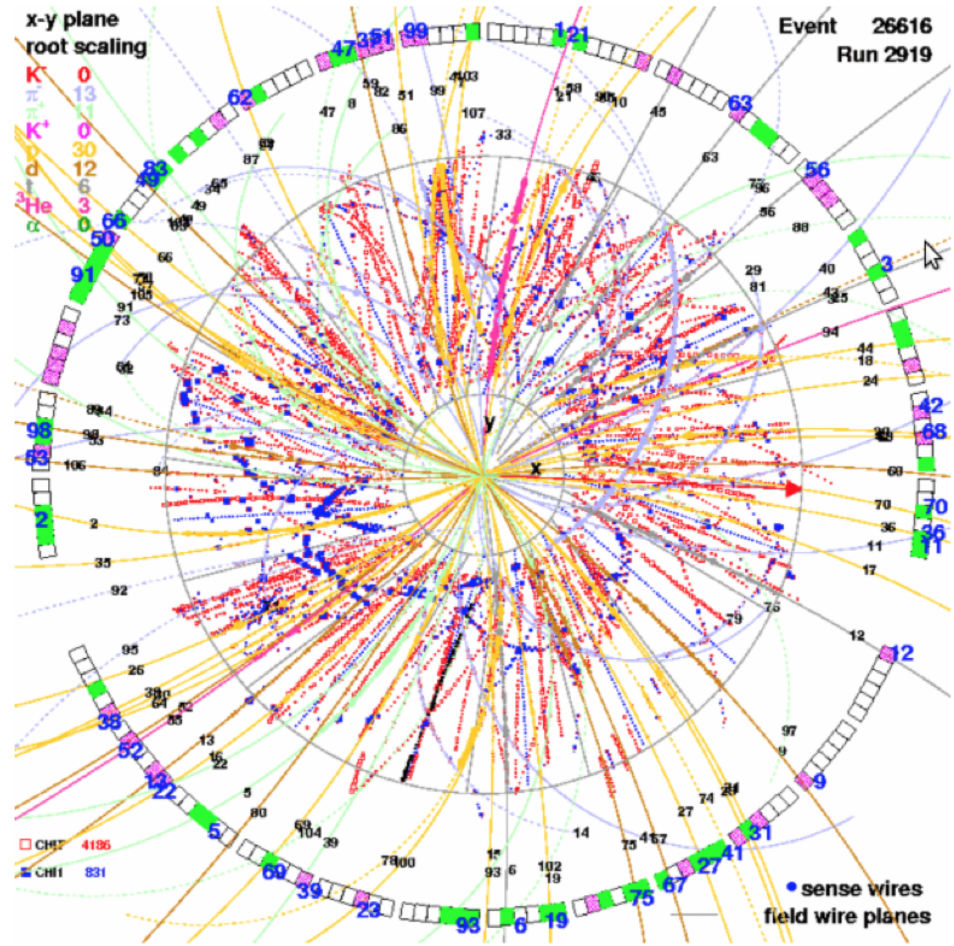

H1 cylindrical drift chamber

Cylindrical
Drift Chamber

[H1 Experiment]

Number of wires: ~ 15000
Total force from wire tension: ~ 6 t

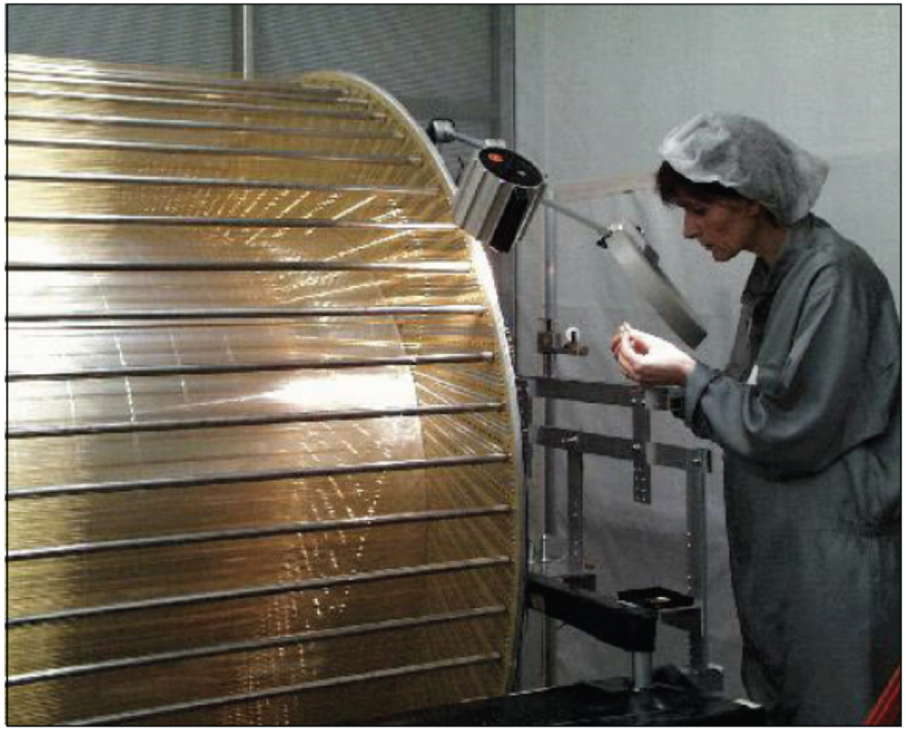

Gaseous detector types

A) Ionization chamber

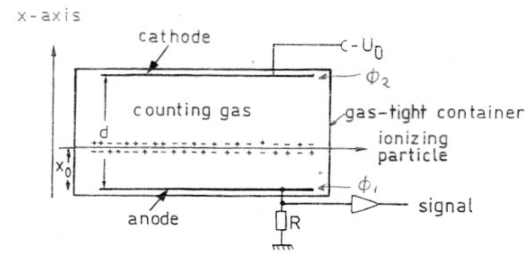

B) Proportional counter

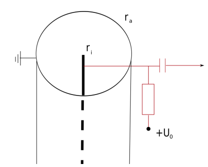

- **Multiwire proportional chambers**

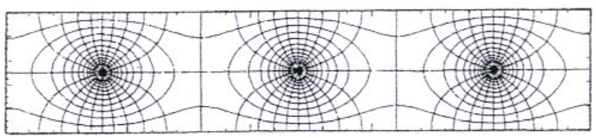

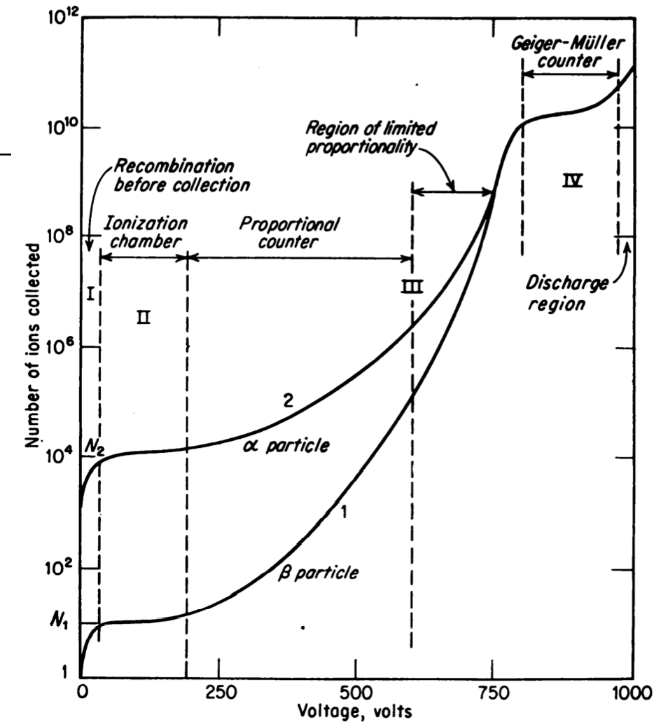

FIG. 2–2. Pulse-height versus applied-voltage curves to illustrate ionization, proportional, and Geiger-Müller regions of operation.

C) Drift chambers

- Cylindrical wire chambers
- Jet drift chambers

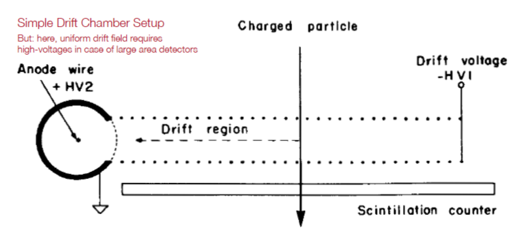

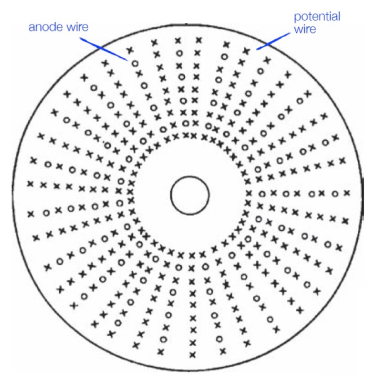

D) Time projection chambers

Time Projection Chamber

"Electronic bubble chamber"

Full 3D track reconstruction

Invented by D. Nygren (1974) at Berkeley National Lab

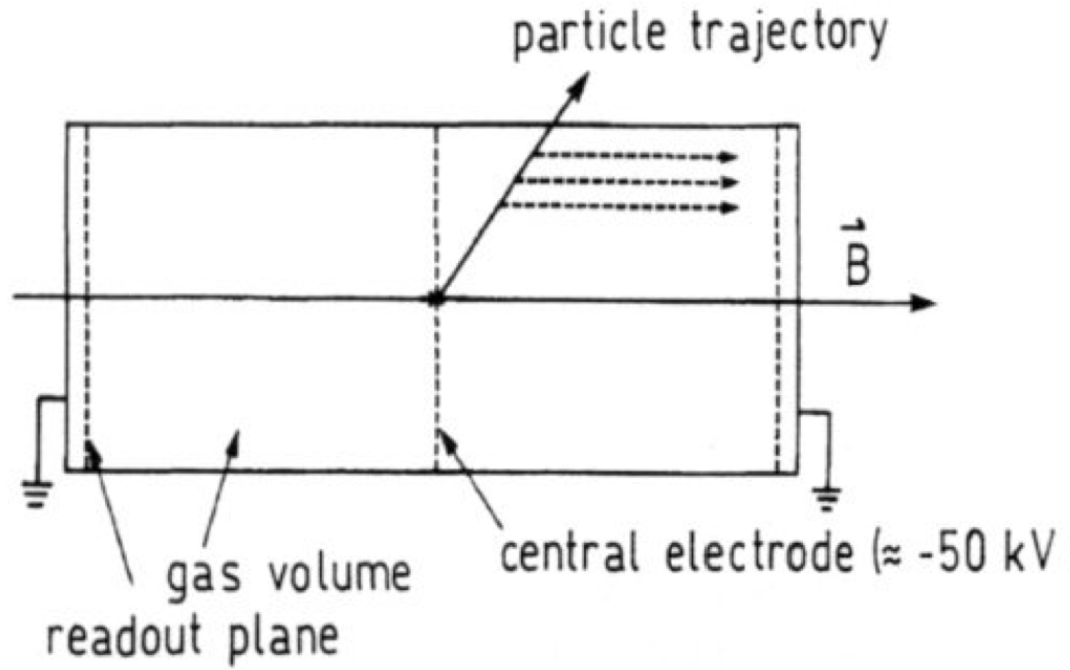

- Mostly cylindrical detectors
- Central HV electrode
- MWPCs at the end-caps
- Usually E||B → Lorentz angle = 0

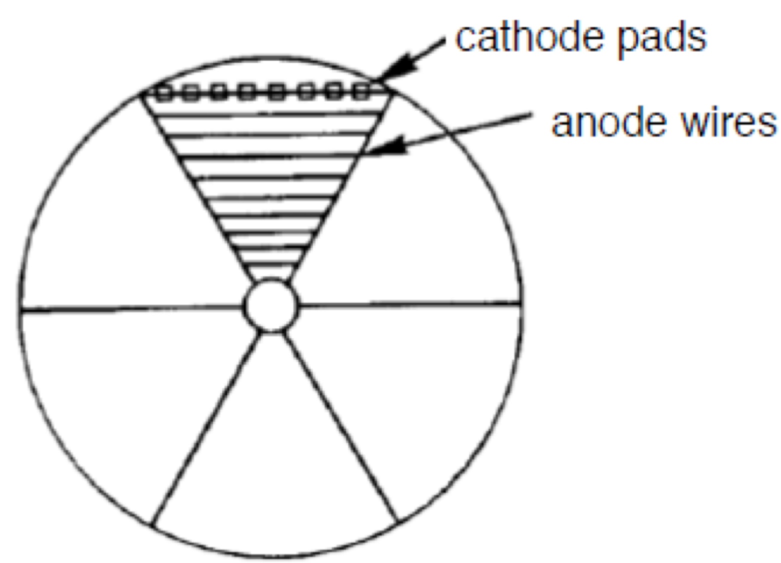

- Particles traversing the gas produce charges by ionization
- Electrons drift towards the MWPC in a highly uniform E field
- Position (2D), arrival time, and energy deposited is measured

TPC

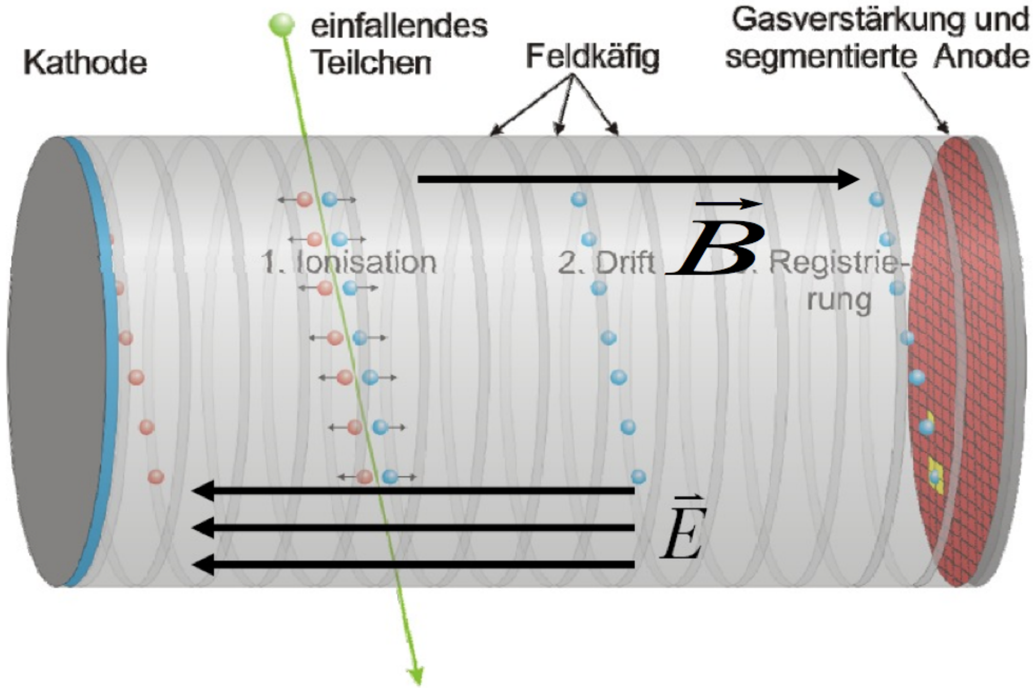

ADVANTAGES:

- Complete track determination within one detector → good momentum determination
- Relatively few wires
- Particle identification via dE/dx thanks to the charge measurement
- Drift parallel to B field → transversal diffusion suppressed by factors 10-100 → good spatial resolution

DISADVANTAGES, CHALLENGES

- Drift time relatively long, 10-100 μs → not a high rate detector. Attachment
- Large volume (precision)
- Large voltage (discharges)
- Large data volume

Structure of a TPC

Watch! We rotate by 90° wrt previous sketches

Highly uniform electric field obtained with field cage

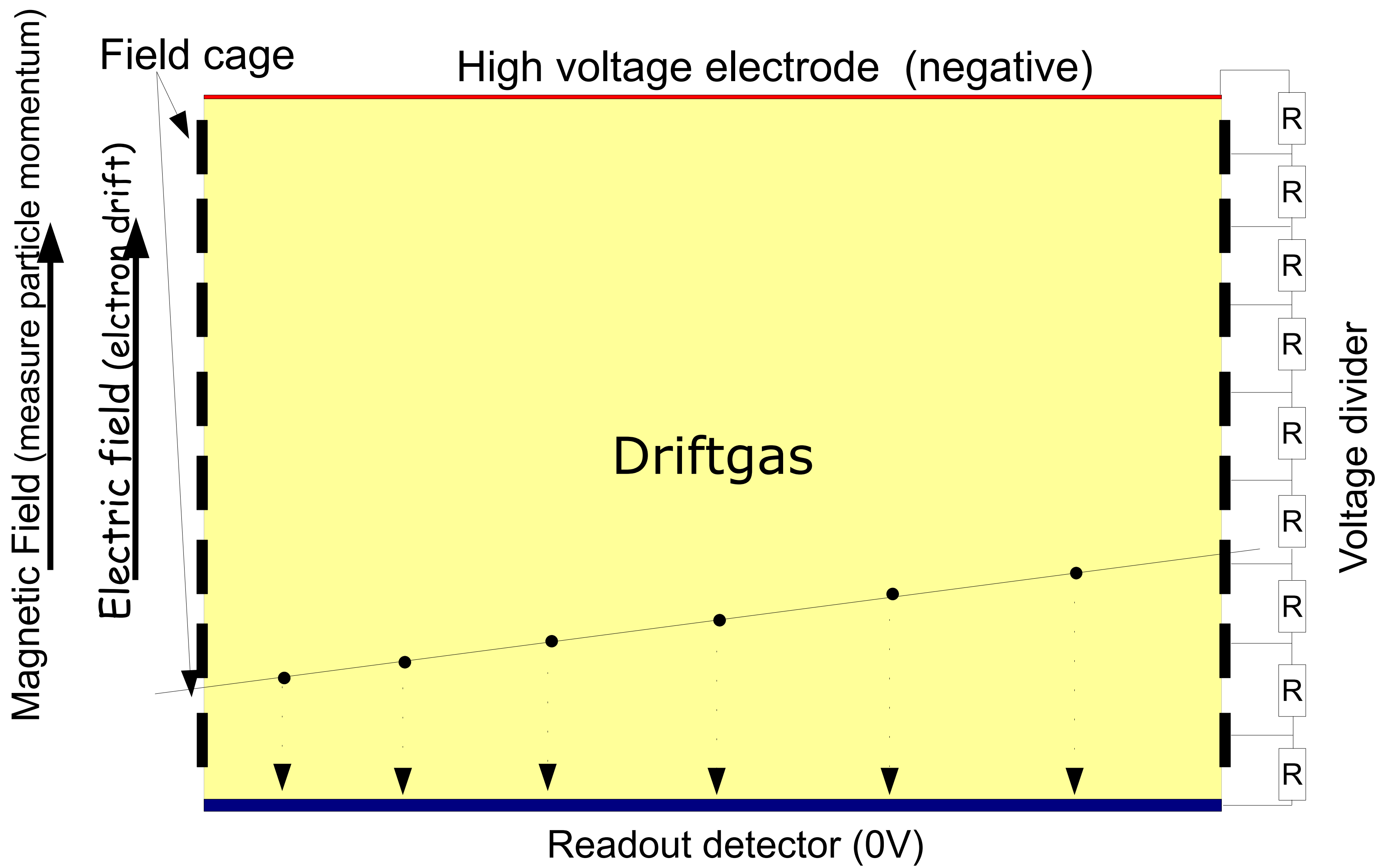

TPC: principle of operation

Ionization electrons move towards the MWPC along the E field lines.

At the end of the long drift path, the signal is induced on the anode wires and the cathode pads. They are continuously sampled.

- Z-coordinate is given by the drift time (v_{drift} critical!)
- X-coordinate is given by charge sharing among cathode pads
- Y-coordinate is given by the wire and pad row number

True 3-dimensional measurement of the ionization points of the entire tracks.

High multiplicity of tracks possible!

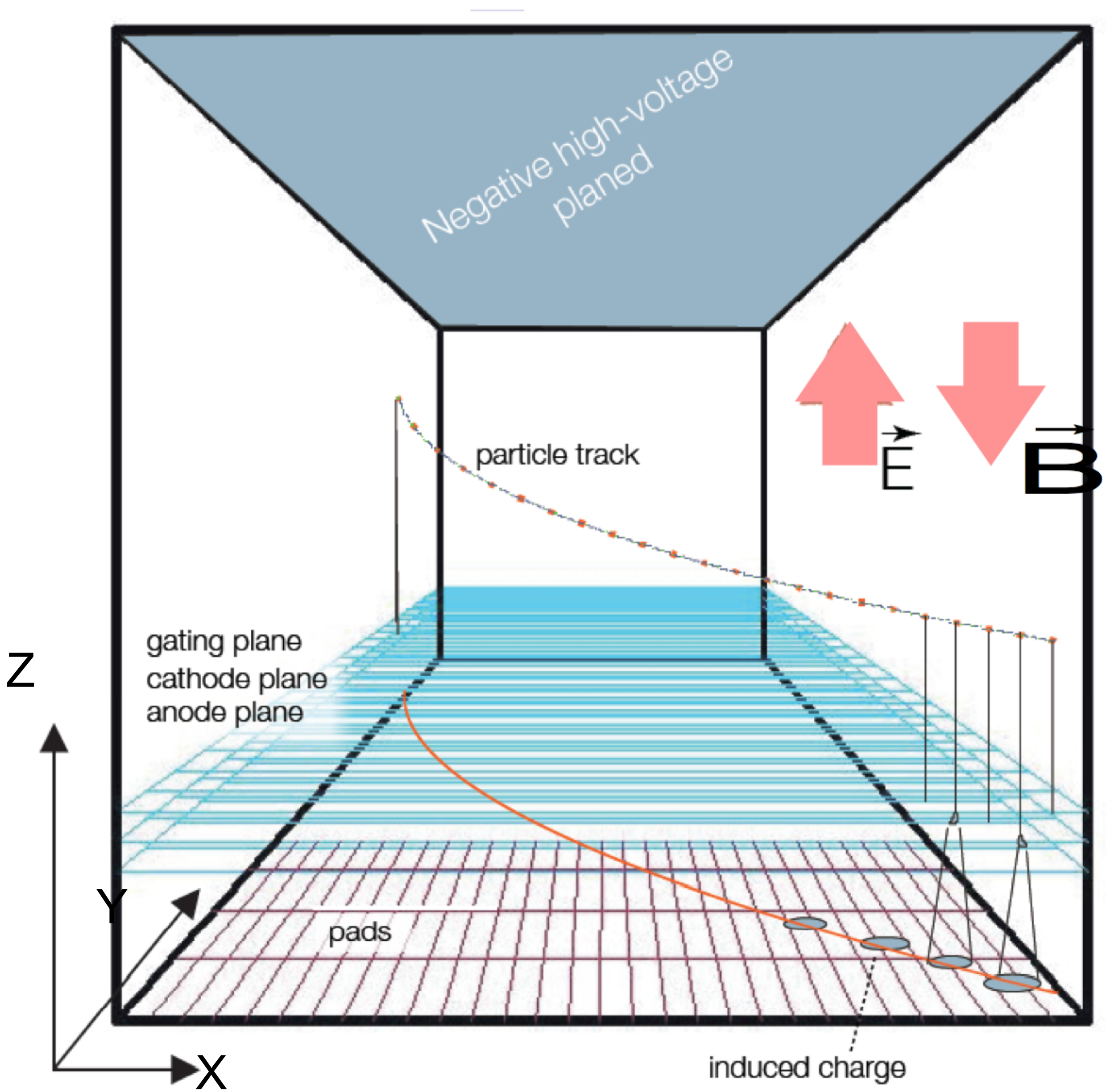

TPC: principle of operation

Ionization electrons move towards the MWPC along the E field lines.

At the end of the long drift path, the signal is induced on the anode wires and the cathode pads. They are continuously sampled.

- Z-coordinate is given by the drift time (v_{drift} critical!)
- X-coordinate is given by charge sharing among cathode pads
- Y-coordinate is given by the wire and pad row number

True 3-dimensional measurement of the ionization points of the entire tracks.

High multiplicity of tracks possible!

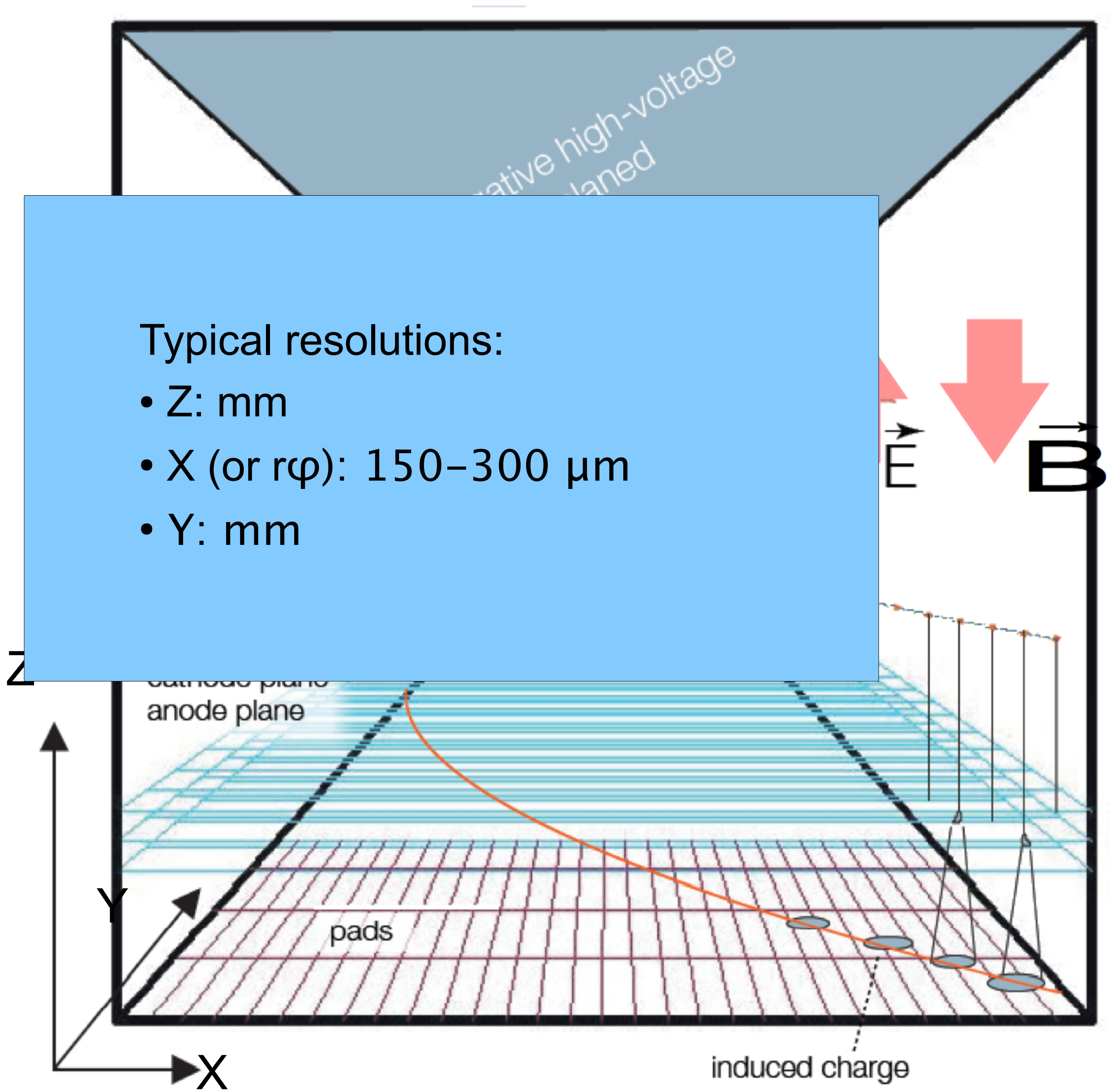

Typical resolutions:
- Z: mm
- X (or rφ): 150–300 μm
- Y: mm

TPC: wire chambers

Several wire planes for optimal field shaping and to stop ion back-flow (see next slide)

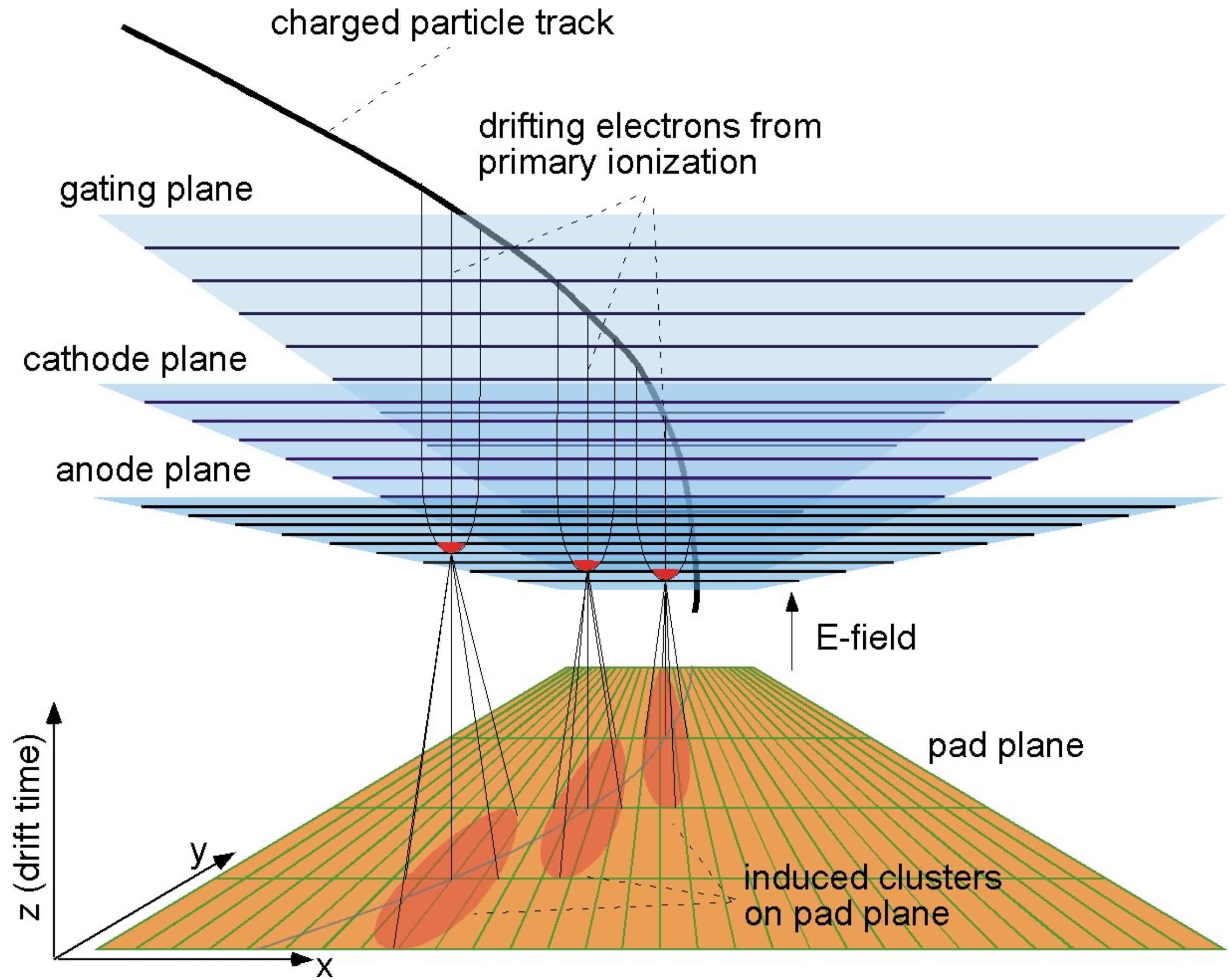

TPC: wire planes

Double layer of wires to shape E-field lines in the region of anode wires

E-Field of a wire grid

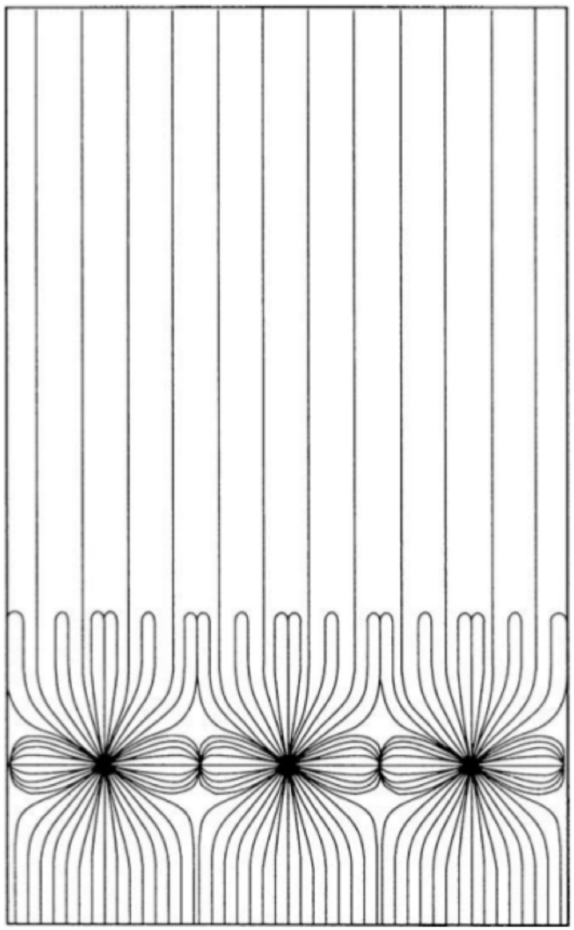

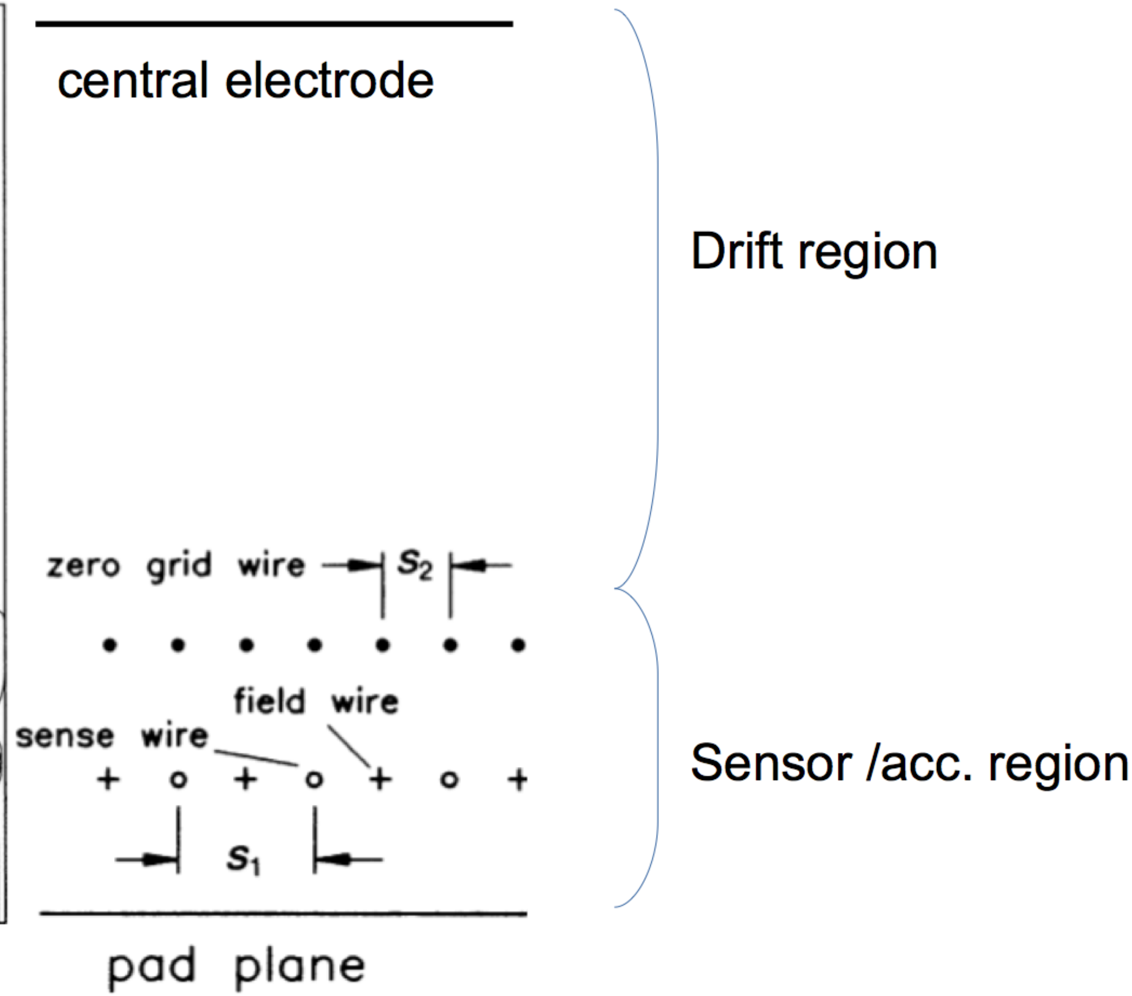

TPC: ion back flow ↔ gating grid

- After the charge multiplication around the anode wires, if the many ions move back to the drift region they would build a substantial space charge. This would cause serious distortions of the drift field!
- Use a **gating grid** which collect the ions and stop them from moving back into the drift region
- The shielding wire layer in between protect the sense wire from possible disturbance while switching

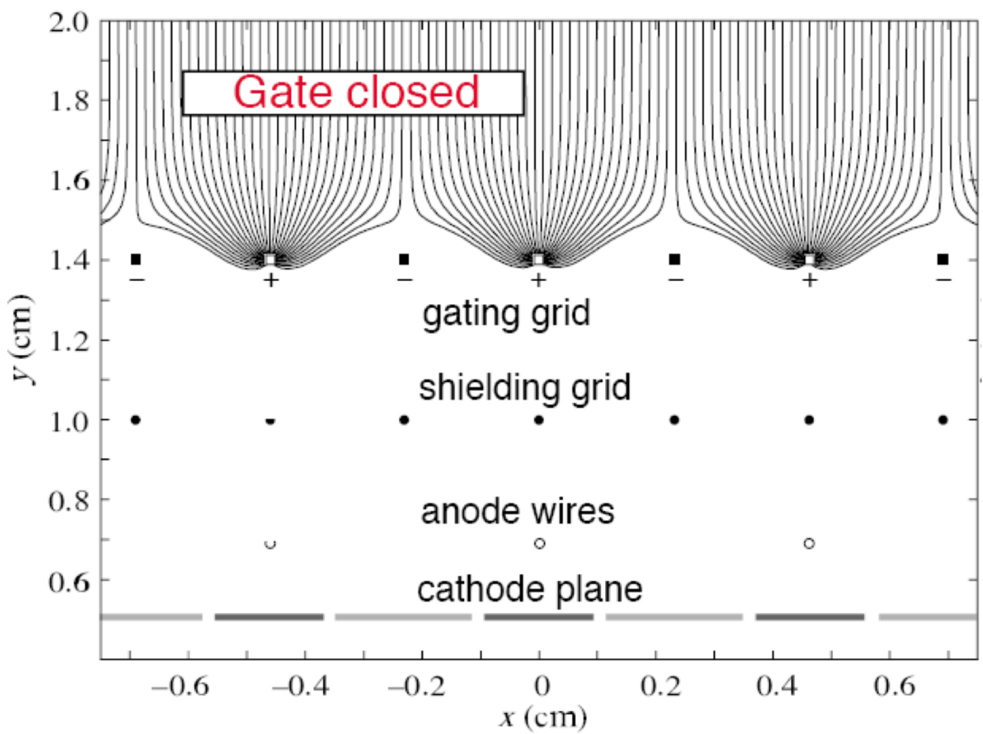

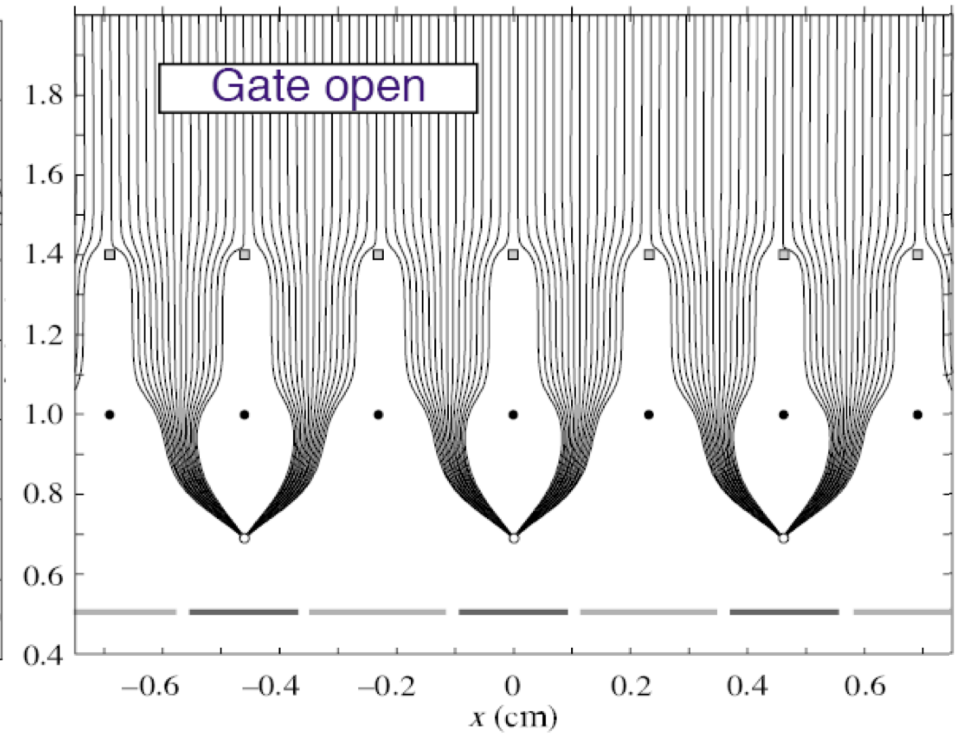

TPC: gating grid

- An external trigger switches the gating grid. It is by default kept closed: upon an interaction trigger, the grid is opened
- It remains opened for the maximal time of drift of electrons from the active volume, then closes again to keep the ions from the amplification away from the drift region

Limitation:

The relatively long drift times (~100 μs for electrons!) and the operation with gating grid limits the effective live time of the detector, and its maximal readout rate!!

→ ALICE TPC upgrade: from MWPC + gating grid → GEM chambers

ALICE TPC

LARGEST TPC EVER BUILT

- Gas volume: ~92 m^3 (active volume)
- Very light giant: 3% X_0 at mid-rapidity
- 72 readout chambers: Multi Wire Proportional Chambers with pad readout
- Half a million pads! (557,568 channels)

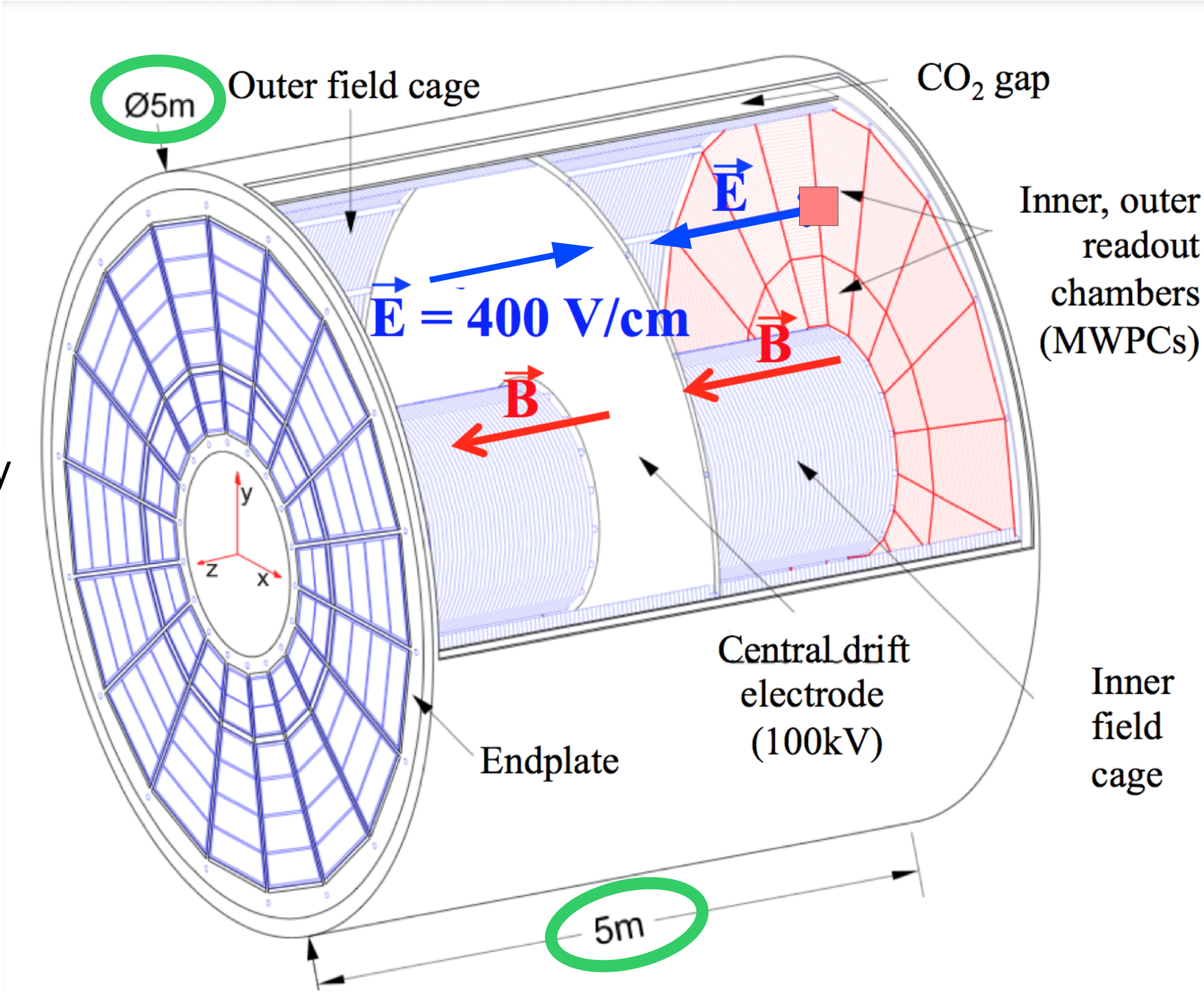

ALICE TPC: the readout chambers

- 2 end-plates with readout chambers, each with 18 sectors
- Each sector:
  - Inner ReadOut Chamber (IROC)
  - Outer ReadOut Chamber (OROC)

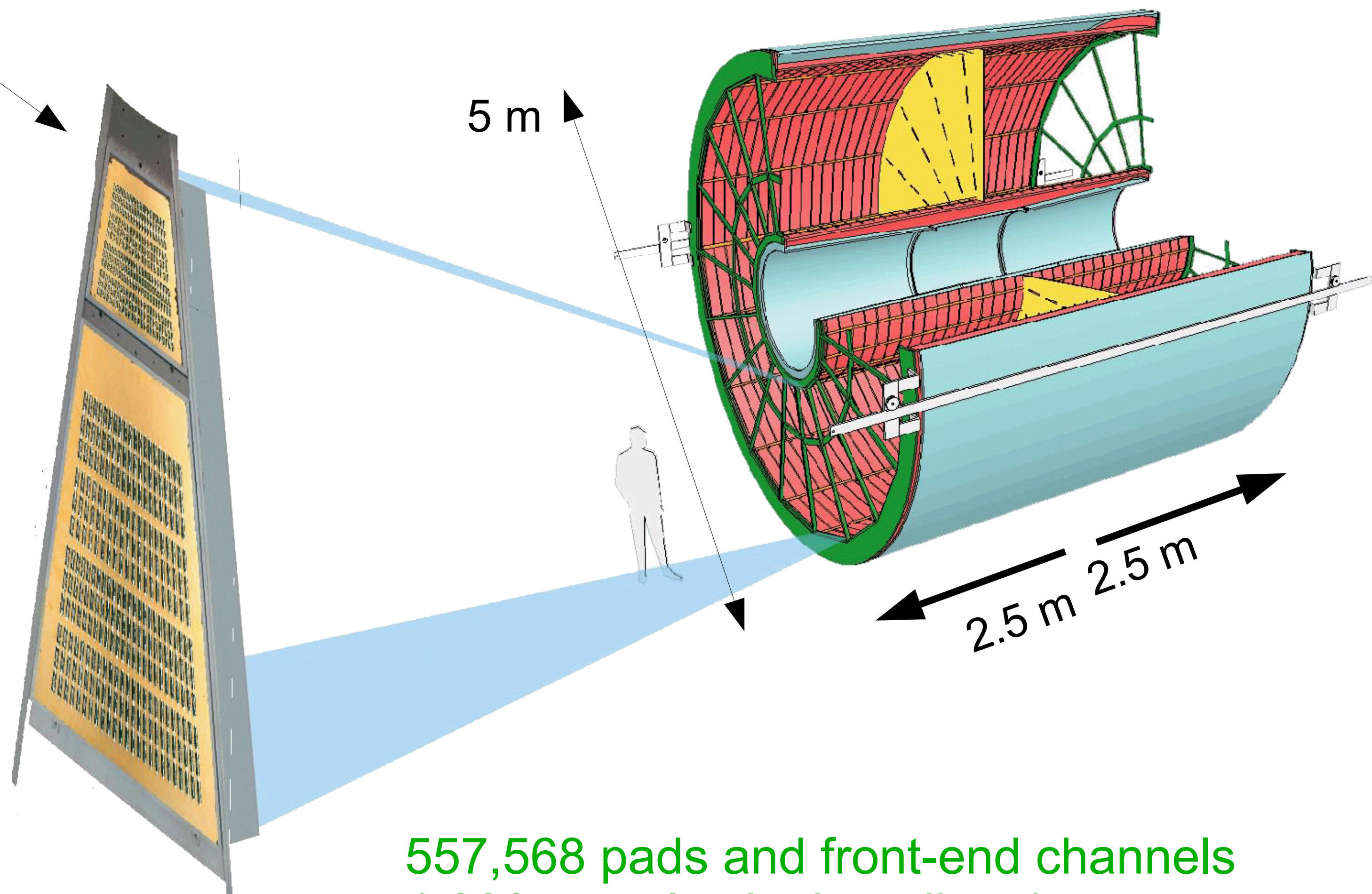

Drift voltage (central electrode): 100 kV
Anode voltage: 1350/1570 V
Nominal gain: 5000 - 8000

557,568 pads and front-end channels
1,000 samples in time direction
557 million voxels

ALICE TPC: dE/dx measurement for PID

Resolution: ~ 5%

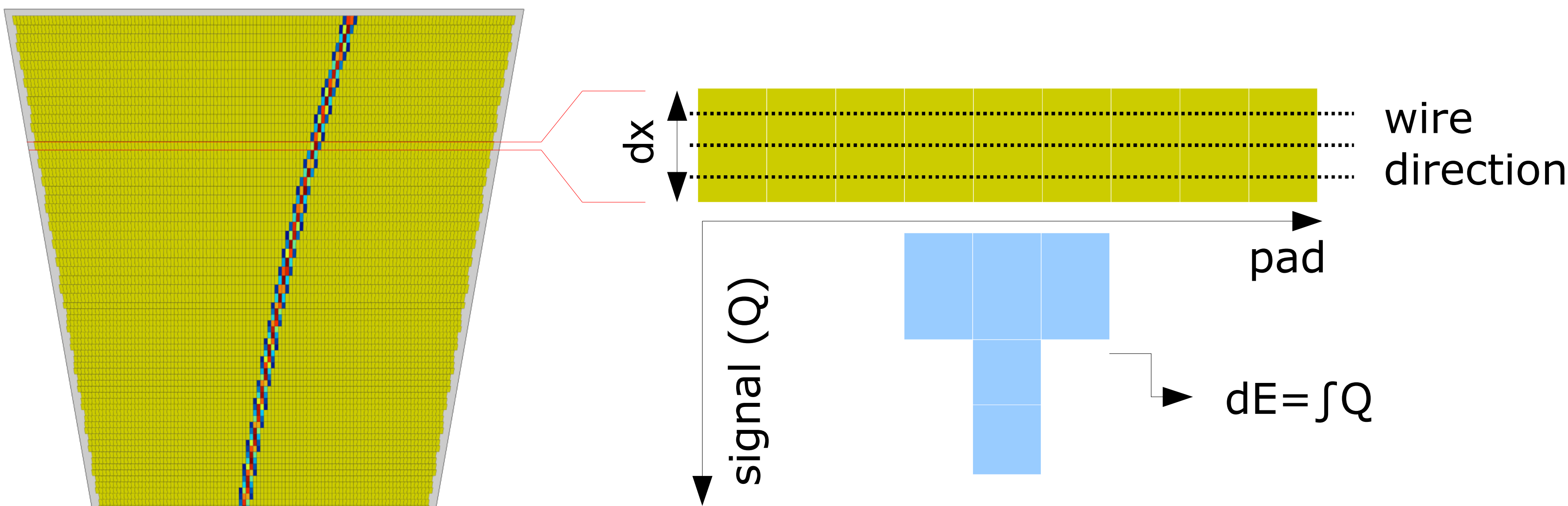

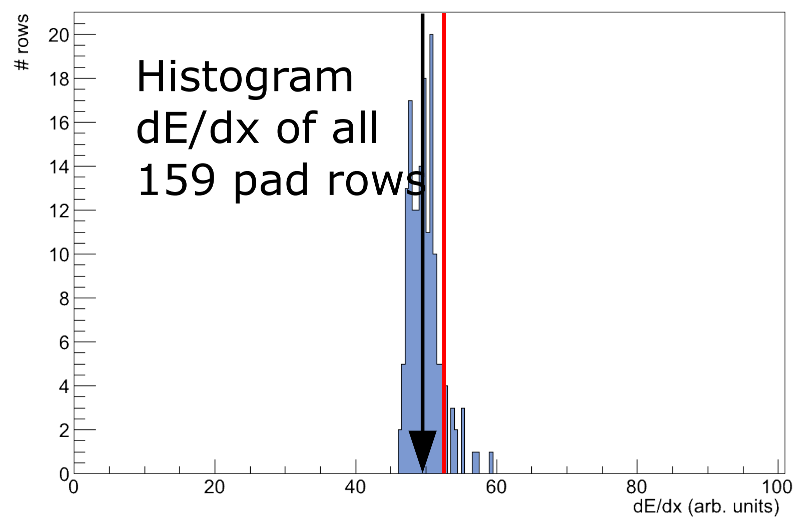

Truncated mean (<dE/dx>) cutting upper 40% of the charge distribution used as PID signal

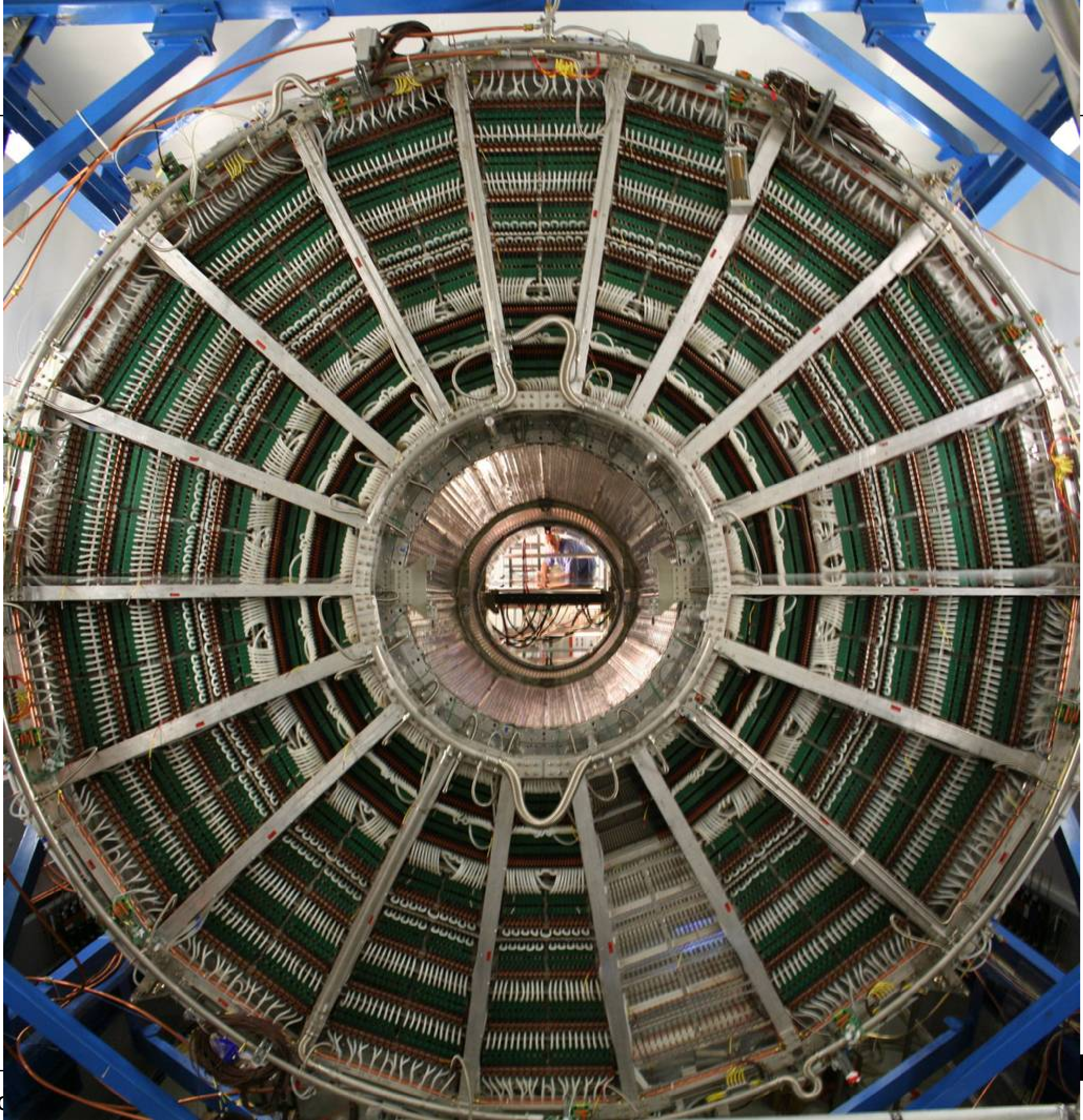

ALICE TPC: event display

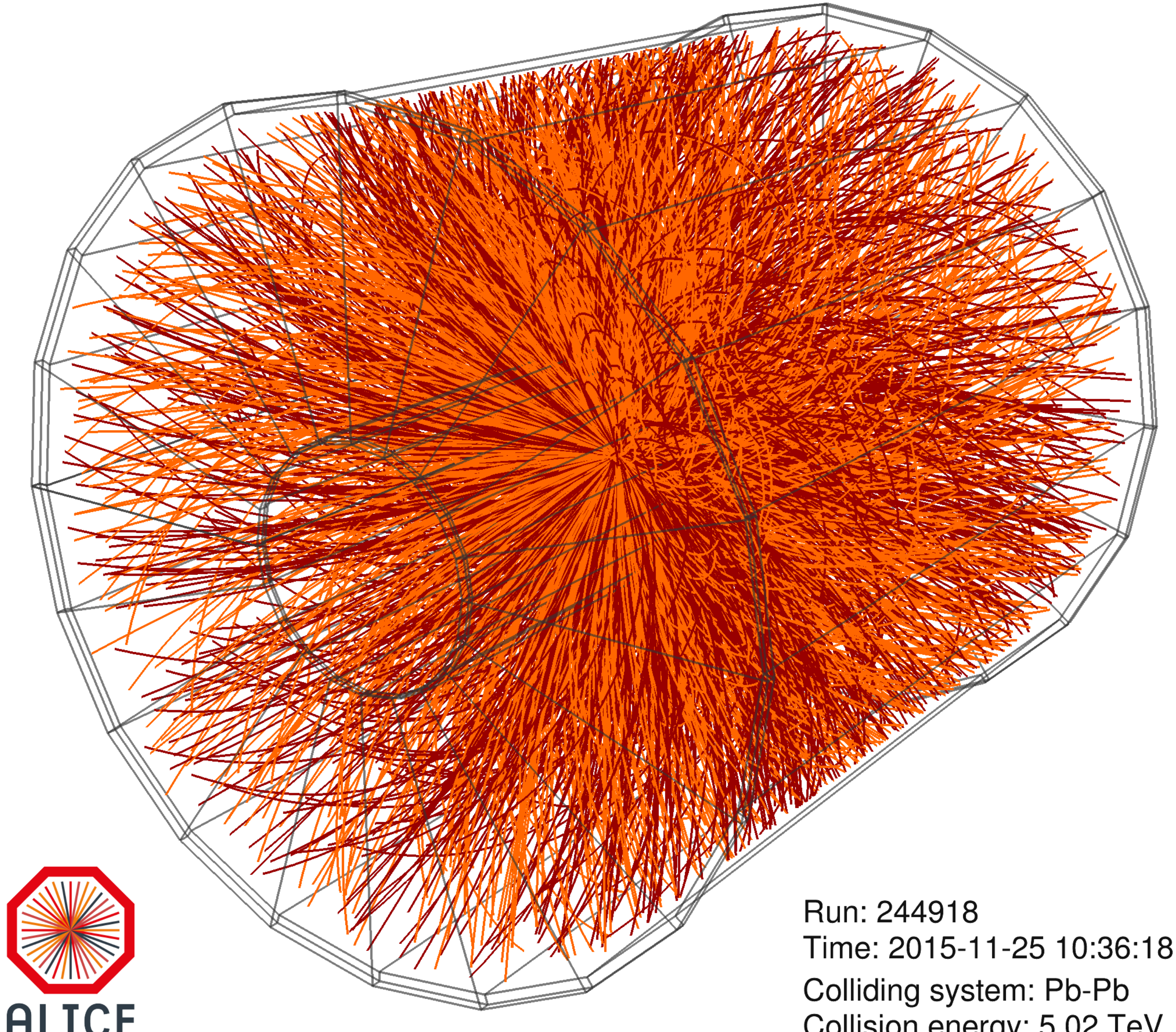

Overview

Ionization mode:

Full charge collection

No multiplication – gain = 1

Proportional mode:

Multiplication of ionization

Signal proportional to ionization

Measurement of dE/dx

Secondary avalanches need quenching

Gain ~ 10^4 – 10^5

Limited proportional mode (saturated, streamer):

Strong photoemission

Strong quenches or pulsed HV

Gain ~ 10^{10}

Geiger mode:

Massive photoemission

Full length of anode wire affected

Discharge stopped by HV cut